TARGETING INFLAMMATION AND NEUROGENESIS IN AN ANIMAL MODEL OF SMALL-VESSEL STROKE

A Thesis Submitted to The College of

Graduate Studies and Research

In Partial Fulfillment of the Requirements

For the Degree of Doctor of Philosophy

In the Department of Physiology

College of Medicine

University of Saskatchewan

Saskatoon

By

RUI HUA

PERMISSION OF USE STATEMENT

In presenting this thesis in partial fulfillment of the requirements for a Postgraduate degree from the University of Saskatchewan, I agree that the Libraries of this University may make it freely available for inspection. I further agree that permission for copying of this thesis in any manner, in whole or in part, for scholarly purposes may be granted by the professor or professors who supervised my thesis work or, in their absence, by the Head of the Department or the Dean of the College in which my thesis work was done. It is understood that any copying or publication or use of this thesis or parts thereof for financial gain shall not be allowed without my written permission. It is also understood that due recognition shall be given to me and to the University of Saskatchewan in any scholarly use which may be made of any material in my thesis.

Requests for permission to copy or to make other use of material in this thesis in whole or part should be addressed to:

Head of the Department of Physiology
University of Saskatchewan
107 Wiggins Road
Saskatoon, Saskatchewan
Canada S7N 5E5

Abstract

Therapeutic strategies of stroke can take two directions: to prevent brain damage from stroke or aid in its repair after a stroke. In this thesis, a rat stroke model, which mimics the human small vessel stroke, was used. Two potential repair strategies were investigated with this model, reduction of inflammatory processes with the aid of minocycline treatment and replacing necrotic neurons with new ones with the aid of neurogenesis of endogenous progenitor cells.

The stroke model is induced by disrupting the medium-size pial vessels within a 5mm-circular brain surface of adult Wistar rats. This leads to a cone-shaped cortical lesion. Therefore it mimics the clinical situation of lacunar infarction, the most frequent outcome of small vessel stroke.

Minocycline, a second-generation tetracycline, prevented cavitation and facilitated the repopulation of the lesion by reactive astrocytes. However, I could not identify the molecular target as the number of activated microglia, infiltrating leukocytes and CD3+ lymphocytes as well as interleukin-1β expression were not significantly altered.

Doublecortin (DCX) is a microtubule-associated protein expressed by migrating neuroblasts and immature neurons. After injury, DCX-positive cells appeared in the neocortex at the base of the lesion. These cells exhibit a morphology resembling differentiated post-migratory neurons with long branched processes. Some of the DCX-positive cells were also immunoreactive for βIII-tubulin, another marker of immature neurons. This might indicate a migratory pathway for developing neuroblasts from the subventricular zone (SVZ) through the corpus callosum to the lesion. SVZ cells were labeled with carboxyfluorescein diacetate, succinimidyl ester (CFSE) stereotaxical injections. Although rostral migratory stream and olfactory bulb were intensely labeled, no CFSE containing cells were found in the cortex underneath the lesion. These results suggest that the DCX-positive cells may not originate from neural precursors from the SVZ, but might be generated from local progenitor cells.

In summary, using the PVD II model, which mimics the lacunar stroke, I found that neuroblasts appeared spontaneously near the lesion in the cerebral cortex and were attempting to upregulate neuronal properties. Reducing inflammation with post-stroke minocycline treatment prevented cavitation. I think both findings open up exciting new avenues for treatment of lacunar infarctions.

ACKNOWLEDGMENTS

I would like to thank my supervisor, Dr. W. Walz, for giving me the opportunity to study in his laboratory. His supervision, guidance and unique personality through this journey have been a genuine gift.

I would like to thank our graduate student chair, Dr. Prakash Sulakhe and all my advisory committee members: Dr. Thomas Fisher, Dr. Michel Desautels, Dr. Ronald Doucette and Dr David Schreyer for their extensive advice and guidance throughout this program. It was my privilege to have all of you as my advisory committee.

I would like to thank the external examiner Dr. James Peeling for taking the time to critique this thesis, and to come to Saskatoon for my defense.

I would like to thank, Lyndon and Margret, the technicians who have worked in Walz lab over the past years. Our daily chats have made my experience here more enjoyable.

During my Ph.D program I was supported by scholarships from the College of Medicine and the College of Graduate Studies and Research of the University of Saskatchewan. The work in this thesis was supported by grants from the Canadian Stroke Network and the Canadian Heart and Stroke Foundation of Saskatchewan.

DEDICATION

To my Loving parents

To my Dear husband

TABLE CONTENTS

LIST OF TABLES

LIST OF FIGURES

LIST OF ABBREVIATIONS

AMPA- alpha-**a**mino-3-hydroxy-5-methyl-4-isoxazolepropionic acid

ANOVA- analysis of variance

Apaf-1- apoptotic protease activating factor 1

ATP- adenosine triphosphate

BBB- blood brain barrier

BDNF- brain-derived neurotrophic factor

bFGF- basic fibroblast growth factor

BrdU- 5-bromo-2-deoxyuridine

BSA- bovine serum albumin

CC- corpus callosum

CD- cluster of differentiation

CFSE- 5-(and-6)-carboxyfluorescein diacetate succinimidyl ester

CINC- cytokine-induced neutrophil chemoattractant

CNS- central nervous system

Cre- cyclization recombination

COX-2- cyclooxygenase-2

CSMN- corticospinal motor neurons

CSF- cerebrospinal fluid

CSPGs- chondroitin sulfate proteoglycans

DCX- doublecortin

DiI- 1,1-dioctadecyl-3,3,3`,3`-tetramethylindocarbocyanine perchlorate

DISC- death-inducing signaling complex

DG- dentate gyrus

DGC- dentate granule cell

DMSO-dimethylsulfoxide

ECM- extracellular matrix

EGF- epidermal growth factor

EGFP- enhanced green fluorescent protein

ELISA- enzyme-linked immunosorbent assay

FGF-2- fibroblast growth factor-2

ET-1- endothelin-1

FITC- Fluorescein

GFAP- glial fibrillary acidic protein

GL- glomerular layer

GCL- granule cell layer

GSAB$_4$- *Griffonia simplicifolia* B$_4$-isolectin

H&E- hematoxylin-eosin

HIF-1- hypoxia-inducible factor-1

HRP- horseradish peroxidase

HSC- hematopoietic stem cells

ICE- IL-1β converting enzyme

ICAM- intercellular adhesion molecule

IFN- interferon

IL- interleukin

IL-1β- interleukin 1β

iNOS- inducible nitric oxide synthase

LCA- leukocyte common antigen

LV- lateral ventricle

***Lox P*-** locus of X-over P1

MCA- middle cerebral artery

MCAO- middle cerebral artery occlusion

MCP-1- monocyte chemoattractant protein-1

mGluR- metabotropic glutamate receptor

MHC- major histocompatibility complex

MMPs- matrix metalloproteinases

MPO- myeloperoxidase

MRF-1- microglial response factor-1

mRNA- message RNA

NeuN- neuronal specific nuclear protein

NF-κB- nuclear factor κB

NMDA- *N*-methyl-D-aspartic acid

NO-nitric oxide

NSCs- neural stem cells

OB- olfactory bulb

PARP- poly (ADP-ribose) polymerase

PG- prostaglandins

PFA- paraformaldehyde

PGE_2- prostaglandin E_2

PMNs- polymorphonuclear neutrophils

PVD II- pial vessel II disruption

RMS- rostral migratory stream

RV- retroviral vector

SEZ- subependymal zone

SGZ- subgranular zone

STAT- signal transducers and activator of transcription protein

SVZa- anterior SVZ

SVZdl- dorsolateral SVZ

S-phase- synthesis phase

TGF- transforming growth factor

TGF-β- transforming growth factor β

TK- thymidine kinase

TNF-α- tumor necrosis factor α

TRITC-tetramethylrhodamine isothiocyanate

tMCAO- transient middle cerebral artery occlusion

tPA- tissue plasminogen activator

TUNEL- terminal deoxyribonucleotide transferase (TNT)-mediated dUTP nick end labeling

1. GENERAL INTRODUCTION

1.1 Stroke

Stroke is a leading cause of mortality and morbidity as well as a major component of health costs in most countries. In Canada alone, around 40,000 to 50,000 strokes and 16,000 stroke-related deaths occur each year with an annual economic cost of around $2.7 billion. Approximately 20% of stroke patients do not survive the first month after a stroke. Another 30% will survive for at least six months, but will be permanently dependent on others. Although a stroke can and does occur in infants and children, it mainly affects adults in the middle and later years of life. Stroke is therefore a major cause of prolonged neurological disability in adults (Warlow et al., 2003). The incidence of stroke-related deaths is predicted to double by 2030 in the USA due to the aging of the population (Frizzell, 2005). This highlights the significance and importance of stroke prevention and treatment.

Stroke is defined by the World Health Organization as a clinical syndrome of rapid onset of a cerebral deficit, lasting more than 24 h or leading to death, with no apparent cause other than a vascular one (Fatahzadeh and Glick, 2006). In humans, stroke is a diverse disease in terms of causes, manifestations, and anatomic sites. Depending on the underlying pathogenesis, strokes are subclassified into ischemic and hemorrhagic types. Approximately 15% of all strokes are hemorrhagic in nature. These are caused by either the rupture of an artery deep within the brain (hemorrhagic stroke, intracerebral hemorrhage), bleeding on the brain surface or bleeding between the brain and the skull (subarachnoid hemorrhage) as a result of trauma or from the rupture of an aneurysm. Approximately 85% of all strokes are classified as cerebral ischemia and result from occlusions of large or small arteries. They may be caused by either atherosclerotic thrombi (thrombus) or distant emboli (embolism) (Fatahzadeh and Glick, 2006).

Ischemic stroke can occur in a discrete area of the brain (focal ischemia) or in the whole brain (global ischemia) (Back et al., 2004). Global ischemia occurs when there is an interruption of blood flow or severe hypoxia to the entire brain. Such situations are mostly caused by cardiac arrest, shock, near drowning or severe systemic hypotension. It seems that different brain regions have different thresholds for ischemia and certain neuronal populations within an individual are selectively vulnerable to ischemia. For instance, white matter is more resilient than gray matter and hippocampal CA1 pyramidal cell neurons are very vulnerable to relatively brief periods of ischemia (Kirino and Sano, 1984; Back et al., 2004).

Focal cerebral ischemia affects restricted brain regions and will impair the function of such areas. In clinical settings, focal ischemia happens more frequently than global ischemia. Regardless of the etiology, the clinical presentation of symptoms depends largely upon the location of the occluded vessels and the presence of collateral circulation (Felberg and Naidech, 2003; Fatahzadeh and Glick, 2006). The symptoms are often transient if the occlusion occurs at one of the small intracerebral vessels. The condition is referred to as lacunar stroke (Frizzell, 2005; Fatahzadeh and Glick, 2006). Around 20% of ischemic strokes are lacunar strokes. Lacunar infarcts are commonly found in the putamen, caudate, thalamus, pons, internal capsule and cerebral white matter, in descending order of frequency (Bamford et al., 1987; Arboix and Marti-Vilalta, 2004). In contrast, large vessel stroke is characterized by extensive cerebral infarction and results from occlusion of a major intracranial vessel. Frequently, high level brain functions are affected and the prognosis is poor.

Unlike global ischemia, which leads to neuronal cell death in vulnerable areas of the brain, focal ischemia produces usually one distinct mass of damaged brain tissue termed infarct. The central region supplied by the affected artery is known as the infarct core, and is often the region with the highest impairment of blood flow. The surrounding area is called the penumbra, often spared from major ischemia impact by the collateral circulation from other arteries. In animal models of middle cerebral artery occlusion [MCAO], the cerebral blood flow within the core decreases to less than 15% of the baseline, whereas the flow in the penumbra is less than 40%. If the blood flow in the

penumbral zone further decreases, the infarct area will inevitably expand (Dirnagl et al., 1999; Hossmann, 2006).

Because the severity and reversibility of the ischemic damage depend on the degree of the flow reduction, there are major physiologic differences between the core and penumbra. Therefore in cerebral ischemia the pathophysiology of core and penumbra differs extensively. The ischemic core, which is subject to the most severe flow reduction, undergoes irreversible damage in a relatively short period of time. In contrast, the ischemic penumbra experiences disturbances of neuronal function that are at least initially reversible. The ischemic penumbra can be "rescued" from infarction if flow is restored or if neuroprotective measures are undertaken. The ischemic penumbra, therefore, is the major target of neuroprotective strategies (Fisher and Garcia, 1996; Hossmann, 2006).

Over the past decades, substantial progress has been made in understanding the pathophysiologic mechanisms of stroke. However, currently only thrombolytic therapy within a narrow time window after stroke onset (Small et al., 1999; Frizzell, 2005) is accepted as a therapeutic option for ischemic stroke. Aspirin, other antiplatelet agents, or anticoagulants are used as preventative therapy for embolic stroke patients (Felberg and Naidech, 2003). Understanding the pathophysiology of brain ischemia is necessary to develop potential therapies for ischemic stroke. In this chapter, the cellular and molecular events leading to brain damage after experimental focal cerebral ischemia are reviewed as well as the therapeutic strategies. The main focus is on possible therapeutic targets based on new discoveries in neuroinflammation and intrinsic regenerative mechanisms of the brain. This chapter is necessarily limited to focal ischemia, as this is the stroke type most often investigated with animal models and it has clinical relevance due to its high prevalence.

1.2 Pathophysiology of Focal Cerebral Ischemia

1.2.1 Overview of the Mechanisms

The current understanding of stroke pathophysiology extends far beyond the immediate effects of the initial impairment of local blood circulation. The events that

take place in the ischemic area are complex and follow a stereotypic temporal and spatial pattern. As the brain has a very high demand for oxygen and glucose, within minutes of cessation of blood flow, brain tissue is deprived of glucose and oxygen and the acidic byproducts of metabolism accumulate, which results in a rapid decline in ATP concentration. The energy deficiency results in failure of the Na^+/K^+-ATPase. The resulting loss of ionic gradients leads to depolarization. The rapidity with which this depolarization occurs depends on the severity and duration of ischemia. Shortly after the onset of ischemia, glutamate is released into extracellular compartments and it activates postsynaptic glutamate receptors, such as ligand-gated ionotropic (NMDA, AMPA) and G-coupled metabotropic (mGluR) receptors. This leads to accumulation of intracellular Ca^{2+} and an increase in intracellular Na^+ and Cl^- concentrations. This massive disturbance of ion homeostasis will eventually lead to cell lysis and cytotoxic edema. The energy failure is probably the predominant mechanism of cell death in the ischemic core (Siesjo, 1992a; Dirnagl et al., 1999; Smith, 2004).

In the penumbra, where the blood flow reduction is not sufficient to cause rapid energy failure, other mechanisms, such as glutamate excitotoxicity, calcium overload and free radical damage, might play major roles. Excessive extracellular glutamate and potassium may diffuse from the core into the penumbral areas and trigger peri-infarct depolarization, which contributes to the expansion of the lesion from the core into the penumbra. Elevated amounts of intracellular Ca^{2+} retard mitochondrial function and cause formation of toxic metabolites, such as proteases, phospholipases, cytochrome oxidase and free radicals. The latter trigger an intracellular 'death' cascade. In addition there is secondary injury as a result of inflammation (Siesjo, 1992a; Dirnagl et al., 1999; Smith, 2004; Hossmann, 2006).

1.2.2 Neuronal Cell Death after Focal Ischemia

Hypoxic neurons die by two different modes: necrosis and apoptosis. Necrotic cell death is more common with more extreme levels of ischemia, whereas apoptotic cell death is more common with less severe insults. Thus, the core tissue of an infarct dies a necrotic death, and, depending on the location within the penumbra, cells die by means of either mode, with apoptosis more common in cells further away from the core.

Necrosis is not an energy-consuming process and is independent of protein synthesis. It is characterized by membrane dysfunction and cell swelling. It usually induces an inflammatory response. In contrast, apoptosis is an energy-dependent programmed cell death (Choi, 1996). The cell requires active gene transcription and protein synthesis to degrade its own DNA. The morphologic features of apoptotic cell death are quite different from necrotic cell death, with DNA laddering and regular clumping of chromatin (apoptotic bodies). Apoptosis is characterized morphologically by primary changes in the nuclei, such as early extensive chromatin condensation, marginalization and segregation followed by fragmentation, whereas the cell membrane and mitochondrial structure are relatively preserved (Snider et al., 1999). In the final stages of cellular dissolution, apoptotic bodies may be formed by cellular fragmentation into spherical vesicles. This is followed by a stereotypical loss of cellular architecture that involves the activity of caspases and other enzyme systems. This process may take several days. This DNA fragmentation can be detected *in situ* in tissue sections by positive terminal deoxyribonucleotide transferase (TNT)-mediated dUTP nick end labeling (TUNEL) (Namura et al., 1998; Ferrer and Planas, 2003).

In experimental rat models of transient focal ischemia, apoptotic neurons were located mainly in the inner boundary zone of infarcts, increasing in number as early as 0.5 h, peaking at 24-48 h, and persisting for 4 weeks after the onset of reperfusion (Li et al., 1995a; Li et al., 1995b). Similar results were described in an ischemic model employing photothrombosis (Braun et al., 1996). Many TUNEL-positive cells were found within the infarct region from 12 h to 3 days. By day 6 they were preferentially located in the boundary zone of the infarct, and by day 14 they had disappeared. A high proportion of TUNEL-positive cells were identified as apoptotic neurons by their morphology. Infiltrating neutrophils were found to be in close contact with apoptotic neurons, which suggests a role for leukocytes in the development of apoptotic neuronal cell death (Li et al., 1995b; Braun et al., 1996). Taken together, these studies point to neuronal death in cerebral ischemia as a prolonged process that involves apoptotic mechanisms. Apoptosis could contribute to the expansion of the primary ischemic region into the periphery. This would explain the dynamics of penumbra evolution (Love, 2003; Smith, 2004).

Apoptosis is characterized by a biochemical cascade which leads to the activation of caspases, a family of proteases that exist as inactivate proenzyme (procaspase) precursor proteins in cells. Once they are cleaved, the active enzymes cleave other proteins, including structural cytoskeletal proteins such as actin and gelsolin, structural nuclear proteins such as lamins, and DNA repair proteins such as the DNA-repairing enzyme PARP and the anti-apoptotic protein Bcl-2 and Bcl-$_{xL}$. This in turn leads to the apoptotic cleavage of nuclear DNA. Caspases 1, 3, 8 and 9 are involved in cerebral ischemia. Caspase 1, also known as interleukin-1 converting enzyme, is involved in the maturation of cytokines and the induction of inflammation. Caspases 3, 8 and 9 are directly involved in apoptosis. There are two pathways of caspase activation: death receptor-mediated (extrinsic) and mitochondrial (intrinsic). The extrinsic pathway starts with the activation of the death receptor. The principal death receptor in cerebral ischemia is Fas. Its activation induces stimulation of a death-inducing signaling complex (DISC) that causes caspase 8 activation, leading to the recruitment of other caspases and activation of the intrinsic apoptotic pathway. In the intrinsic pathway, cytochrome C is released from the mitochondrial membrane and then in turn activates downstream caspases 3, 6 and 7, of which caspase 3 acts as a final common pathway. It is responsible for inactivating PARP, thus disabling DNA repair mechanisms. The result is cellular death. Cytochrome C is a member of the mitochondrial electron-transport chain which is required for the generation of ATP. It is not only essential for energy production, but it is also a central mediator in the caspase activation cascade. Once it is released from the mitochondria into the cytoplasm, it binds to apoptotic protease activating factor 1 (Apaf-1) and forms the apoptosome together with ATP and procaspase 9. The apoptosome activates caspase 9 and leads to sequential activation of downstream caspases. The balance between pro-apoptotic (Bid, Bax, Bad, Bag) and anti-apoptotic (Bcl-2, Bcl-$_{xL}$) proteins in the Bcl-2 family plays a crucial role in the release of cytochrome C (Snider et al., 1999; Ferrer and Planas, 2003; Friedlander, 2003; Love, 2003; Sugawara et al., 2004).

A large body of evidence shows that brain ischemia causes activation of caspases. Up-regulation and activation of caspases have been observed to precede the death of neurons in models of transient focal ischemia (Namura et al., 1998; Hermann et

al., 2001), permanent focal ischemia (Velier et al., 1999; Sasaki et al., 2000; Harrison et al., 2001) and global ischemia (Ni et al., 1998; Ouyang et al., 1999).

1.2.3 Gliosis in Focal Ischemia

In histological analysis, infarction is characterized by pannecrosis of neurons and glial cells. Within the first few hours after injury, not only neurons but also all the glial and vascular cells in the infarct core area undergo cell death, as reviewed in the previous section. At the same time, brain damage initiates a series of cellular and molecular events that evolve over several days. The main cell types involved in these changes are astrocytes, microglia, and oligodendrocyte precursors, with some involvement of meningeal cells if the injury penetrates the meninges. In addition, neural stem cells and/or neural progenitors may be involved. Macrophages from the bloodstream and microglia migrate into the injured area from the surrounding tissue within hours of injury. After several days, large numbers of oligodendrocyte precursors are recruited. With time, these cells decrease in number, and the injury area is surrounded by reactive astrocytes. This process is called reactive gliosis or glial scarring (Fawcett and Asher, 1999).

1.2.3.1 Astrocytes

Astrocytes are the principal macroglial cells in the CNS and make up about 50% of human brain volume. They participate in regulation of microvasculature, maintenance of ionic homeostasis and control of neuronal transmission. They also play an important role in the plasticity after injury. Accordingly, they are essential for normal neuronal activity, critically influence neuronal survival during ischemia and participate in repair and regeneration in the post-injury period (Walz and Juurlink, 2002).

Within the ischemic lesion, astrocytes exhibit swelling, fragmentation of processes and disintegration at the same time as or before neuronal changes. Subsequently, expression of the astrocytic marker glial fibrillary acidic protein (GFAP) is decreased and barely detectable anymore (Chen et al., 1993). However, starting 4-6 h after ischemia, the astrocytes surrounding the area of ischemia become reactive. This activation is characterized by hypertrophy and/or proliferation. The response is enhanced

by the migration of microglia and macrophages to the damaged area. Astrocytes activated by injury change shape by enlarging their cell bodies and extending many processes. These processes tightly interweave and are bound together by gap junctions. One major change of reactive astrocytes is the up-regulation of their intermediate filaments, which is directly associated with morphological changes (Stoll et al., 1998). In both the MCAO and cortical photothrombosis ischemia models, the number and intensity of reactive astrocytes at the lesion site steadily increase over approximately 1 week (Inuzuka et al., 1996; Yamashita et al., 1996). Some of these cells co-express other intermediate filament proteins, such as vimentin and/or nestin, which are normally found in immature astrocytes (Ridet et al., 1997). At later times after ischemia, reactive astrocytes in the immediate vicinity of the injury interweave their processes to form a barrier, termed the glia limitans, which consists mainly of a tightly packed meshwork of astrocytic processes and a large amount of ECM in a limited extracellular space.

The function of the glia limitans is to insulate the brain parenchyma from the non-brain compartments, replacing the destroyed blood brain barrier (BBB) or the pia mater. Although its functional role is not completely understood, this can be considered as a response by the brain to prevent further spread of damage and to restore homeostasis through isolation of the damaged region. However, glial scar formation has also been regarded as the major impediment to axonal regeneration and CNS repair (Ridet et al., 1997; Sofroniew, 2005). GFAP-knockout mice or mice treated with GFAP antisense RNA show enhanced expression of laminin and become more permissive to neurite growth (Sofroniew et al., 1999; Costa et al., 2002). This suggests that cytoskeletal proteins may contribute to the barrier effect of the glial scar for axonal extension. In addition reactive astrocytes secrete collagens and sulfate proteoglycans which also impede neurite growth (Fidler et al., 1999; Liesi and Kauppila, 2002). Recent studies suggest that astrocytes are involved in guiding axons and newly generated neurons and that they have trophic effects on neurite outgrowth and neurogenesis (Chen and Swanson, 2003). This appears to contradict the previous view. Reactive astrocytes increase the expression of several growth factors, such as basic fibroblast growth factor (bFGF), brain-derived neurotrophic factor (BDNF) and neuregulins, which are know to stimulate neurite outgrowth (Ridet et al., 1997; Tokita et al., 2001). *In vitro* studies show

that astrocytes induce neurogenesis in adult neural stem cells in culture (Song et al., 2002). The recent discovery of neurogenesis triggered by focal ischemia suggests that reactive astrocytes might be essential in neuronal differentiation processes.

Although astrocytes have a reputation for providing trophic support for neurons, recent studies have shown that they participate in the inflammatory response after ischemia. Activated astrocytes can express the inducible form of nitric oxygen synthase (iNOS) within a few hours and up to 3 days after ischemia in the rat (Iadecola et al., 1995). iNOS activates nitric oxide, a reactive oxygen species that contributes to neuronal cell death (Hewett et al., 1994). Reactive astrocytes also have the capability to produce various proinflammatory cytokines, such as IL-1ß, TNF-α, interferon, highly cytolytic proteins, complement proteins and prostaglandins (Chen and Swanson, 2003; Panickar and Norenberg, 2005). Furthermore, there are also reports that astrocytes are capable of phagocytosis (Aloisi, 1999). Therefore, astrocytes play a major role in the neuroinflammatory cascade and contribute to the neuronal damage in cerebral ischemia.

1.2.3.2 Microglia / Macrophages

Microglia are resident brain macrophages that are derived from the monocytic lineage. In the normal adult brain, they are in a quiescent state showing a typical ramified morphology with short branched processes and expressing few surface molecules. Rapid activation of glial cells occurs prior to any obvious signs of neuronal death. Microglia activate at a very early stage in response to CNS injury. After activation, they exert multiple functions by transforming into phagocytes. The initial activation is characterized by morphological changes, involving enlarged cell bodies and contraction of processes, as well as up-regulation of the surface molecules isolectin-B4, complement type 3 receptor (CR3, CD11b/CD18 complex), and microglial response factor-1 (MRF-1). In this partially activated state, microglia proliferate and migrate to the sites of injury, but they are not phagocytic and do not produce cytotoxic molecules. In the presence of dying neurons, microglia become further activated and at this stage, they are true phagocytes with amoeboid morphology. They express the same markers as the cells of the peripheral macrophage lineage, including MHC class I, MHC class II,

leukocyte common antigen (LCA) and CD4. In this state they are virtually indistinguishable from blood-borne macrophages (Kreutzberg, 1996; Streit et al., 1999).

In transient MCAO, by day 1, activated microglia are found in the penumbra close to the neurons, their processes often encircling the neurons. The entire infarct area is covered by round and amoeboid macrophages within 3 days after MCAO induction. Within 4 weeks, the debris was completely cleared by these phagocytes (Kato et al., 1996; Lehrmann et al., 1997; Zhang et al., 1997). In fact, these macrophages contain two different pools, activated microglia and blood-borne monocytes/macrophages. Monocytes/macrophages infiltrating from the blood stream into an ischemic area are recruited with a delay in comparison with resident microglia/macrophages (Schroeter et al., 1997).

The overall role of microglia, whether it is beneficial or detrimental in cerebral ischemia, is not clear at present. Activated microglia/macrophages produce toxic molecules such as nitric oxide (NO), oxygen radicals, arachidonic acid derivatives, chemokines and cytokines. In particular, proinflammatory cytokines such as TNFα, IL-1, and IL-6 play important roles as mediators of the inflammatory phase of cerebral ischemia. *In vitro* studies suggest that microglia kill neurons by secreting NO, oxygen free radicals, glutamate, and other cytotoxic substances (Farber and Kettenmann, 2005). On the other hand, in areas of severe damage, microglia can phagocytose debris and attack microorganisms that may infect the damaged area. In addition, microglia produce neurotrophins *in vitro*, as well as TGF-ß and plasminogen, which are involved in tissue repair and neurite outgrowth (Streit, 2002). Thus, it is very likely that microglia play different roles at different time points: amplifying the effects of neuroinflammation and mediating cellular degeneration in the brain as well as protecting the CNS, with these protective or regenerative activities occurring days or even weeks after the onset of ischemia (Streit et al., 1999; Streit, 2002).

1.2.3.3 Neutrophils and Macrophages

Circulating leukocytes invade and contribute to the developing infarction (Tomita and Fukuuchi, 1996). In response to an injury, the resident inflammatory brain cells, microglia, are activated and lead to local generation of various cytokines. These in

turn act on the endothelial cells lining the local blood vessels, induce an increased BBB permeability and start expressing various adhesion molecules. These events trigger a roll-on of circulating leukocytes. They adhere to endothelial cells, and eventually transmigrate into the damaged cerebral parenchyma. Various leukocyte subpopulations are recruited at different times (Stoll et al., 1998). Neutrophils are the first hematogenous leukocytes that appear in the brain in response to focal ischemia, followed by monocytes/macrophages and some lymphocytes. Monocytes/macrophages are the most abundant leukocytes that enter the brain after focal ischemia. After transient MCAO in rats, neutrophils can be detected in microvessels of the ischemic hemisphere as early as 30 min after the occlusion with a peak at 12 h, whereas intraparenchymal neutrophils are most numerous at 24 h and decline rapidly thereafter. Lymphocytes can be found accumulating in the border zone of an infarct by day 1, peaking by day 3 in the photothrombosis and permanent MCAO models in rats (Schroeter et al., 1994; Jander et al., 1998). Blood-borne monocytes/macrophages arrive at the ischemic zone together with the lymphocytes, but persist up to day 14 (Jander et al., 1998). The accumulation of these microvasular leukocytes was originally believed to contribute to local debris removal and scar formation in the infarcted area. However, recent studies show that these cells generate and release highly reactive oxygen species (free radicals) (Huang et al., 2006). Their toxic enzymes such as myeloperoxidase have been shown to degrade components of the basal lamina and to contribute to the neuroinflammatory response. As well they directly release inflammatory mediators, such as IL-1ß, TNF-α and CINC, which contribute to irreversible infarction (Huang et al., 2006).

In summary, brain ischemia produces a well-defined gliotic response, which involves several cell types. The activation, proliferation and hypertrophy of these cells are the hallmark of this reaction. The primary goal of this response is to destroy and clear up damaged cells, tissue and foreign substances, to mediate repair by restoring blood supply, re-establishing the integrity of the blood-brain barrier and promoting homeostasis in and around the injury. However, activated microglia / macrophages, neutrophils, and astrocytes can release many toxic substances, such as cytokines. They contribute to the disruption of the BBB and the resulting edema, and release cytokines, which contribute to the inflammation and secondary damage following brain ischemia

(Barone and Feuerstein 1999). Indeed, it seems there is a close relationship between inflammation and gliosis since gliosis can be induced by cytokines (Barone and Feuerstein 1999). Activated glial cells then secrete cytokines, which in turn contribute to CNS inflammation and gliosis.

1.3 Potential Treatments for Stroke Therapy

In the past, neuroprotection has been the only goal of basic scientists and clinical investigators. Neuroprotection, a therapeutic intervention, is designed to target the acute events triggered by focal perfusion deficits in the brain. This strategy would reduce the volume of cerebral infarction, which would in turn reduce functional deficits. However, the recent discovery of neural stem cells/multipotent precursors and continuous neurogenesis in the adult brain, has revolutionized the view of brain plasticity and has suggested new therapeutic strategies for degenerative CNS disorders and cerebral ischemia. From a therapeutic point of view, the recruitment of adult intrinsic stem cells for structural brain repair or the activation and expansion of isolated adult stem cells will be of great importance. Therefore, current experimental studies of stroke therapy in animals have focused on two aspects:

1. Neuroprotection: targeting the acute events triggered by the focal perfusion deficits in brain, to reduce brain damage and create a better outcome (Romero et al., 2006).

2. Regeneration: targeting the chronic events and aspects of neuronal plasticity and regeneration to improve recovery (Smith, 2004).

1.3.1 Targeting Neuroprotection to Improve Outcome

With the better understanding of the complex cascade of brain damage after ischemia, a greater number of neuroprotective interventions targeting different pathological elements have been tested and developed in animal models of stroke. These various interventions include calcium channel blockers, anti-excitotoxic substances (such as a variety of glutamate receptor antagonists), free radical scavengers, anti-apoptotic drugs and anti-inflammatory agents (Liebeskind and Kasner, 2001; Turley et al., 2005). Unfortunately, clinical trials for most of these approaches have not proven

safe or did not show improved stroke outcomes, despite repeated successes in animal trials. One of the possible causes for this discrepancy between the animal studies and clinical tests is that the windows for the treatment were set too late to target the desired molecular pathways (Hossmann, 2006). For instance, the increased glutamate level after injury lasts only for 10-30 min and most of the damage related to its excitoxicity may occur within the first 60 min (Ikonomidou and Turski, 2002). After that, glutamate may serve in a neuroprotective and a regenerative function (Ikonomidou and Turski, 2002). Calcium levels plateau within minutes of the onset of damage, and in most of the animal studies, calcium channel blockade was started within 1 hour of ischemic onset (Horn and Limburg, 2001). Therefore, by the time patients are available for treatment damage caused by these mechanisms might be largely completed.

Unlike these early events leading to damage, post-ischemic inflammation evolves within hours and lasts for several days. It is a dynamic process, potentially providing a longer therapeutic window. Immediate early response genes are expressed within 2 h and inflammatory cytokines, chemokines and adhesion molecules are produced, inducing the leukocyte accumulation and migration as well as microglia activation (Hossmann, 2006). Glia scarring and tissue remodeling are followed and associated with healing of infarct tissue. As an essential component of pathological mechanisms responsible for ischemic stroke, inflammation may also contribute to the secondary brain damage following ischemia, as well as being a potential cause for the exacerbation of ischemic brain injury. In addition, inflammatory mechanisms are not fundamental for physiological brain functions. Thus interference with these secondary responses may not result in intolerable side effects (Barone and Feuerstein, 1999). Therefore, post–ischemic inflammation is a promising target for therapeutic intervention in ischemic stroke. The inflammation reaction is an attractive pharmacologic opportunity, considering its rapid initiation and progression over many hours after stroke and its contribution to the evolution of tissue injury. Therefore, inflammation provides a much longer therapeutic window and it is more practical to design effective therapeutic interventions targeting the inflammation pathway. One might therefore expect a reasonable probability for this intervention to be successful in the treatment of the stroke patient. Since the cellular components of inflammation have already been reviewed in

the gliosis section, the major molecular elements that trigger and promulgate inflammatory signals will now be reviewed, since these signals may provide the targets for therapeutic intervention. Experimental attempts have explored the possible beneficial effects of pharmacologic manipulation of certain inflammatory elements. The effects of minocycline, an antibiotic exhibiting an anti-inflammatory ability in CNS injury and experimental ischemic models, will also be reviewed.

1.3.1.1 Brain Inflammatory Response to Ischemia: a Potential Therapeutic Opportunity

Focal cerebral ischemia causes a strong inflammatory response involving a complex set of interactions between vascular structures and inflammatory cells (Stoll et al., 1998). The vascular endothelium promotes inflammation through the up-regulation of adhesion molecules such as ICAM, E-selectin, and P-selectin that bind to circulating leukocytes and facilitate their migration into the CNS. At the same time, pro-inflammatory cytokines act directly on endothelial cells causing increased BBB permeability and activation of intracellular adhesion molecules, such as ICAM-1, P-selectin, and E-selectin (Danton and Dietrich, 2003). This helps the circulating leukocytes migrate into the damaged tissue. These peripheral inflammatory cells include neutrophils, T- lymphocytes and mononuclear phagocytes. Microglia, the resident brain inflammatory cells (reviewed in the gliosis section), are activated early in response to ischemic insults, producing pro-inflammatory cytokines (Danton and Dietrich, 2003; Huang et al., 2006).

Post-ischemic inflammation exerts its influence primarily through a complex cytokine network. Often cytokines are divided into pro- and anti-inflammatory mediators based on their ability to promote or suppress immunoactivation. Among them, IL-1ß and TNF-α are the most important and well-studied in mediating the inflammatory reaction. It has been shown in the CNS that activated microglia are the primary cells to produce and release IL-1ß and TNF-α (Arvin et al., 1996; del Zoppo et al., 2000). Neurons, astrocytes and endothelial cells also produce these cytokines (Wang and Shuaib, 2002). Increased IL-1ß and TNFα mRNA and protein levels have been found in both focal and global ischemia (Wang and Shuaib, 2002). IL-1ß and TNF-α are involved

in different aspects of post-ischemic inflammation. IL-1ß can induce gene expression of phospholipases A2, iNOS and cyclooxygenase-2 (COX2), which leads to the production of the potent pro-inflammatory mediators prostaglandins (PG) and NO, thus furthering the neuroinflammatory cascade (Wang and Shuaib, 2002). TNF-α has been shown to increase BBB permeability and facilitate the entry of peripheral inflammatory cells into the brain (Pan et al., 1997) and may also contribute to the prolonged activation of microglia in an autocrine fashion (Kuno et al., 2005).

Recent studies have shown that several transcription factors, such as nuclear factor (NF-κB), hypoxia-inducible factor-1 (HIF-1), interferon regulatory factor-1, and signal transducers and activators of transcription (STATs) are activated by hypoxia. These factors activate TNF-α and interleukin-1β (IL-1β) within 2 h after the onset of ischemia. These cytokines activate glial cells, which then produce more cytokines, such as TNF-α, IL-1β and IFN-α. NF-κB was also shown to be involved in the production of iNOS and COX-2, which are important inflammatory mediators (Huang et al., 2006).

Experimental attempts have therefore been made to diminish certain inflammatory elements in order to block the inflammatory response and explore the possible beneficial effects after focal ischemia. These strategies include anti-leukocyte infiltration, cytokine inhibition and anti-adhesion molecules (Danton and Dietrich, 2003; Zheng and Yenari, 2004). Recent experiments showed that minocycline, an antibiotic, has the potential to inhibit inflammatory pathways and therefore exert neuroprotective effects in different CNS injuries (Danton and Dietrich, 2003).

1.3.1.2 Minocycline in CNS Injury

Minocycline is a second generation tetracycline derivative with antimicrobial activity. Recently it has been shown to have neuroprotective properties in animal models of acute CNS injury and neurological diseases, including brain ischemia (Yrjanheikki et al., 1998; Yrjanheikki et al., 1999), spinal cord injury (Lee et al., 2003; Wells et al., 2003; Teng et al., 2004), traumatic injury (Sanchez Mejia et al., 2001), Huntington's disease (Chen et al., 2000), Parkinson's disease (Du et al., 2001), and amyotrophic lateral sclerosis (ALS) (Zhu et al., 2002). Most of the evidence suggests that the neuroprotective effect of minocycline is associated with inhibition of iNOS as well as

IL-1β converting enzyme (ICE) expression, thereby preventing IL-1β formation following injury (Yrjanheikki et al., 1998; Chen et al., 2000; Du et al., 2001). Minocycline treatment also reduces expression of the matrix metalloproteinases (MMPs), which are involved in the breakdown of the blood-brain barrier and subsequent infiltration of inflammatory cells into the brain (Brundula et al., 2002; Koistinaho et al., 2005). In addition to anti-inflammatory effects, minocycline can also modulate neuronal cell death by a direct interaction with the apoptotic machinery, possibly acting on caspase-dependent and –independent cell death mechanisms (Chen et al., 2000; Zhu et al., 2002; Wang et al., 2003).

However, these encouraging results were not found in all studies. Lately, several studies found that minocycline lacks a beneficial effect or may even have detrimental effects. This was shown for Huntington's disease (Diguet et al., 2003; Smith et al., 2003), Parkinson's disease (Yang et al., 2003; Diguet et al., 2004b), hypoxic-ischemic brain injury (Tsuji et al., 2004) and spinal cord injury (Zang and Cheema, 2003). It has even been suggested that many negative effects were never reported and therefore the record of minocycline may be more questionable than the literature suggests (Diguet et al., 2004a).

With regards to stroke, minocycline showed beneficial effects in different animal models of global ischemia (Yrjanheikki et al., 1998; Yrjanheikki et al., 1999), transient and permanent focal cerebral ischemia (Yrjanheikki et al., 1999; Xu et al., 2004; Koistinaho et al., 2005) and hypoxic-ischemic brain injury in neonatal rats (Yrjanheikki et al., 1999; Arvin et al., 2002; Fox et al., 2005). However, Tsuji et al. (2004) reported that minocycline could exacerbate hypoxic-ischemic brain injury in the developing mouse while providing mild protection in rat pups. Fox et al., (2005) found only a transient protection in rat pups. In a permanent MCAO in adult mice, minocycline treatment started before MCAO reduced the infarct size, whereas treatment initiated after MCAO was not protective (Koistinaho et al., 2005).

Minocycline has been used in humans for decades as an antibiotic, particularly for treatment of acne and more recently has been used in the treatment of rheumatoid arthritis, proving to be safe. The half-life of minocycline in humans is between 16 and 20 hours and it can be administered orally. It penetrates well into the brain and the

cerebrospinal fluid (CSF) and it is well tolerated by patients (Breedveld et al., 1990; Tilley et al., 1995). These characteristics make minocycline an appealing candidate in experimental studies and clinical trials for cerebral ischemia.

1.3.2 Enhancing Adult Neurogenesis to Improve Recovery

Neural cell replacement therapies are based on the premise that neurological function lost to injury or neurodegenerative disease can be improved by introducing new cells to replace the function of the lost neurons. These new neurons could improve the functional recovery of the host by integrating into the existing microcircuitry of the nervous system, therefore replacing lost neuronal circuits. Alternatively, newly introduced cells could constitutively secrete growth factors to support the survival or regeneration of existing neurons (Ferretti, 2004; Lindvall et al., 2004; Lindvall and Kokaia, 2006).

That continuous neurogenesis exists in the adult mammalian brain has been well accepted now. As well, there is recent documentation of increased endogenous neurogenesis in the adult mammalian brain after various brain injuries. This opens up the possibility to manipulate endogenous multipotent precursors *in situ* to replace lost or damaged neurons. Manipulation of endogenous precursors may have advantages over transplantation-based approaches as there is no need for external sources of cells, which are normally derived from either embryonic tissue or non-human species (Emsley et al., 2005). In fact, neurogenesis has been documented in several focal ischemic models. However, the number of spontaneously regenerating neurons detected so far is low. Recent evidence of spontaneous neurogenesis, angiogenesis and synaptogenesis distant from the ischemic lesion points to a remodeling of the surviving tissue that may promote post-lesional brain plasticity (Roitberg, 2004). Understanding these processes may unveil hitherto unknown mechanisms that may become targets of future therapeutic interventions. However, the mechanisms underlying the beneficial effects of these therapies have not been fully investigated. Understanding endogenous neurogenesis after stroke may provide insights into enhancement of functional improvements. The following sections review research of normally occurring neurogenesis, findings from

experiments demonstrating endogenous neurogenesis after experimental focal ischemia, and finally, experiments regarding neocortical neurogenesis.

1.3.2.1 Neurogenesis in the Adult Brain

The consensus definition of neural stem cells (NSCs) remains controversial. In this thesis, the terms, "NSC", "progenitors", and "precursor cells" will be defined as recommended by recent reviews (Lledo et al., 2006; Sohur et al., 2006). Neural stem cells are rigorously defined as cells from the nervous system that are capable of self-renewal, proliferation and multipotent differentiation into different neuroectodermal lineages of the CNS, including the multitude of different neuronal and glial subtypes. Multipotent neural progenitors of the adult brain are proliferative cells with limited self-renewal that can differentiate into at least two different cell lineages. CNS stem cells and all progenitors are generally referred to as precursors or precursor cells.

Adult neurogenesis is referred to as a process of generating functional neurons in the adult brain. It is comprised of the entire series of events starting from the proliferation of precursor cells and ending with the functional integration of new mature neurons (Ming and Song, 2005; Lledo et al., 2006; Sohur et al., 2006). The adult brain has long been regarded as a non-regenerating organ. However, the recent development of new techniques for labeling dividing cells, the development of neuron-specific immunocytochemical markers, and confocal microscopy has resulted in the identification of continuous neurogenesis and possible multipotent neural progenitors in many parts of the adult mammalian brain. Contrary to previous beliefs about the adult brain, it is in fact capable of generating new neurons that can integrate into its complex circuitry.

It is now well established and accepted that active neurogenesis in the normal adult rodent brain is not widespread, but is largely restricted to the two germinal areas, the hippocampal dentate gyrus (DG) and the subventricular zone (SVZ) of the lateral ventricles (Alvarez-Buylla and Lim, 2004; Lledo et al., 2006). The new neurons are found in the olfactory bulb (OB) and granule cell layer of the DG. They are derived from the neural stem cells residing in the SVZ and the subgranular zone (SGZ) of the DG, respectively. Neurons are generated continuously in the SVZ and migrate through the

rostral migratory stream [RMS] in the OB where they differentiate into interneurons. In the DG of the hippocampus, new granule neurons remain near their site of generation and become incorporated into the DG cell layer (Taupin, 2006a). The present study focuses on the neurogenesis in the SVZ-RMS-OB axis.

1.3.2.1.1 Neurogenesis in the SVZ-RMS-OB

The SVZ (in some literature, it is also called subependymal layer/zone) is a remnant of the enlarged perinatal periventricular germinative area. During development, this germinative area narrows to the most rostral part of the lateral ventricle and forms the SVZ, which persists through adulthood (Tramontin et al., 2003). In the perinatal period the SVZ can be subdivided into several anatomical regions. The anterior SVZ (SVZa), which is located rostral to the frontal tip of the lateral ventricle, has been characterized as the major source of the cells in the RMS. The dorsolateral SVZ (SVZdl) is a large pocket of cells situated at the dorsolateral aspect of the lateral ventricle at the level of the anterior commissure that is regarded as a major source of forebrain neuroglia (Brazel et al., 2003). Only neurogenesis in the SVZa persists to adulthood. When retrovirus, bromodeoxyuridine (BrdU) or vital dye is microinjected into the anterior portion of the SVZ of adult rodents, labeled cells migrate through the RMS and are eventually found in the OB. Once reaching the OB, these labeled cells migrate radially and differentiate into olfactory granule neurons and to a much lesser extent, peri-glomerular interneurons (Luskin, 1993; Lois and Alvarez-Buylla, 1994). However, *in vitro*, cells can be isolated from the adult SVZ and expanded in culture to form neurospheres, which generate both neurons and glia (Reynolds and Weiss, 1992; Lois and Alvarez-Buylla, 1993). As such, the SVZ represents an important reservoir for precursors in the adult brain and could potentially provide a useful resource for neurogenerative therapy.

The continuous neurogenesis in the adult SVZ suggests that the neural stem cells/ multipotent progenitors reside in this germinal area. To date, at least four different cell types have been identified in this SVZ-ependymal region: types A, B and C and ependymal cells, which line the lateral ventricle and separate the SVZ from the ventricle cavity (Doetsch et al., 1997). Type A cells are migrating neuroblasts (young migrating

neurons) and they organize as chains in the SVZ and RMS. Type C cells are highly proliferative precursors (fast dividing transient amplifying cells) scattered in small clusters along the chains of migrating neuroblasts (A cells). Type B cells are GFAP and nestin expressing astrocytes. They were named SVZ astrocytes because they express astrocytic intermediate filaments, such as GFAP, vimentin and nestin. Despite the nomenclature of these cells, it is important to distinguish between true astrocytes and GFAP-expressing SVZ cells. It has been reported that the GFAP-expressing astrocytes in the SVZ have a bipolar or unipolar morphology that has significantly fewer processes than true astrocytes. Type B cells form a tube-like structure ensheathing the chains of migrating neuroblasts and they also interact closely with the ependymal cells separating lateral ventricle from the SVZ. Similar to what has been observed in embryonic neural progenitors, type B cells also contain single cilia that extend into the ventricle lumen through the ependymal barrier. Type C cells are the most frequently dividing cells in the SVZ, but both B and A cells also undergo cell division. One hour after a single [^{3}H]-thymidine injection, 52% of the labeled cells in the SVZ were type C cells, 15% are type A, and 12% were type B. The remaining 21% were not identified. Based on the proportions of the different cell types in the SVZ, it seems that type C cells are 10 times more likely to divide than type A or B cells (Doetsch et al., 1999).

The nature of the stem cells in the SVZ has been the subject of controversy for a long time. Two potential sources have been suggested: ependymal cells or GFAP-expressing astrocytes (Chiasson et al., 1999; Doetsch et al., 1999; Johansson et al., 1999). Eventually, this later theory has been confirmed by the work of Alvarez-Buylla and his colleagues (Doetsch et al., 1999). In this paper, they showed that after elimination of immature precursors (type C cells) and neuroblasts by antimitotic treatment, only the SVZ astrocytes were left. This cell type divided to generate immature precursors and neuroblasts. In addition, using a transgenic mouse expressing the receptor for an avian retrovirus under the control of the GFAP promoter, after specifically labeling astrocytes of the SVZ by targeting an avian retrovirus carrying the reporter gene to this region, they found labeled neurons in the OB. They showed that SVZ astrocytes are able to give rise to cells that grow into multipotent neurospheres *in vitro* (Doetsch et al., 1999). Since then, more studies have confirmed that the SVZ GFAP-expressing

astrocytes are the primary progenitors *in vivo* (Imura et al., 2003; Garcia et al., 2004). By employing a transgenic GFAP-TK mouse, which expresses virus thymidine kinase (TK) under mouse GFAP promoter, the authors showed that the new neurons in the OB are depleted after elimination of the GFAP-expressing cells by the antiviral agent ganciclovir. In addition, they used Cre/lox technology and generated GFAP-Cre reporter mice in which all GFAP-expressing cells and their progeny expressed the reporter even if the expression of GFAP and Cre was downregulated (Garcia et al., 2004). Results from these transgenic mice show that all new neurons generated in the adult mouse forebrain are derived from GFAP-expressing cells. Overall, both *in vivo* and *in vitro* evidence shows that GFAP-expressing type B cells function as neural stem cells / multipotent precursor cells. In the adult SVZ, the slowly proliferating GFAP-expressing astrocyte-like cells (type B cells) differentiate to become rapidly dividing immature progenitors (type C cells) and generate migrating neuroblasts (type A cells), which migrate in chains through the RMS to the OB.

Once neuroblasts are born in the SVZ, they migrate along the RMS to their final destination in the OB. This is a 5-8 millimeter distance in the mouse. For a cell that is only 10-30 μm long, this translates into a long distance to migrate within only 2 to 9 days (Doetsch and Alvarez-Buylla, 1996). How do these cells move such a long distance and transverse the dense parenchyma of the adult brain? Neuroblasts in the SVZ of adult rodents, unlike the neuroblasts in the developing cerebellum, cortex, or adult avian telencephalon, use a novel form of neuronal migration, called tangential chain migration. As mentioned above, in adult rodent SVZ and RMS, migrating neuroblasts (A cells) form a long chain and move along each other and are surrounded by a tube-like structure, which is formed by processes from astrocytes (type B) (Lois and Alvarez-Buylla, 1994; Jankovski and Sotelo, 1996). Migrating neuroblasts have elongated morphologies with a leading process tipped by a growth cone (Lois and Alvarez-Buylla, 1994). Chain migration has been demonstrated *in vitro* using explant cultures of the SVZ. In these cultures, neuroblasts escape the explant, assemble as chains and move in incremental steps at an average speed of 120 μm/h by sliding along each other (Wichterle et al., 1997). Constantly using their leading processes to explore the surrounding environment, these cells appear to respond to unidentified signals that trigger the cell

body to move. Chain migration *in vitro* occurs in conditions completely devoid of glial cells.

Neuroblasts are produced in excess by the SVZ and they migrate to the OB, where they arrive 3 to 5 days later. Over the course of the next 10-25 days, they migrate into their proper positions in the OB, mature and become interneurons. More than 30,000 neuroblasts exit the rodent SVZ for the RMS each day (Alvarez-Buylla et al., 2001). Many die, probably during migration, and 50% or more are lost 15 to 45 days after they arrive in the OB (Petreanu and Alvarez-Buylla, 2002). Once the cells reach the core of the OB, they are separated from the chains, migrate radially to more superficial layers (granule cell and external plexiform layers), where they differentiate into the olfactory inhibitory interneurons of two main types, granule neuron and periglomerular neurons. Both type of interneurons lack an axon and instead have reciprocal dendro-dendritic synapses with mitral and tufted cells, modulating the processing of sensory information (Carleton et al., 2003; Lledo et al., 2006).

1.3.2.1.2 Neurogenesis in the DG of the Hippocampus

The neural progenitors in the adult hippocampal dentate gyrus are located in the SGZ of the hippocampus, which is at the border of the hilus and dentate granule cell layer. In the SGZ of the hippocampus, it was also shown that GFAP-expressing SGZ astrocytes are the primary neural precursors (Picard-Riera et al., 2004). These astrocytes with their cell bodies in the SGZ have radial processes going through the granule cell layer and short tangential processes extending along the border of the granule cell layer and hilus. These GFAP- and nestin-expressing astrocytes divide via asymmetric division and give rise to amplifying progenitors that proliferate in clusters and generate DCX+ and PSA-NCAM+ neuroblasts. Over 9,000 neuroblasts are produced per day in young adult rats (Cameron and McKay, 2001). These neuroblasts disperse and migrate a very short distance into the granular cell layer of the DG, where they differentiate into granule neurons. Later, the newly generated DGCs send axonal projections to the CA3 area. During this early postmitotic stage, the new neurons are apparently recruited in a

functional role, or die (Kempermann et al., 2004). The adult-born DGCs are morphologically and electrophysiologically indistinguishable from the existing cells and appear to functionally integrate into the circuitry of the dentate gyrus (Emsley et al., 2005; Lichtenwalner and Parent, 2006). Although the precise functional role of hippocampal neurogenesis in the adult mammalian brain is unknown, it is suggested that the new neurons might play a role in hippocampal-dependent learning and memory (Lledo et al., 2006).

1.3.2.1.3 Neurogenic Potential of the Cortex and other Regions of the Mature Brain

Although ongoing neurogenesis in the adult DG of the hippocampus and OB is widely accepted, whether neurogenesis exists in other brain regions in adulthood remains a topic of debate. Reports of persistent neurogenesis in the cortex can be traced as far back as several decades (Altman, 1963; Kaplan, 1981). Although neural multipotent progenitors have been isolated from the cortex (Palmer et al., 1999), it is still very controversial whether neurogenesis persists *in vivo* in the neocortex of the adult mammalian brain (Lichtenwalner and Parent, 2006). A research group claimed the existence of an extremely low level of neurogenesis in the neocortex of the adult primate (Gould et al., 1999). Later on, this group modified their interpretation by stating that the existence of these neurons was only transient (Gould et al., 2001). However, other groups disputed these results primarily on methodological grounds (Kornack and Rakic, 2001; Koketsu et al., 2003), and a recent study suggested there is no neurogenesis in the neocortex of adult human brain (Bhardwaj et al., 2006).

In addition, there are some reports of the production of new neurons in the adult amygdala (Bernier et al., 2002), substantia nigra (Zhao et al., 2003), dorsal vagal complex of the adult brainstem (Bauer et al., 2005), primary visual cortex (Kaplan, 1981), spinal cord (Yamamoto et al., 2001) and striatum (Dayer et al., 2005). These reports suggest that the existence of low-level neurogenesis in the adult mammalian brain might be a widespread phenomenon. However, some of these results have been disputed (Cooper and Isacson, 2004; Frielingsdorf et al., 2004).

In vitro results suggest that neural progenitor cells may also reside in other regions of the adult brain (Gottlieb, 2002). Multipotent neural progenitors have now

been isolated from various non-neurogenic regions of the adult mammalian CNS, such as spinal cord (Weiss et al., 1996; Shihabuddin et al., 1997), striatum (Reynolds and Weiss, 1992; Palmer et al., 1995), optic nerve (Palmer et al., 1999), retina (Tropepe et al., 2000), corpus callosum (Kondo and Raff, 2000), septum (Palmer et al., 1995) and hypothalamus (Lie et al., 2002). When cultured in the appropriate media, these cells have been shown to have multilineage potency and self-renewing ability. When exposed to high concentrations of mitogens, such as FGF-2 and / or EGF in serum-free medium, isolated precursor cells proliferate. After withdrawing the mitogen or exposing the cells to instructive factors, these cells promptly differentiate into three main cell types of the CNS; neurons, astrocytes and oligodendrocytes *in vitro* (Gage, 2000). It has to be pointed out that although these studies contribute useful information, one should not forget that cell culture systems are highly artificial in many respects and do not reproduce *in situ* conditions very well (Sohur et al., 2006). *In vivo*, precursor cells are accompanied by other cells and their microenvironment is inseparable from their inherent properties.

These *in vivo* and *in vitro* studies suggest that multipotent neural progenitors may be present throughout the adult CNS and their neuronal differentiation could be influenced by their local environment. The nature of the signals and factors that promote neuronal differentiation of these precursors is still unknown.

1.3.2.1.4 Neurogenesis in Adult Human and Nonhuman Primates

Dentate granule cells (DGCs) continue to be generated throughout life in adult human and nonhuman primates. Several groups have shown neuronal birth in the dentate gyrus of monkeys by showing that cells incorporating the S-phase markers tritiated thymidine or BrdU differentiate into neurons several weeks later (Kornack and Rakic, 1999). In the human dentate gyrus, new DGCs continue to be generated even as late as the seventh or eighth decade of life (Eriksson et al., 1998).

Neuronal production also appears to continue in the adult SVZ-olfactory bulb pathway of primates (Kornack and Rakic, 2001). The adult primate SVZ underlies the ventral and lateral walls of the lateral ventricle. SVZ neuroblasts migrate in the RMS as a thick chain surrounded by an astrocytic net (Pencea et al., 2001a). Neurospheres can be

generated from the adult human subependymal zone of the lateral ventricle. Similarly to rodents, these adult human neurospheres give rise to functional neurons and glia (Westerlund et al., 2003). Chain migration of neuroblasts away from the lateral ventricles is not apparent in the human adult brain (Sanai et al., 2004). It has also been suggested that similar migrations may occur in the infant human brain (Weickert et al., 2000). Evidence suggests, however, that new neurons are added to the adult human olfactory bulb (Bedard and Parent, 2004) and their source therefore is uncertain. By utilizing the ^{14}C integration and BrdU techniques, a recent study suggested no neocortical neurogenesis exists in the adult human brain. The neurons in the human neocortex are generated perinatally, but not generated in adulthood at detectable levels (Bhardwaj et al., 2006).

1.3.2.2 Post-stroke Neurogenesis

The presence of ongoing neurogenesis and multipotent neural progenitors in the mature forebrain raises the question: Could these precursor cells serve as an endogenous source for replacement after neural loss associated with brain injury? Several investigations have found increased cell proliferation and neurogenesis in the adult rodent forebrain SVZ after various forms of injury, such as cortical aspiration (Szele and Chesselet, 1996), inflammatory demyelination (Calza et al., 1998) and focal ischemia (Jin et al., 2001; Zhang et al., 2001). The increased neurogenesis in the SGZ has also been demonstrated in different experimental stroke models, such as transient global ischemia in the gerbil (Liu et al., 1998), mouse (Takagi et al., 1999), rat (Yagita et al., 2001) and in the rat MCAO model of focal ischemia (Arvidsson et al., 2001; Dempsey et al., 2003). With regards to stroke, it has been found that cerebral ischemia enhances not only neurogenesis in the SVZ and SGZ, the neurogenic areas of adult brain, but also the non-neurogenic areas such as striatum, cortex and hippocampus. Newborn neurons have also been observed in the ipsilateral striatum (Arvidsson et al., 2002), neocortex (Jiang et al., 2001), in animal models of MCAO and in the degenerated hippocampal CA1 (Nakatomi et al., 2002). Some studies suggest that a small portion of these newly generated neurons is functionally integrated in the circuits (Chen et al., 2004). These data highlight the potential of endogenous precursors for cellular therapy. Understanding

of the contribution and mechanisms of stroke-induced neurogenesis to the pathophysiology of cerebral strokes will allow significant advances in the understanding of cerebral strokes, and their therapy.

To study neurogenesis, BrdU is often used as a marker for dividing cells. BrdU, a thymidine analog that is incorporated into the DNA of dividing cells during S-phase, labels dividing cells and passes the label on to the progeny. BrdU can be detected by immunocytochemistry and can be combined with double or triple labeling with the neuron-specific markers. It therefore allows the detection of newly generated neurons. The first evidence of regenerative neurogenesis was reported in the neocortex by Magavi et al., (2000). They used a biophysical approach to induce synchronous apoptotic degeneration of corticothalamic neurons in layer VI of the anterior cortex of adult mice. Importantly, other cells in the regions surrounding those neurons targeted for death were not injured. Using BrdU as well as phenotype specific markers of progressive neuronal differentiation, they found that newborn cells (BrdU+) progressively developed expression of the mature neuronal marker NeuN, and survived to at least 28 weeks. Two weeks after injury, they also found subsets of BrdU+ cells with morphology of migratory neuroblasts expressing doublecortin (DCX), a protein found exclusively in migrating neurons, and Hu, an early neuronal marker. A subset of these newly generated mature BrdU+ and NeuN+ positive neurons were also able to form appropriate long-distance thalamic projections as shown with the retrograde label FluoroGold. Where do these new-born neurons originate? Although there are no detailed studies of the exact locations of the endogenous precursors, in this paper (Magavi et al., 2000) the authors suggested two potentially co-existing sources: the main source appeared to originate in the SVZ, whereas a small source appeared to be precursors resident within the cortex itself. More recently, the same group modified the location of targeted cell death to the corticospinal motor neurons in Layer V of the motor cortex in adult mice (Chen et al., 2004). They found that BrdU+/DCX+ cells, adopted the morphology typical of migrating neurons in the developing brain. These cells are located only in or under the corpus callosum and cortical layers VI and V undergoing targeted CSMN degeneration. Later, BrdU+ newborn cells expressed the early neuronal marker Hu. NeuN, a mature neuronal marker, was expressed within 2 to 4 weeks in the same region

where BrdU+/DCX+ cells were found. These newborn neurons survived for at least 56 weeks and a portion of the new neurons extended axons to the spinal cord and formed long-distance corticospinal connections (Chen et al., 2004). When immature neurons or neural precursors were transplanted into this degenerating cortex, they could migrate selectively to the appropriate cortical layer and differentiate into projection neurons, receive afferent synapses, express appropriate neurotransmitters and receptors, and form appropriate long-distance connections to the original contralateral targets of the degenerating neurons (Snyder et al., 1997; Sheen et al., 1999).

Taken together, these results demonstrate that endogenous neural precursors can be induced *in situ* to differentiate into cortical neurons, survive for many months and form appropriate long-distance connections in the adult mammalian brain and the microenvironment plays a very important role in influencing the potential of neural precursors (Sohur et al., 2006). However, it seems the production and integration of these newborn neurons are relatively low and the functional consequences of this neurogensis after this specific injury remain to be determined. Moreover, it is possible that the adult cortex undergoes targeted apoptotic degeneration of projection neurons and forms an instructive environment for guiding the differentiation of neural precursors. This lesion might have only destroyed the targeted neurons without inducing inflammatory responses, gliosis, or activated cytokine-release stage microglia (Sheen and Macklis, 1994; Wang et al., 1998b). Ischemic injury is a more complicated process than the targeted apoptotic model system.

Accumulating evidence suggests that ischemic injury can induce neurogenesis in the hippocampus and striatum, and possibly neocortex as well. This section will focus on the recent studies addressing the response to ischemia and whether neuronal replacement from endogenous precursors occurs in regions of the adult brain that do not normally undergo neurogenesis. This includes the neocortex, striatum and hippocampal CA1 area following focal ischemia.

1.3.2.2.1 Post-stroke Neurogenesis in the Hippocampal Formation

Increased neurogenesis in the SGZ has been demonstrated in different experimental stroke models, such as the transient global ischemic model of the gerbil

(Liu et al., 1998), mouse (Takagi et al., 1999) and rat (Yagita et al., 2001), and the rat MCAO model of focal ischemia (Arvidsson et al., 2001; Dempsey et al., 2003). These studies provide no evidence of neuronal replacement of dead neurons in the lesioned region, such as CA1. However, recent studies showed that new neurons are found at the sites of the lesioned area after transient global ischemia, such as the CA1 area of the hippocampus. Nakatomi et al. (2002) reported a modest regeneration of CA1 pyramidal neurons (BrdU+ cells co-expressing neuronal markers such as Hu, NeuN, and ßIII -tubulin) within 4 weeks after a transient global ischemic model, induced by transient four-vessel occlusion and systemic hypotension in adult rats. Intraventricular infusion of epidermal growth factor and FGF-2 during the first week after global ischemia leads to a remarkable increase of regeneration in damaged CA1 neurons. These neurons differentiate into electrophysiologically functional neurons with the morphological characteristics of pyramidal cells and integrate into existing brain circuitry, contributing to the amelioration of the special learning deficits caused by global ischemia. Cell tracing studies using retrovirus and DiI labeling revealed that the newly generated neurons in the CA1 area might arise from the progenitors that reside in both the posterior periventricular region near the hippocampus and hippocampal parenchyma. Neurogenesis in the hippocampal pyramidal cells has also been reported in an adult gerbil model of transient global ischemia (Schmidt and Reymann, 2002). However, other studies in the gerbil model have not found CA1 neuron regeneration (Liu et al., 1998).

1.3.2.2.2 Post-stroke Neurogenesis in the Striatum

Neurogenesis in the ipsilateral striatum has been reported in animal models using MCAO in both rats and mice (Arvidsson et al., 2002; Parent et al., 2002; Jin et al., 2003; Zhang et al., 2004; Nygren et al., 2006b; Yamashita et al., 2006). At around 2 weeks after injury, migrating neuroblasts / immature neurons were observed in the striatum as indicated by the expression of neuronal cell lineage markers such as DCX and / or βIII-tubulin. Some of these cells also co-labeled with BrdU. This indicates that they are newly generated (Arvidsson et al., 2002; Parent et al., 2002). Almost all of the DCX expressing cells after stroke in the striatum also expressed βIII-tubulin (Yamashita et al.,

2006), the marker Meis2, and Pbx proteins, which are normally expressed within developing striatal medium-sized spiny neurons (Toresson et al., 2000; Arvidsson et al., 2002). A small percentage of DCX+ cells also expressed the mature neuronal marker NeuN (Arvidsson et al., 2002; Jin et al., 2003). At weeks 5-6 after a stroke, the new neurons had the typical morphology of mature neurons and expressed NeuN as well as mature striatal medium-sized spiny neuron markers, such as DARPP-32 and calbindin. They were found in the damaged area and in the unaffected medial striatum (Arvidsson et al., 2002; Parent et al., 2002; Yamashita et al., 2006). Months later, although some of the newly generated neurons die through caspase mediated apoptosis, a subset of these newborn neurons were found to form synapses with neighboring striatal cells in the damaged striatum (Thored et al., 2006; Yamashita et al., 2006). Thus, the new neurons differentiate into the phenotype of most of the neurons that were destroyed by the ischemic lesion. These data strongly suggest that the endogenous precursor cells can be induced to differentiate into functional mature neurons and can replace some of the damaged neurons.

There are two possible sources for the newly generated neurons in the ischemic striatum after MCAO. The first possible source is the SVZ, as the neuroblasts born in this location might migrate toward the ischemic striatum. DCX+ cells forming chain-like structures extending from the SVZ toward the ischemic striatum were observed (Jin et al., 2003; Zhang et al., 2004). This migratory appearance is similar to the normal RMS chain migration of SVZ neuroblasts to the OB. These chains were closely associated with thin astrocytic processes and blood vessels (Yamashita et al., 2006). The second possible source is the striatal parenchyma, because it also contains latent progenitors that can be activated and become neurogenic when stimulated by neurotrophic factors (Palmer et al., 1995; Pencea et al., 2001b). Using the Cre-loxP recombination system, which enables region-specific cell labeling and long-term tracing, Yamashita et al. (2006) confirmed that the SVZ cells were the primary source of this newly generated striatal neurons after MCAO. Furthermore, using the cell-type-specific viral infection method, which only labels SVZ GFAP-expressing cells, they confirmed that SVZ GFAP-expressing cells are the primary source of striatal neurogenesis after MCAO.

1.3.2.2.3 Post-stroke Neurogenesis in the Cortex

As mentioned above, cortical neurogenesis can be induced in the injured adult neocortex by targeting apoptotic degeneration (Magavi et al., 2000; Chen et al., 2004). However, this lesion is very different from ischemic injury because it only destroyed the targeted neurons without induction of gliosis. Whether neurogenesis can still occur after a stroke that has caused extensive cortical damage is not clear. Although the MCAO induced excessive injury in both the striatum and cerebral cortex, the reports of whether neurogenesis in the peri-infarct cortex occurs, are not consistent. It has been shown in a cortical reversible photothrombotic stroke model that a small subset of dividing and BrdU+ cells co-expressed the neuronal markers Map-2 and NeuN in the peri-infarct area, and was distributed randomly in the cortical layers II-VI (Gu et al., 2000). Later on, the same group reported the presence of double-labeled cells by BrdU and other neuron-specific markers, Map-2, β-tubulin III, and NeuN in the peri-infarct of both damaged cerebral cortex and striatum after tMCAO (Jiang et al., 2001). A similar presence of immature neurons in the cortex after MCAO was reported (Jin et al., 2003). This cell-tracking study using the lipophilic carbocyanine tracer DiI suggests that the SVZ cells migrate via the lateral cortical stream into the penumbra of the ischemic cortex and striatum. However, four other studies (Arvidsson et al., 2002; Parent et al., 2002; Zhang et al., 2004; Yamashita et al., 2006), did not detect any BrdU+ cells co-labeled with neuronal markers in the injured cortex following MCAO despite their appearance in the striatum. In an irreversible ischemic cortical injury, induced by thermocoagulation of pial blood vessels, cells expressing DCX, a protein exclusively expressed by migrating neuroblasts and immature neurons, were present in the striatum and corpus callosum but not in the peri-infarct cortex 5 days after initiation of the injury. Furthermore, one month later, no BrdU+ cells expressing NeuN were detected in any region. These results suggest that new neurons do not form or survive in the neocortex under this experimental condition. A recent study has reported a substantial production of new neurons in response to a cortical focal ischemic injury. One week after a cortical ischemic injury, more than 10,000 neuroblasts (DCX+) cells per animal were present in the peri-infarct neocortex. Three months later, it seemed that around 10% of these neuroblasts survived and differentiated into mature neurons in the peri-infarct area as

suggested by the number of BrdU+/NeuN+ cells (Ohab et al., 2006; Tsai et al., 2006). Using genetic and viral labeling methods, the authors showed that cortical ischemic injury induced the production of new neurons from the SVZ via GFAP-expressing cells and migration of these newborn neurons into a unique neurovascular niche in peri-infarct cortex (Ohab et al., 2006; Tsai et al., 2006).

Taken together, these results suggest that endogenous neural precursors are potentially capable of being recruited and induced to differentiate into cortical neurons in the ischemically damaged cortex, but only if the instructions or survival cues necessary for neurogenesis are present and are not suppressed. Elucidation of the appropriate signals necessary for neuronal differentiation or survival could enable CNS repair after stroke.

1.4 Animal Models of Focal Ischemia

To understand the pathogenesis of stroke and to evaluate preventive or therapeutic strategies, experimental animal models of focal and global ischemia have been developed in many different species, both small and large (e.g., mice, rats, gerbil, cats and primates). Rodent models are most commonly used due to their low cost, easy maintenance and reproduction, and close resemblance to higher species (Traystman, 2003). Although many animal stroke models have been developed, however, there is no one perfect model which alone is able to mimic human stroke conditions. This is because of the diversity of human stroke in terms of the cause, manifestation and anatomic sites of the ischemic lesion (Traystman, 2003).

Animal models of cerebral ischemia are divided into global and focal. Essentially, cerebral ischemia in both focal and global models consists of the reduction of oxygen and glucose supply to brain tissue. Global ischemia occurs when cerebral blood flow is reduced throughout most or all of the brain, whereas focal ischemia is represented by a reduction in blood flow to a very distinct, specific brain region (Ginsberg and Busto, 1989). An important variable affecting stroke outcome is the presence or absence of reperfusion following an ischemic event. Reperfusion occurs in a substantial proportion of human stroke patients, due to spontaneous early clot lysis, collateralization or clinical intervention, such as tPA treatment (Richard Green et al.,

2003). Accordingly, there are two basic classes of the experimental focal ischemic model: reversible (transient) and permanent. In permanent focal ischemia, the arterial blockage is maintained permanently throughout the experiment, whereas in transient focal models, vessels are blocked temporarily, usually from 1 to 3 h, to mimic the prolonged reperfusion in clinical settings (Aronowski and Labiche, 2003). It appears that early reperfusion after a stroke is beneficial and capable of reversing the majority of ischemic dysfunctions, whereas, in some instances, late reperfusion may contrarily trigger deleterious processes and lead to more ischemic damage (Aronowski and Labiche, 2003; Schaller and Graf, 2004).

The most commonly used focal ischemia models often involve permanent or temporary occlusion of the middle cerebral artery and are widely used to mimic the human stroke condition of large artery occlusion (Ginsberg and Busto, 1989). MCA supplies the basal ganglia, internal capsule and the lateral surface of the cerebral cortex (Aronowski and Labiche, 2003) and 25% of first-time human ischemic strokes involve infarcts in the MCA territory (McAuley, 1995; Richard Green et al., 2003). Therefore, the MCAO model has great relevance for human ischemic stroke. Different occlusion sites and techniques are therefore used and there are many versions of MCAO models, such as: proximal MCAO model (Tamura model); intravascular thread model (Koizumi model); distal MCAO with bilateral common carotid artery occlusion model (Chen model); and photothrombosis model (Watson model). To obtain reproducibility of flow reduction and lesion size in MCAO, two principal occlusion sites are used: proximal and distal. Proximal MCAO leads to an extensive infarction of the basal ganglia and the neocortex, whereas a more distal occlusion leads to a smaller infarct, including neocortical infarction only (McAuley, 1995). Permanent occlusion can be obtained by microsurgical coagulation, by introducing an embolism or by insertion of an intraluminal suture (Windle et al., 2006). If the thread is withdrawn, conditions of reversible reperfusion are mimicked. Transient MCAO can also be induced by injection of endothelin-1 (ET-1) (Robinson et al., 1990). MCAO models produce a substantial amount of injury in many different brain regions but do not normally affect the motor cortex. These models mimic large artery occlusion in humans (Carmichael, 2005).

Human strokes are mostly small in size (Carmichael, 2005) and can occur as end-arteriolar or small vessel occlusion (McAuley, 1995). In rodents, small-size infarction of the motorsensory cortex has been induced by different techniques, such as photothrombosis, ET-1 injection, or devascularization. Each model has its own advantages and disadvantages. Photothrombosis induces small vessel occlusion and is achieved by systematic injection of Rose-Bengal or other photosensitive dyes. Focal illumination of the targeted brain area through the intact skull leads to platelet aggregation with formation of clots and thrombotic occlusion of small intracerebral vessels (Watson et al., 1985; Dietrich et al., 1987a). The advantages of this model are the small size of infarcts, the ability to place the infarct within distinct functional subdivisions of the cortex and the minimal surgical manipulation of the animal. However, it was shown that Rose Bengal interferes with glutamate transport, which somewhat invalidates this model (Ogita et al., 2001). Another technique to induce ischemic cortical infarct is the use of ET-1, which is a potent and long-acting venous and arterial vasoconstrictor (Macrae et al., 1993; Reid et al., 1995). Intracortical injection or topical application of ET-1 produces a local dose-dependent well-defined ischemic lesion (Hughes et al., 2003). However a variation of this model used by other groups produced injuries that varied in size (Adkins-Muir and Jones, 2003) or no dose-dependency at all (Windle et al., 2006). The optimal placement of the ET-1 dosage for a reproducible cortical infarct and for sensorimotor deficits has not yet been established. Devascularization of all the cortical pial vessels of an exposed cortical surface is also used to induce cortical injury (Conner et al., 1998; Kolb et al., 2006). All three models have the advantage of providing a precise injury location whereas the photothrombosis model and intracortical injection of ET-1 model require less surgical intervention of the animals. The devascularization model was criticized because mechanical removal of the pial surface vessel might induce mechanical injury.

2. RATIONALE & OBJECTIVES

Animal models of focal ischemia are useful tools in understanding the pathology and treatment of human stroke. Recent developments in the genesis and pathophysiology of experimental stroke in animal models suggest that protection and repair processes ***after*** such an injury should be the major focuses of therapeutic approaches in future stroke (Hossmann, 2006).

Ischemic stroke causes not only localized ischemic cell death in the brain but also triggers a strong inflammatory response, gliosis and a regenerative response in the tissue surrounding the ischemic area core. Post-ischemic inflammation plays an important role in secondary brain damage following stroke. Therefore, anti-inflammatory intervention has been considered important for therapeutic approaches based on neuroprotection. Minocycline, a second generation of tetracycline, has been shown to have neuroprotective effects in different animal models of acute and chronic neurodegenerative disease including stroke, possibly through its anti-inflammatory and anti-apoptotic effects (Yong et al., 2004). Stroke also triggers a regenerative response in the tissue surrounding the area of cell death. Stroke enhances neurogenesis in both neurogenic and non-neurogenic areas. In the rodent brain, post-stroke neurogenesis has been observed in the peri-infarct of striatum (Arvidsson et al., 2002) and/or the cerebral cortex (Ohab et al., 2006) in the MCAO model. SVZ, the biggest pool of neural stem cell/neural progenitors of adult brain, seems to be the principle source of this post-stroke neurogenesis after MCAO (Jin et al., 2003; Yamashita et al., 2006).

In the past, most focal cerebral ischemic investigations have focused on the occlusion of very large blood vessels, such as in the MCAO model. However, small vessel stroke does regularly occur in human stroke and accounts for approximately one third of human strokes (McAuley, 1995; Greenberg, 2006). If only large size animal stroke models are used, this will lead to a potential bias against the clinical situation

(Carmichael, 2005). In this thesis, a rat stroke model was selected, which mimics the human small vessel stroke, and two potential mechanisms, depressing inflammation with minocycline and neurogenesis of endogenous progenitor cells, have been applied to this model.

I hypothesize that targeting the non-neuronal cells in a small-vessel stroke will improve the outcome. The detailed objectives are as follows:

1. To use a modified cortical devascularizing model, pial vessel II occlusion model, and to evaluate its usefulness in novel strategies of neuroprotection.

2. To compare the effectiveness of this irreversible stroke model with another model of focal stroke, but with reversible blood flow obstruction.

3. To assess the potential benefits of minocycline treatment ***after*** such an experimental stroke and analyze its mode of action.

4. To compare the effectiveness with which various tracing techniques label cells migrating out of the SVZ.

5. To examine whether new migrating neuroblasts appear near the lesion.

6. To identify the source of such migrating neuroblasts.

3. MATERIALS AND METHODS

3.1 Animals

Adult male Wistar rats (250g-350g) were used for the Pial vessel II disruption model (PVD II) and Long Evans rats (250g~350g) were used for the topical application of ET-1 model. All the rats were supplied by Charles River Inc. (St. Constant, QC, Canada). After arrival, all animals were housed in cages of two rats each, and were kept for at least 1 week before being used in any procedure. They were exposed to a 12 hour light and dark cycle. Animals had free access to standard food and water. The guidelines of the Canadian Council of Animal Care in conjunction with the University Committee on Animal Care and Supply were followed for all experimental procedures (Protocol identification number 20020024).

3.2 Surgical Procedures

The equipment and surgical area were sterilized in accordance with institutional guidelines. The head of the anesthetized animal was shaved around the surgical area before being mounted in the stereotaxic frame. The scalp was sterilized with povidone iodine twice followed by alcohol.

Two animal models, (topical endothelin-1 application and modified cortical devascularizing model) were used.

3.2.1 Topical Endothelin-1 Application

Long Evans male rats were anesthetized by inhalation of halothane in 100% oxygen using a Boyle anesthetic machine. The induction of anesthesia was obtained by 4~5% halothane inhalation for 5 to 10 minutes in a sealed box. After the loss of response to the pinch test of the hind paws and tail (pedal reflex), the rats were shaved and placed into a stereotaxic apparatus. The anesthesia was maintained by the administration of a

concentration of 1~2% halothane via a nose cone. During the course of the surgery, the halothane level was carefully adjusted to maintain surgical anesthesia as judged by the absence of pedal and tail reflex but presence of proper breathing pattern, heart rate and pink appearance of the paws.

After a midline incision was made on the scalp, a craniotomy was performed on the right hemisphere overlying the M1 region of the cortex using a 5 mm diameter drill trephine centered at 1 mm anterior and 3 mm lateral to the bregma (-1.5 mm to 3.5 mm anterior and 0.5 mm to 5.5 mm lateral to bregma). Cool sterile saline was applied intermittently to prevent overheating from the high-speed drilling. After removing the piece of skull, the dura was carefully removed without damaging any of the cortical surface underneath or the overlying pial vessels. ET-1 (100 pmol/µl in saline) was applied to the exposed cortex in two 5 µl applications separated by an interval of 3 min, using a microsyringe. Three minutes later, another 10 µl was applied and the surface covered immediately with a piece of sterile gelfoam soaked with an additional 10 µl of ET-1. This was intended to slowly release the drug over the exposed cortex. A total of 3,000 pmol ET-1 was applied. The opening in the skull was enclosed with a sheet of Parafilm® glued to the adjoining skull surface. Control animals were subjected to all of the procedures, except that ET-1 was replaced with sterile saline.

3.2.2 Modified cortical devascularizing model (Pial Vessel II Disruption Model)

Adult male Wistar rats were anesthetized with an intraperitoneal injection of a ketamine (125 mg/kg) and xylazine (7 mg/kg) mixture. After surgical anesthesia was achieved, the rats were immobilized in a stereotaxic frame. The craniotomy was performed with a 5 mm diameter drill trephine positioned on the right and rostral side of the bregma adjacent to the coronal and sagittal sutures. Cool sterile saline was applied intermittently to prevent overheating from the high-speed drilling. After removing the dura, the cortical surface and the overlying pial vessels were exposed. Medium-size (class II) pial vessels, but not large ones (class I) (Bar, 1980) were disrupted using

fine-tip forceps (Fine Science Tools). Cool sterile saline was used to prevent bleeding before replacing the bone fragment.

3.2.3 Wound Closure and Postsurgical Care

The scalp was closed with a wound clip and buprenorphine (0.035 mg/kg) was injected subcutaneously for pain management. The body temperature was monitored throughout the surgery by a rectal probe and maintained at 37ºC with a heating pad. Animals were kept in separate cages, one animal per cage under a warm lamp during anesthesia recovery.

3.3 Minocycline Treatment

The minocycline regimen used was chosen based on data obtained from previous stroke studies on acute neuroprotection (Yrjanheikki et al., 1999). Due to the low solubility in saline, minocycline HCl (Sigma) was dissolved in sterile distilled water at a concentration of 15 mg/ml. Minocycline was stirred in distilled H_2O, with heat as needed, until it yielded a clear, yellow to amber solution. The solution was stored at 4°C and protected from light.

Minocycline was given intraperitoneally at a dose of 45 mg/kg 1 hour and 12 hours after lesioning, followed by 22.5 mg/kg, given twice daily until 6 days after lesioning (Yrjanheikki et al., 1999). An equivalent amount of distilled water was used in controls.

3.4 *In Vivo* Labeling of SVZ cells in Adult Rats

To develop a reliable and reproducible method for *in vivo* labeling large amounts of SVZ cells, three methods have been used and tested in the normal and ischemic rat brain.

3.4.1 BrdU Loading

BrdU (5-bromo-2-deoxyuridine), a thymidine analog, is incorporated into newly synthesized DNA thus providing a marker for proliferating cells. BrdU (Sigma) was

administered intraperitoneally daily for two days at the concentration of 100 mg/kg, dissolved in 0.9% NaCl with 0.007 M NaOH. The first injection started 2 days prior to perfusion in the normal animal or prior to the induction of ischemic injury. An antibody directed against BrdU allows the identification of cells that have already incorporated BrdU, thus providing a marker for proliferating cells (see the immunostaining section for the detailed procedure).

3.4.2 Retroviral Vector (RV)

Retroviruses are known to infect predominantly proliferating cells. When such a virus is stereotaxically injected into the lateral ventricle, it will only be taken up by mitotic cells, such as neural precursor cells. The BAG replication-deficient RV was utilized to label proliferating subventricular cells *in vivo* as a non-diluting lineage marker. They carry the Lac-Z gene, which is responsible for coding the enzyme ß-galactosidase into a vector that was derived from the Moloney murine leukemia virus (Price et al., 1987). Briefly, RV was collected from confluent φ 2BAG alpha cells, supplemented with 1 µl/ml polybrene, filtered through a 0.45 mm filter, aliquotted and frozen at -80 ºC. The titer was 2.5 x 10^5 to 2.5 x 10^7 colony forming units. The retrovirus supernatant was kindly provided by Dr. Doucette (Department of Anatomy and Cell Biology, University of Saskatchewan), in whose laboratory all procedures were undertaken.

I injected stereotaxically 2~4µl of RV supernatant into the lateral ventricle in the time period before the pial vessel disruption (AP = -0.7 mm, ML = 1.3 mm from bregma, DV = +4.7 mm from the skull). The injection rate was 0.5µl/min. The animals were sacrificed on day 4, 6 or 14. All the procedures involving handling of the retroviral supernatant were performed in accordance with requirements and standards of the Biosafety Code of the University of Saskatchewan (endorsed by the Board of Governors on March 29, 2001), the Laboratory Biosafety Guidelines (Laboratory Center for Disease Control, Health Protection Branch, Health Canada, Second Edition, 1996), as well as the policies of the Department of Health, Safety and Environment and the Biosafety Advisory Committee of the University of Saskatchewan. Use of the RV in these experiments was covered by Biosafety Permit #ANA-02. All of the *in vitro* work

using the RV was done in a Biosafety Level 2 hood in a designated biohazard room.

3.4.3 Fluorescent Dye

Two neural tracers, DiI and CFSE, were tested for their ability to label migrating cells in the SVZ.

DiI (Molecular Probes), a fluorescent lipophilic tracer, can passively diffuse across the plasma membrane. It fluoresces orange-red when viewed with a TRITC filter. DiI labeling does not appreciably affect cell viability, development, or basic physiological properties (Holmqvist et al., 1992). 2.5~5 µl DiI (0.25% in DMSO) were injected into different brain areas to test for the efficiency of labeling SVZ progenitor cells. 2.5~5 µl DiI was injected into the lateral ventricle (AP = -0.7 mm, ML = 1.3 mm, DV = 4.7 mm from bregma skull) and SVZa at four coordinates (AP = 0 mm, ML = 1.4 mm, D = 4.8 mm from bregma skull; AP = 0 mm, ML = 1.4 mm, D = 4.6 mm from bregma skull; AP = 0.5mm, ML = 1.4, D = 4.8 from bregma skull; AP = 0mm, ML = 1.5, D = 3.3 from bregma dura) lateral and deep. For the labeling in the PVD II rats, DiI was injected right before the induction of the PVD II at an injection rate of 0.5 µl/min. The animals were sacrificed at different survival times, from 2 days to 2 weeks.

Carboxyfluorescein diacetate, succinimidyl ester (CFSE, Molecular Probes) is also a lipophilic dye, which passively diffuses across the plasma membrane. Unlike DiI, CFSE is colorless and nonfluorescent until it is transported into the cells, where its acetate groups are cleaved by intracellular esterases and then it yields highly fluorescent, amine-reactive carboxyfluorescein succinimidyl ester. The succinimidyl ester group of CFSE reacts covalently with intracellular amines, which enable CFSE to be well-retained in the cytoplasm. The fluorescence is inherited by daughter cells after cell division, or cell fusion, and is not transferred to adjacent cells in a population (Li et al., 2003). Due to its instability, CFSE solution (in dimetheylsulfoxide) was made right before the *in vivo* injection. The fluorescein filter set was used to directly visualize CFSE labeled cells. 200 nl of 10 mM CFSE (500*u*g CFSE in 90 µl dimetheylsulfoxide) was injected into SVZa (AP = 0 mm, ML = 1.4 mm, DV = 4.7 mm from bregma skull) at a speed of 0.1 µl/min. For the study of neuroblast migration after the ischemic injury, CFSE was injected either right before the induction of the PVD II or 2, 3 or 5 days after

PVD II. The rats were sacrificed at different survival times, from day 1 to 2 weeks.

3.4.4 Craniotomy and Stereotaxic Injection

Adult, male Wistar rats (270-330g) were anesthetized with ketamine and xylazine as described above. A small midline incision was made to expose the skull and the rats were then placed into the stereotaxic apparatus (Harvard Apparatus, ASI Instruments). The head was stabilized and adjusted with ear bars to obtain a flat skull position. A dremel with a 1 mm drill bit was used to drill a burr hole at the appropriate coordinates without damaging the dura and the underlying cortex.

The stereotaxic injection was done using a 5 µl Hamilton syringe with a 32-gauge needle attached to a microinjector. Three minutes after the needle was placed into the right position, the injection was started and it lasted 2 min. The syringe was left in place for an additional 3 min before a slow withdrawal was initiated to prevent any backflow. The scalp incision was closed with a suture.

3.5 Histology and Immunocytochemistry

3.5.1 FAM Fixed Paraffin-embedded Sectioning

Rats were anesthetized with a ketamine (125 mg/kg) and xylazine (7 mg/kg) mixture as described above. For evaluating the ischemic animal models and assessing the neuroprotective effects of minocyline, FAM (formalin: acetic acid: methanol 1 : 1 : 8) fixed paraffin-embedded sections were used. One, 3, 6, or 21 days after lesioning, rats were intracardially perfused with approximately 300 ml PBS (pH 7.4), followed by 300 ml FAM solution. Brains were then removed and post-fixed in the same fixative overnight at 4°C. Brains were paraffin-embedded and cut into 10 µm thick coronal sections with a microtome. Sections were mounted on 3-amino-propyltriethoxysilane (APS)-coated (silanized) slides, dried at 37°C overnight and stored at room temperature.

3.5.2 4% PFA Fixed-Cryostat Sectioning

FAM-fixed and paraffin-embedded sections were superior in reproducing morphological details of cells and immunostaining with some antigens, such as GFAP. To obtain better antigen preservation and thus to enhance immunostaining, especially for the neurogenesis and migration part of the project, 4% formaldehyde-fixed cryostat sections were used. In brief, rats were intracardially perfused with 1% sodium nitrite in 0.1 M PBS (sodium nitrite dilates blood vessels thereby helping to flush out the blood from the vascular system), followed by cold freshly depolymerized 4% formaldehyde (FA) in 0.1 M PBS (pH 7.4). The brains were removed, post-fixed in 4% FA overnight and then moved into 30% sucrose solution and stored at 4°C before sectioning. Brains were embedded in Tissue-Tek optimal cutting compound (OCT; Sakura Finetek, Torrance, CA), frozen in liquid nitrogen-cooled isopentane and sectioned at 40 µm on a cryostat. Sections are mounted on the slides (Superfrost@ plus, VWR international) and stored at -20°C before labeling.

3.5.3 X-Gal Staining of Tissue Sections

X-Gal staining is used to detect β-galactosidase expression in the RV-infected cells. Nuclear Fast Red was used for high-contrast counterstaining. Tissue sections were incubated in a 0.1% x-Gal solution for 48 hours at 37°C and then submerged in 0.1% Nuclear Fast Red solution containing 5% ammonium sulfate for 2 min. Sections were then rinsed in phosphate buffer, dehydrated and coverslipped with Cytoseal (Richard-Allan Scientific).

3.5.4 Lectin Histochemistry

Lectin histochemistry was used to assess microglial / macrophage activation. B_4-isolectin from *Griffonia simplicifolia* ($GSAB_4$, Sigma) was used, as it specifically binds to alpha-D-galactosyl residues and labels all activation stages of microglia (Streit, 1990). Deparaffinized sections were quenched with 0.3% hydrogen peroxide and pretreated in Citrate buffer (pH 6.0) at 90°C for about 45 minutes. After blocking in 1% bovine serum albumin, sections were incubated with biotin-labeled $GSAB_4$ (10 µg/ml,

Sigma) in 1% bovine serum albumin (BSA) at 4°C overnight (Savchenko et al., 2000). Horseradish peroxidase (HRP)-conjugated streptavidin (1 µg/ml, Jackson Laboratories) was applied for 2 hours at room temperature. TRITC conjugated goat anti-HRP (1:25, Jackson Laboratories) was applied for visualizing the binding site. The nuclei were counterstained with Hoechst (see the following section).

3.5.5 Immunofluorescence Staining

Single and double-label immunofluorescence histochemistry was performed on paraffin-embedded or cryostat sections following a two-step immunofluorescent staining procedure.

The sections were blocked in PBS containing 5% donkey serum and Triton X-100 (0.02% Triton X-100 for 10 µm paraffin-embedded sections; 0.3% Triton X-100 for 40 µm cryostat sections) and incubated with primary antibodies overnight at 4ºC. The following primary antibodies were used: mouse anti-BrdU (1:200; Sigma-Aldrich), guinea pig anti-DCX (1:100, Chemicon), mouse anti-NeuN (1:100, Chemicon), rabbit anti-GFAP (1:100, Sigma) or goat anti-GFAP (1:25, Santa Cruz), rabbit polyclonal antibody against Ki67 (1:200, Novocastra), rabbit polyclonal antibodies against MPO, (1:100, Neo Markers), mouse monoclonal antibody against rat CD3 (1:25, Serotec), mouse monoclonal antibody anti-neuronal class III β-Tubulin (TuJ1 clone, 1:500, Covance), mouse anti-polysialic acid-NCAM IgM (clone 2-2B, 1:300, Chemicon), and mouse anti-NG2 (1:100, Chemicon). Negative controls omitting the primary antibodies were carried out in all experiments for all the secondary antibodies used. After washing in PBS, sections were incubated with secondary antibodies conjugated with fluorescence dyes (TRITC, FITC) at room temperature for 2 h in blocking solution without Triton X100. The secondary antibodies included donkey anti-guinea pig IgG conjugated to TRITC or FITC, donkey anti-mouse IgG conjugated to FITC or TRITC, donkey anti-rabbit IgG conjugated to FITC or TRITC, donkey anti-mouse IgM conjugated to FITC or TRITC and goat anti-mouse IgG conjugated to FITC or TRITC. All secondary antibodies were used at 1:100 or 1:200 dilutions, and were species cross-adsorbed from Jackson Immunoresearch Laboratories (West Grove, PA).

Sections were rinsed three times in PBS and coverslipped with anti-fade mounting medium (Citifluor glycerol/PBS, Marivac). Paraffin-embedded sections went through deparaffinizing and rehydrating steps before the immunostaining procedure was applied. For nuclear counterstain, sections were incubated with Hoechst 33243 (1 µg/ml) for 15 min. They were washed three times in PBS before coverslipping.

Heat-induced antigen retrieval (AR) technique was used in $GSAB_4$ histochemistry and MPO, CD3, DCX and Ki67 immunostaining. This allowed for the retrieval of antigens that had been masked by formalin fixation (Boenisch, 2001). The slides were immersed in citrate buffer (pH 6.0) at 90^{o}C for about 45 minutes to 1 hour. This resulted in a stronger intensity of the immunohistochemical staining.

3.6 Assessment of Lesion Volume and Cystic Cavity

By day 6, the cortical devascularizing lesion was filled with cellular material (mostly macrophages and microglia) and had a distinct border. By day 21 it turned into a fluid-filled cyst with a glia limitans. Thus, a well-demarcated cortical lesion was observed by day 6 and a cystic cavity developed at 21 days. The quantification of the lesion volume was achieved by hematoxylin and eosin (H&E) staining on 6 days post-surgery animals. Every tenth section of a series of 10 µm-thick sections was stained with H&E. The sections were captured by digital camera (Coolsnap fx) mounted on a microscope (Olympus IX71) and the border traced on the electronic image. The lesioned area on each section was computed from the border outline using ImagePro software. The total lesion volume was calculated by summation of the areas multiplied by the interslice distance (100 µm).

The fluid-filled cystic cavity appeared between day 14 and 21. It was evident from the cell-free area encased by a glia limitans (Wang and Walz, 2003; Wang et al., 2004) and did not need any staining in order to be recognizable. As minocycline completely prevented the appearance of such a cell-free space (see Results) and resulted in a cavity space of zero, quantification and statistical analysis was not necessary for the experiments dealing with cavitation.

3.7 Enzyme-linked Immunosorbent Assay for IL-1β

Twenty-four hours following PVD II, the rats were perfused with ice-cold PBS and the ischemic ipsilateral and non-ischemic contralateral cortices were removed, snap frozen in liquid nitrogen and stored at -80°C until assayed. For extraction of proteins, the tissue was homogenized in 250 µl of homogenization buffer consisting of: 50mM Tris-HCl, pH 7.3, 5mM EDTA, 1% protease inhibitor cocktail (Sigma, P8340) for every 50 mg wet weight. The samples were centrifuged at 4^{o}C for 20 min at 13,000 RPM and the supernatant was aliquotted. The IL-1β protein concentrations in rat brain tissue homogenates were quantified using ELISA Duoset kits (R&D Systems). Initial studies showed that IL-1β recovery from brain tissue spiked with known concentrations of IL-1β was in the range of 85%-120%. Tissue extracts (100 µl) were applied to each well for the ELISA and all the samples were in duplicate. IL-1β protein concentrations were normalized based on the original wet weight of the brain tissue samples.

3.8 Cell Counting and Image Analysis

The images of stained specimens were captured by a photometrics CoolSnap fx CCD camera mounted on a microscope (Olympus IX71) and analyzed with Image-Pro Plus software (Version 4.5). Cellular co-localization was confirmed using confocal microscopy (Zeiss, LSM-410). Single confocal images were taken as 1 µm optical sections from 40 µm cryostat sections. All tissue sections to be used for cell counting were counterstained with Hoechst prior to mounting to ensure that the only positive profiles counted were those associated with a nucleus.

Microglial/macrophage activation was assessed at 6 days post lesioning based on $GSAB_4$ histochemistry on 10 µm paraffin-embedded sections. For quantification, at least 3 sections per area of interest were stained and counted from each animal. Only $GSAB_4$+ cells with nuclei were counted for the peri-infarct areas. Cell population density was calculated by dividing the cell number by the brain section volume. The results were corrected with the use of Abercrombie's technique, allowing assessment of the real density of microglia (Savchenko et al., 2000). The calculation was carried out using the formula: $N = n \times T / (T + D)$, where N is the estimate of the true cell number, n is the number of nuclear segments, T is mean section thickness and D corresponds to a mean

nuclear diameter. The number of MPO-positive cells in the entire lesion was counted and normalized to the area of infarct.

DCX+ cell counting was performed on 40 µm-thick PFA-fixed cryostat sections. For quantification of the DCX+ cells, three to six parasagittal sections through the lesion (1.4~2.4 mm lateral to the bregma) were examined. DCX + cells in the cortex surrounding the injury, between the injury and corpus callosum and in the corpus callosum were quantified. Only DCX+ cells with a nucleus were counted. DCX+ cells (TRITC filter) were identified at 20X magnification, the filter was then switched to view Hoechst 33243 in order to determine if the cells were Hoechst+. A higher magnification (40X) was used to confirm that DCX and the nucleus were in the same cell by focusing up and down through the cell volume and ascertaining that cytoplasmic DCX immunoreactivity completely enveloped the nucleus. Results were expressed as the average number of DCX+ nuclei per 40 µm cryostat section between the lesion and RMS.

3.9 Statistical Analysis

All values are expressed as the mean ± standard error of the mean (SEM). The significance level was set at $P < 0.05$. Paired two-tail t-test was used to investigate significant differences between control and experimental groups regarding the lesion volume, the numbers of microglia/macrophage cells, MPO cells and body weight. For statistical analysis for IL-1β protein concentrations, the two-way analysis of variance [ANOVA] was used with ischemic- and drug-treated animals as the two variables. The one-way ANOVA was used to compare the number of DCX+ cells in experimental rats to control rats with days post-ischemia being the independent variable; the numbers of DCX+ cells in corpus callosum and neocortex was analyzed separately for statistical significance. Multiple post hoc comparisons between the different Groups were performed with Bonferonni's multiple comparison post-test with the significance level being set at $p < 0.05$.

4. VALIDATION OF AN APPROPRIATE FOCAL ISCHEMIA MODEL IN ADULT RATS

4.1 Introduction

There are a number of rodent focal ischemia models but the most commonly used involve occlusion of the MCA. The use of this model results in a substantial lesion, which encompasses the neocortex as well as the striatum . However, malignant human stroke (brain infarction >200 cm^3, or 39% of the ipsilateral brain hemisphere) is observed only in 10% of the cases (Carmichael, 2005). Many human strokes are of small size and of lacunar nature (Carmichael, 2005). This is a type of small vessel stroke, which constitutes approximately 25% of first ischemic strokes in humans (Lammie, 2000). If only the large size stroke animal models were used, this would lead to a potential bias against the clinical situation (Carmichael, 2005). There is an urgent need to focus on more research of the small vessel brain disease variety, which is the one prevalent in silent strokes and gives rise to cavitation (Greenberg, 2006).

In rodents, small size infarction in the motorsensory cortex has been induced by different techniques, such as photothrombosis, ET-1 injection, or devascularization. As reviewed in Section 1.4, all animal models have advantages and disadvantages. The traditional pial vessel disruption model, often referred to as the devascularization model or pial stripping model, was induced by complete termination of all the vessels overlying the exposed cortex (Funnell et al., 1990; Fedoroff et al., 1997; Conner et al., 1998; Farr and Whishaw, 2002; Gonzalez and Kolb, 2003; Kolb et al., 2006). This model most often results in a massive rectangular cortical infarct, extending far into the corpus callosum, and it creates hemorrhage due to stripping off the large class I vessels (Bar, 1980). The drawback of this model is that it mimics neurotrauma rather than ischemia due to its massive impact. In order to avoid these problems, the devascularizing model has been modified in our lab

and a rat model developed that is initiated by disruption of the medium size pial vessels (class II) ***only*** (Bar, 1980). This modified cortical devascularizing model (called *pial vessel II disruption model*) was applied to a smaller brain surface, a 5 mm circular area overlying the motor cortex. Instead of scraping off all the pial vessels in the exposed area with a mechanical device, a pair of fine forceps was used to disrupt the tip of medium size pial vessels (class II) only to minimize the mechanical damage. This modified method introduces a small cone shaped cortical lesion, with the tip often reaching into layers IV and V of the cortex. The tip never reaches deep enough to touch the corpus callosum. After two weeks, cavitation develops at the site of the lesion (Fig 4-1) (Wang and Walz, 2003).

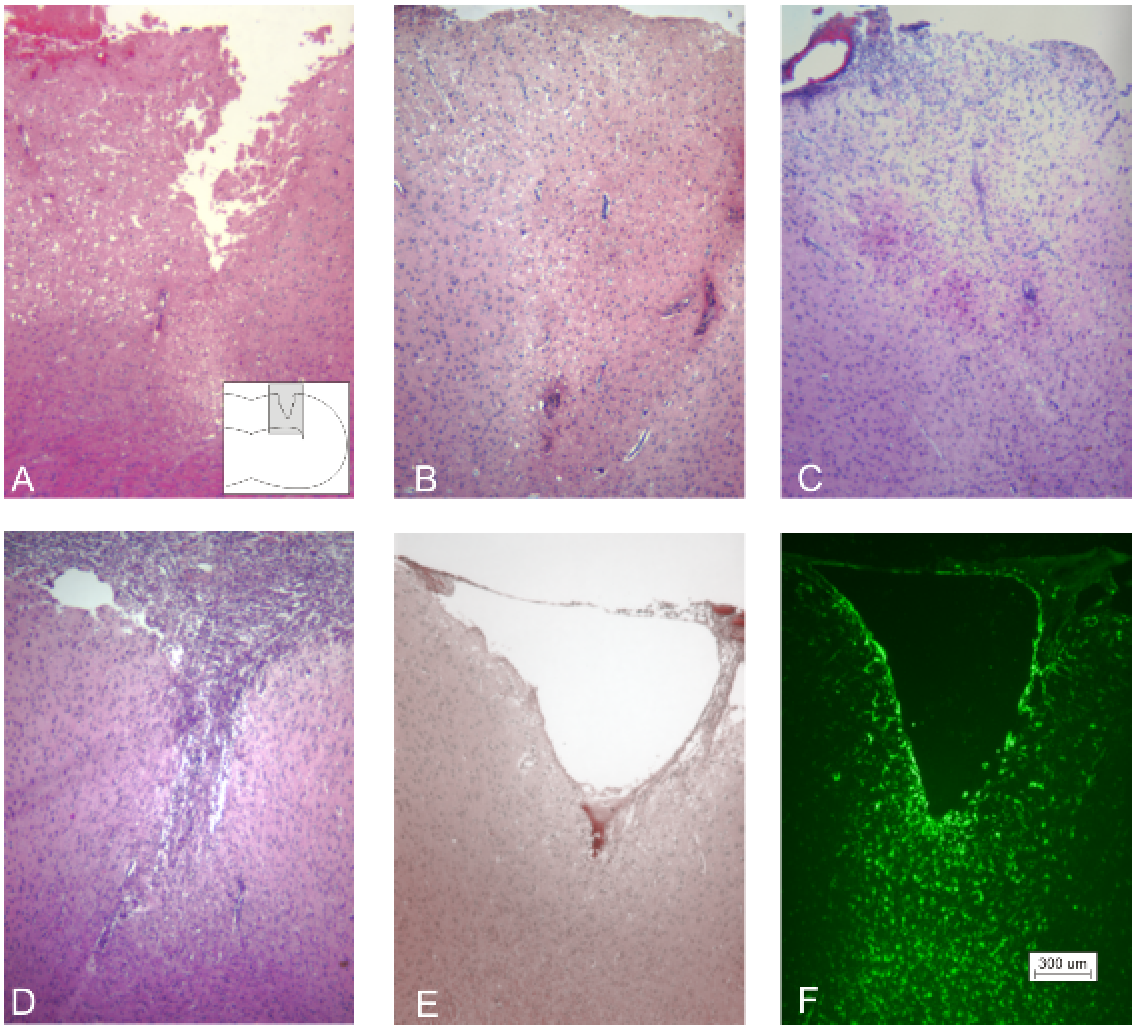

Figure 4-1. H&E stained sections illustrating the development of the lesion following PVD II. The insertion in A illustrates the typical PVD II lesion and sections were from the area depicted by the shaded box. A: 1 day, B: 2 days, C: 3 days, D: 6 days, E: 21 days, F: same animals as E but stained for GFAP. The lesion turns into a fluid filled cystic cavity surrounded by the glial limitans by day 21. Scale bar: 300 µm applies to all sections (from Wang and Walz, 2003).

PVD II mimics irreversible focal ischemia. Permanent occlusion of blood vessels has proved a useful model but the persistence of the occlusion differs from occlusion stroke in humans, where reperfusion frequently occurs (after a variable time) in a high proportion of patients (Carmichael, 2005). We therefore compared the PVD II model with a similar, but reversible model.

ET-1 is a 21 amino acid peptide with potent vasoconstrictor properties (Reid et al., 1995). Direct injection or topical application of ET-1 to the brain tissue or to the middle cerebral artery revealed a reversible vasoconstriction of the artery that resulted in profound reductions in local cerebral blood flow and the development of cerebral infarction (Robinson et al., 1990; Macrae et al., 1993; Fuxe et al., 1997). In order to be comparable to the PVD II model, ET-1 was topically applied to the exposed cortical surface area. The purpose of this section is to examine whether this model, which allows reperfusion, is superior to PVD II. If successfully reproducible, it would offer a simple model with the advantage of combining primary focal cerebral ischemia with a secondary phase of reperfusion.

4.2 Results

27 adult male Long Evans rats were used to evaluate the topical ET-1 application model. All rats tolerated the surgical procedure well and there was no mortality due to the surgery. Rats were sacrificed 1 (n=5), 3 (n=13) and 6 (n=9) days post surgery and every tenth section of a series was stained with Harris hematoxylin and eosin (H&E) to identify the lesioned area as well as gliosis. Following surgery, the majority of animals (24 out of 27) developed a complete bowl-shaped infarct, which was confined to the sensorimotor cortex as judged by histological assessment. The depth of the lesion varied among the animals, extending from the cortical surface ventrally to different layers or even to the corpus callosum (Fig 4-2, A, B, C). As shown in the figures, the typical lesion appeared to cross right through the neocortex. In approximately 50% of the rats, the lesion also extended into the corpus callosum. However, direct subcortical structural damage, such as in the striatum, was not evident. In a small set of rats (3 out of 27), a complete cortical infarct did not form or was in a completely irregular shape as judged by H&E staining.

The developing infarct shows a progression of pathological events similar to those observed in the PVD II model (Wang and Walz, 2003). As determined by H&E staining, a cortical infarct was apparent one day after topical application of ET-1. Neurons appeared angulated and slightly shrunken (Fig 4-2, D). By one day neurons with shrunken nuclei and hypereosinophilic cytoplasm were evident within and surrounding the lesions. On day 3, most of the neurons in the lesion were gone and the lesion was surrounded by a rim of activated microglia/macrophages that had begun to infiltrate the lesion area (Fig 4-2, E). A well-demarcated infarct was formed at day 6, surrounded and filled with a rim of activated microglia/macrophages (Fig 4-2, F).

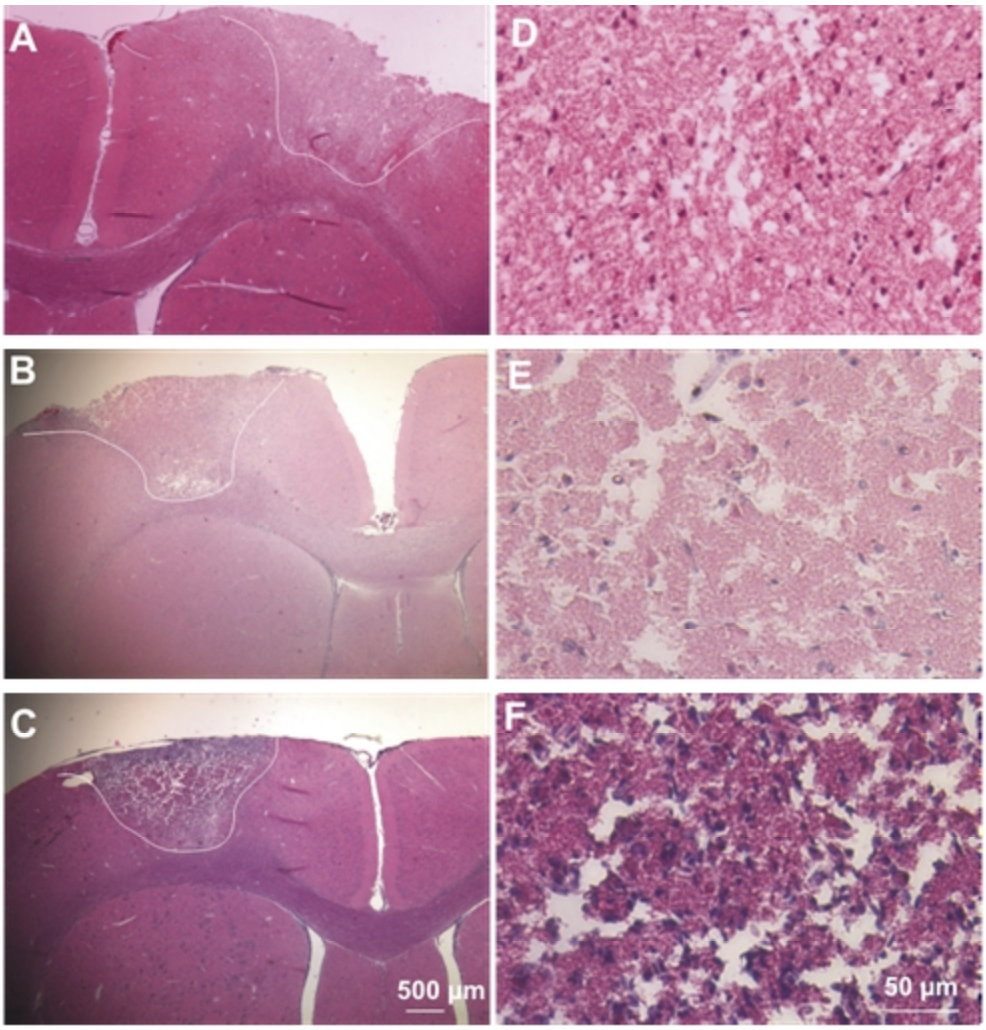

Figure 4-2. Distribution of cortical infarction and the development of the lesion induced by the topical ET-1 application model. Paraffin-embedded sections of H&E staining at different magnifications, showing representative lesions at 1 day (A, D), 3 days (B, E) and 6 days (C, F) after topical application of ET-1 onto the pial surface. The white outlines represent the extent of the cortical infarct. Higher magnification views of the infarct showed the histopathological changes in the lesion at 1 day (D), 3 days (E) and 6 days (F) after topical application of ET-1. Scale bar: 500 µm (A, B, C), 50 µm (D, E, F).

The occlusion and reperfusion of the brain surface vasculature therefore resulted in a progressive infarction in a small cortical volume of a large percentage of animals. However, it also introduced a variety of anatomical distortions into the brain tissue. The damaged tissue was swollen, so that it frequently protruded out of the skull. In some cases, the caudate-putamen was also distorted and pushed upward. In some rats it resulted in substantial brain edema (Fig 4-3). There was no obvious cortical neuron damage or brain edema observed in sham animals. Table 4-1 represents a summary of the degree of brain damage observed in each time point following topical ET-1 application.

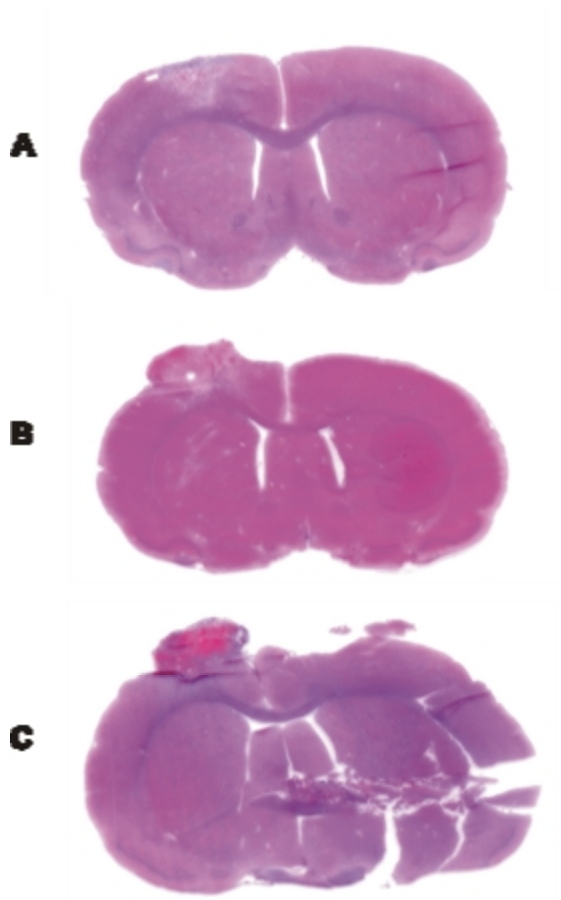

Figure 4-3. Images of H&E-stained 10 μm-thick coronal brain sections at the level of the largest lesion extension, six days after topical application of ET-1. A: Representative section shows no obvious edema of the ipsilateral hemisphere and there is no blood on the brain surface indicating no submeningeal bleeding. B: Representative section shows severe pulling up of tissue in the wound area, edematous tissue is observed in the damaged area. C: The edematous tissue along the hematoma is evident.

Table 4-1. A summary of the degree of brain injury observed at each time point following topical ET-1 application.

	Day1 (n=5)	Day3 (n=13)	Day6 (n=9)
Irregular shape lesion/incomplete infarct	1	1	1
Lesion without tissue protrusion	1	3	4
Lesion with medium tissue protrusion	1	5	3
Lesion with severe tissue protrusion	2	4	1
Hematoma observed in damaged tissue	3	3	4

The numbers were the numbers of rats in each category. The degree of tissue protruding (no, medium, severe) was determined under microscopy.

4.3 Discussion

For the study of the pathology and potential therapeutic strategies of cerebral ischemia, it is crucial that reproducible *in vivo* animal models are used. In the past, most focal cerebral ischemic investigators have used the various MCAO models. However, as pointed out above, there is a real need for models reproducing aspects of small-vessel occlusion. Most human strokes are small in size and the massive infarctions, also called malignant hemispheric infarctions, only account for about 10% of human strokes (Carmichael, 2005). Using only large size stroke models induces a potential bias against smaller stroke types.

In this study, I have demonstrated that the topical application of ET-1 to the pial surface results in ischemic damage to the underlying cortical gray matter in a high percentage of the cases, therefore providing a useful technique for inducing cortical ischemic injury. However, tissue deformation and brain edema were observed in many animals. The occurrence of brain edema, tissue deformation and hemorrhage makes this model inappropriate for studying neuroprotective agents. The impact of treatment on infarct volume is difficult to judge. The tissue deformation due to edema makes the accurate measurement of a relative small lesion volume very difficult and will result in inaccurate measurements. Another disadvantage of the ET-1 model is that ET-1 and both subtypes of the ET-1 receptor are found not only on endothelial cells, but also on neurons and astrocytes (Reid et al., 1995). It has been reported that ET-1 application induces astrocytosis (Hama et al., 1997), cortical spreading depression (Dreier et al., 2002) and that it affects gap junction permeability (Sanchez-Alvarez et al., 2004). These findings suggest that ET-1 exerts a direct, receptor-mediated signaling effect on astrocytes and neurons that may exacerbate the ischemic damage and complicate the interpretation of therapeutic or neural repair experiments.

The associated occurrence of the brain edema and distortion of the cortex and basal ganglia suggested that ipsilateral brain edema was occurring. Indeed, the dosage of ET-1 used in this study is higher than the dose used in some other studies (Fuxe et al., 1997; Adkins-Muir and Jones, 2003). The high dosage of ET-1 may have induced prolonged reductions in cerebral blood flow. Delayed reperfusion can induce increases

in vascular permeability during reperfusion, which aggravates brain edema formation, especially the vasogenic component, and parenchymal hemorrhages (Siesjo, 1992b; Schaller and Graf, 2004). Disruption of the BBB after reperfusion has been observed with transient MCAO, but not after permanent MCAO (Kastrup et al., 1999) and the disrupted BBB is known to contribute to vasogenic edema (Dietrich et al., 1987b; Kimelberg, 1995). It has also been reported that ET-1 induced focal cerebral ischemia is associated with acute but reversible hemispheric swelling during the early phase of reperfusion (Gartshore et al., 1997) and this early swelling might worsen and contribute to tissue deformation. A lower dose of ET-1 may be all that is needed to produce a consistent cortical lesion and yet reduce the brain edema and tissue protrusion.

Another possible cause for the anatomical distortion / histological changes might be the location of the lesion. In this model, the lesion was placed right on top of the lateral ventricle, therefore, the removing of the skull and tissue damage right above the lateral ventricles may result in pressure that gradually will push the tissue up. Even more extensive brain distortion was reported in a cortical lesion placed on the cortex right above the lateral ventricle and induced by wiping off all the pial and blood vessels as well as the suctioning off 1 of mm^3 pieces of brain tissue (Whishaw, 2000). It is, however, noteworthy that more laterally (Adkins-Muir and Jones, 2003; Luke et al., 2004) or more caudally (Fuxe et al., 1997) placed lesions have not been reported to produce similar degrees of tissue distortion. Indeed, in the PVD II model, the lesion is placed 1.5 mm anterior as compared to this injury and the damaged tissue upswelling and protruding was observed only rarely. The profound local tissue upswelling limits this model in its application to the study of neuroprotection after stroke.

In summary, topical administration of ET-1 (3,000 pmol) to the pial surface induces, in most of the animals, a pan-necrotic infarct by day 1 and a well-defined infarct surrounded by a rim of microglia/macrophages by day 6. Wang and Walz (2003) established the development of histological damage in the PVD II model. In comparison with the PVD II model, the topical ET-1 application model also provides a cortical infarct with precise injury location and a high reproducibility. It therefore provides a good model of the mechanistic aspects of focal ischemia. Indeed, vascular damage caused by prolonged cerebral ischemia can lead to brain edema and hemorrhage

formation in ischemic stroke patients (Fagan et al., 2004a). Therefore, the topical ET-1 model incorporates some useful conditions that may be observed in human ischemic stroke, e.g., brain edema, bleeding, or reperfusion. Therefore, it provides a useful model to study the mechanisms involved in ischemic pathology and neural repair. However, the occurrence of brain edema and tissue protrusion complicates the volume estimation of ischemic lesions because the entire affected hemisphere (still containing non-affected tissue) may be swollen and enlarged compared to the contralateral side, which results in inaccurate measurements. In addition, the existence of the edematous damaged area makes the accurate measurement of a relatively small lesion volume very difficult. As the infarct volume is a major parameter for neuroprotective evaluation this model needs further improvement.

The PVD II model creates a consistent and reproducible cortical injury with very rare occurrence of tissue protrusion and upswelling (Wang and Walz, 2003; Wang et al., 2004). It should be noted that the lesions produced by PVD II were smaller than those in many studies of the effects of "focal" cortical damage, especially the photothrombosis model, ET-1 model (intracerebral injection and topical application) and the traditional cortical devascularization model with class I vessel disruption (Fig 4-4). Instead of scraping/tearing off ***all*** pial vessels in the exposed area, the big vessels, which supply the white matter (Bar, 1980) are salvaged, and the medium pial vessels are disrupted by using fine forceps to minimize the mechanical damage and subsequently bleeding. This prevents hemorrhage and causes a cone shape lesion exclusively located in the cerebral cortex. As with all models of ischemia there are disadvantages and advantages with using the PVD II model for studying neuroprotective agents. This model creates a pure cortical injury, small in size and allows the flexibility of changing the injury site, which mimics small-vessel stroke in the clinic. The disadvantages stem from the mechanical disruption of the vessels although there is no obvious damage in the control animals as evidenced by microscopic observation (Wang and Walz, 2003). Obviously, this model causes an irreversible interruption of blood flow and therefore appears not to take into account reperfusion. However, about 80% of reperfusion in human stroke is not through clot lysis, but through collateralization (Carmichael, 2005). Collateralization will not be affected in this PVD II model. It has been suggested that a

permanent ischemic model should be used to test the efficacy of potential neuroprotective drugs to enhance clinical success (Richard Green et al., 2003). On balance, I decided to use the PVD II model for the assessment of the potential benefits of minocycline.

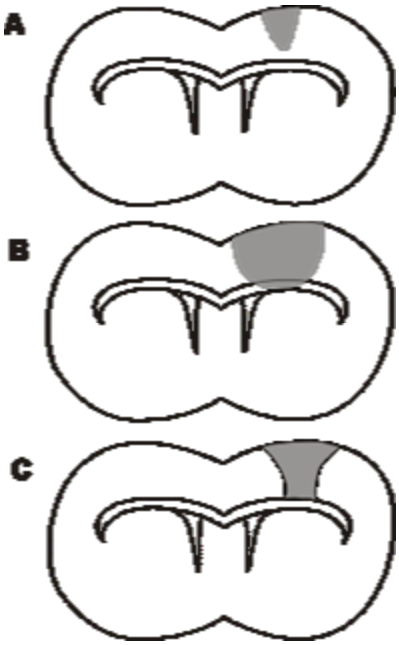

Figure 4-4. Schematic drawing of lesion sizes in three different stroke models. The typical lesion in the coronal brain sections with the corpus callosum and lateral ventricles (dotted lines) in the PVD II model (A), conventional pial vessel disruption model (B) and topical ET-1 model (C). A: PVD II model introduces a small cone-shape cortical lesion. The tip never reaches deep enough to touch the corpus callosum. B: conventional pial vessel disruption model results always in a massive rectangle cortical infarct, extending far into the corpus callosum. C: the topical ET-1 model induces a bowl-shaped infarct. The depth of the lesion varied among the animals. In 50% animals, the lesion reaches into the corpus callosum.

5. ASSESSMENT OF THE NEUROPROTECTIVE EFFECT OF MINOCYCLINE IN A PIAL VESSEL II DISRUPTION MODEL

5.1 Introduction

Minocycline, a second-generation tetracycline, has been shown to have neuroprotective properties in animal models of acute CNS injury and chronic neurological diseases (reviewed in section 1.3.1.2). A heterogeneity of beneficial effects have been proposed: anti-inflammation, anti-apoptotic, anti-oxidant and a paucity of negative side effects as well (Domercq and Matute, 2004; Stirling et al., 2005). With regards to stroke, minocycline showed beneficial effects in different animal models of global ischemia (Yrjanheikki et al., 1998; Yrjanheikki et al., 1999), transient and permanent focal cerebral ischemia (Yrjanheikki et al., 1999; Xu et al., 2004; Koistinaho et al., 2005), intracerebral hemorrhage model (Power et al., 2003) and hypoxic-ischemic brain injury in neonatal rats (Yrjanheikki et al., 1999; Arvin et al., 2002; Fox et al., 2005). However, there are also contradictory results showing that minocycline has no beneficial effects (Fox et al., 2005) or even that it exacerbates injury (Tsuji et al., 2004). In a permanent MCAO in adult mice, if minocycline treatment was started before the insult, the drug reduced the infarct size, whereas if the treatment was started after the insult, minocycline was not protective (Koistinaho et al., 2005). Before minocycline can be used in clinical trials with stroke patients, it must be shown to be effective in several types of stroke models with drug delivery times that are clinically realistic (Diguet et al., 2004a; Yong et al., 2004). To date, the dominant model used in studying minocycline actions is the MCAO model. If only the large size stroke animal models are used, this will lead to a potential bias against the clinical situation

(Carmichael, 2005). Therefore, in the present study, the PVD II model was used to test the effects of minocycline treatment. Standard minocycline treatment was started an hour after lesioning and the outcome was evaluated based on histological and immunohistochemical parameters.

5.2 Results

5.2.1 Minocycline Treatment Prevents Formation of the Cystic Cavity and Glia Limitans

The PVD II model was applied to adult rats with or without minocycline treatment. One day after injury, the damaged area was identified as less densely stained with dying neurons present, which lack stainable nucleic acid. After 3 days all cells (neurons and non-neuronal cells) in the lesion disappeared. Microvessel proliferation and a massive infiltration of blood-borne cells was observed in the infarct area. A well-demarcated cortical lesion was observed by day 6 and a cystic cavity developed by 21 days (see Fig 4-1) (Wang and Walz, 2003).

Since the lesion developed a distinct border by day 6, day 6 was chosen as the time point to measure the volume of the cortical lesion from the H&E stained sections. Minocycline treatment did not reduce the lesion volume (1.09 ± 0.30 mm^3) compared to the control group (injected with equivalent amount of distilled H_2O, see Materials and Methods Section 3.3) (0.91 ± 0.15 mm^3, n=6) (Fig 5-1). However, by day 21, in the minocycline-treated group, only 1 out of 6 animals had developed a cavity in contrast to 5 out of 6 animals in the control group that exhibited a cystic cavity in the lesion area (Fig 5-2 A, B).

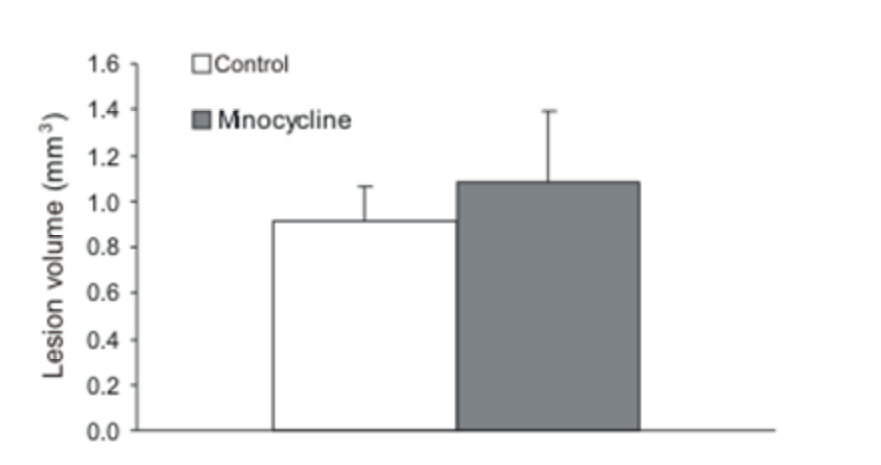

Figure 5-1. Lesion volume 6 days after PVD II in control and minocycline- treated rats as measured with H&E (n=6). There is no significant difference (P=0.63). Data are shown as mean ± SEM.

The cystic cavity is surrounded by a glia limitans (Wang and Walz, 2003). Since minocycline treatment prevented the cavitation, this study investigated whether the rescued tissue is part of the brain parenchyma and therefore within the tissue enclosed by the glia limitans, or outside the glia limitans. GFAP immunostaining was therefore used as a marker of astrogliosis. In the control group all animals developed a glia limitans on day 21 following injury (Fig 5-2 A, C). With minocycline treatment, the glia limitans was absent in 5 out of 6 treated rats (Fig 5-2 B, D) and the rescued tissue space was filled with reactive GFAP+ astrocytes (Fig 5-2 D). However, the appearance and distribution of GFAP+ cells in the tissue surrounding the lesion is not changed by minocycline treatment on days 1, 3 and 6 after injury (Fig 5-3).

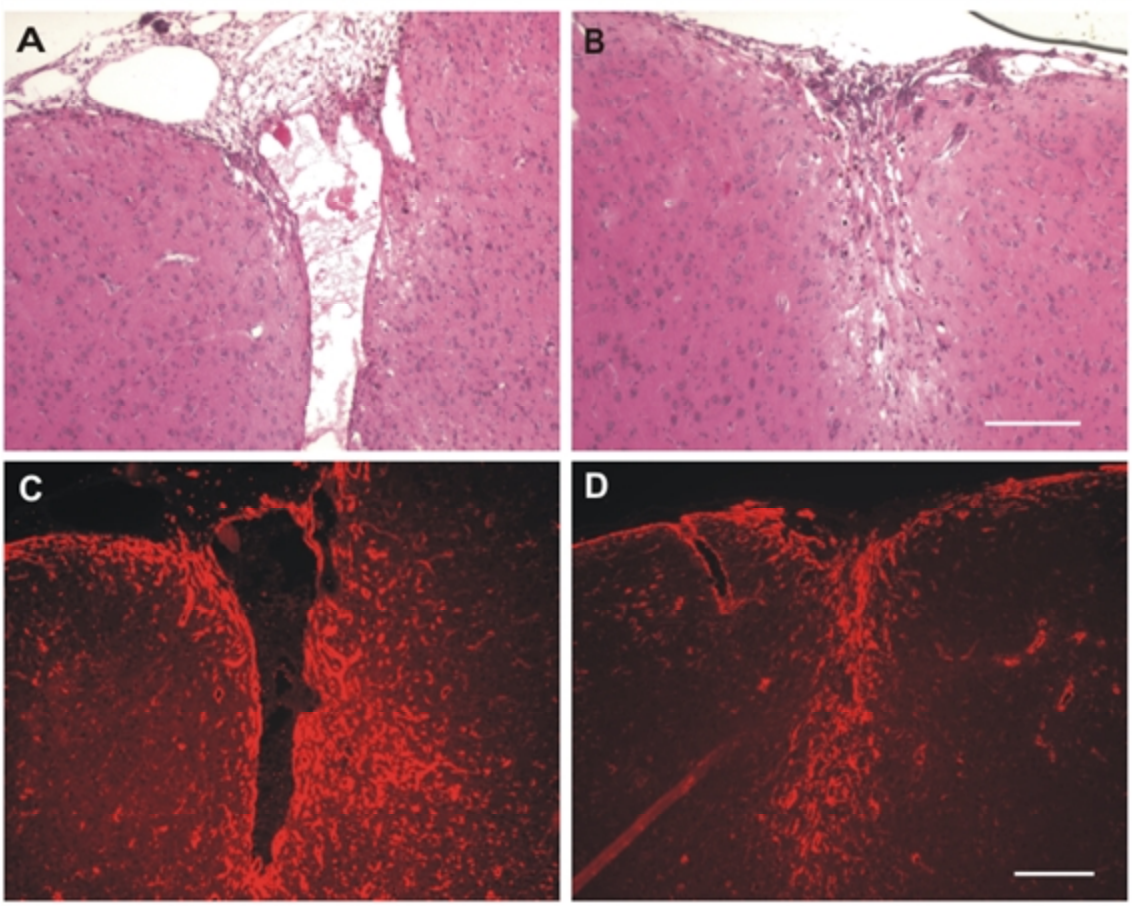

Figure 5-2. Effect of minocycline on cystic cavity and glia limitans 21 days after PVD II. A cystic cavity and glia limitans developed between days 14 and 21 in the control group (n=6; A, C). With minocycline treatment, the glia limitans was absent and the injured area was filled with reactive GFAP+ astrocytes (n=6; B, D). A, B: Representative H&E stained sections. C, D: Adjacent sections stained for GFAP. Scale bar: 200 μm.

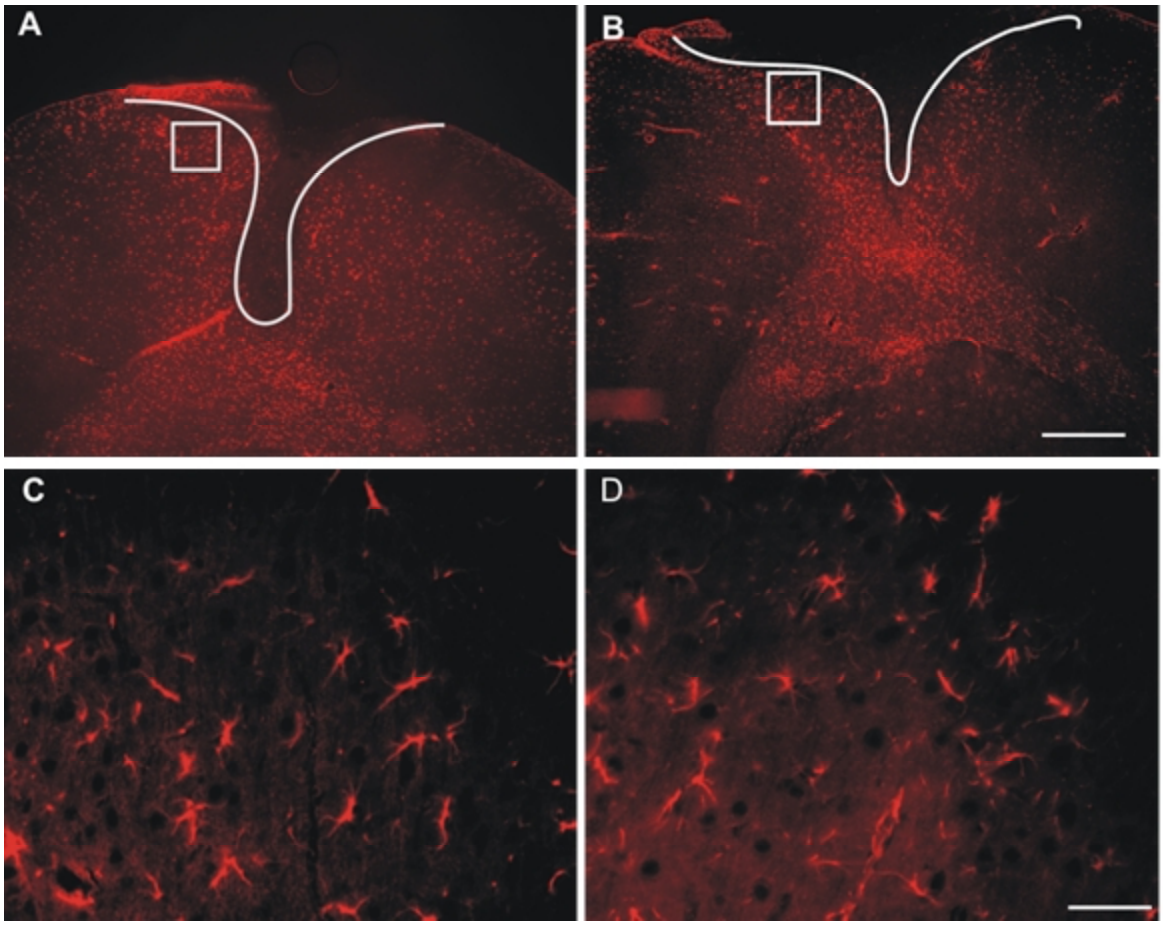

Figure 5-3. Comparison of GFAP staining in control (A, C) and minocycline treated rats (B, D) six days after PVD II. A, B: The overview pictures include cortical lesion and peri-lesion areas. White outline delineates the lesion. C, D: high magnification of the square outlined areas in A, B. Scale bar: 500 μm (A, B); 50 μm (C, D).

5.2.2 Minocycline Treatment and Inflammatory Response after Pial Vessel Disruption

5.2.2.1 Microglia Activation

There is evidence that the neuroprotective effect of minocycline is related to the inhibition of microglial activation (Tikka et al., 2001). To determine whether minocycline affects glial cell activation, lectin histochemistry was used to determine the microglia morphology. Microglia were identified by means of lectin histochemistry with B_4-isolectin from *Griffonia simplicifolia* ($GSAB_4$, Sigma), which specifically binds to alpha-D-galactosyl residues. It stains microglia during all stages of activation (Streit, 1990). The following classification was used to describe the stages of microglial activation (Ziaja and Janeczko, 1999; Kato and Walz, 2000).

1. Resting microglia, which are ramified microglia and present in the normal brain. They have round, small cell bodies with radiating long, thin, branched processes.
2. Activated microglia, which are cells responding to ischemia with morphological and immunophenotypic changes, but which are not phagocytic. Their morphological changes include enlarged cell bodies and contraction of their processes to show a more stout morphology. Two major morphological types were detected in this model: a highly ramified shape, with an enlarged cell body giving rise to ramified tapered process; a bushy shape, a very large cell body with thick, short processes.
3. Phagocytic microglia, which are full-blown brain macrophages with an amoeboid or round morphology, and with expression of a number of immunomolecules that are shared with hematogenous macrophages.

As described in detail in Methods and Materials, microglial activation after PVD II is classified into 3 stages/types: resting microglia, activated microglia, and phagocytic microglia/macrophages. The typical morphology of these three types/stages of $GSAB_4$+ microglia in the control group is shown in Fig 5-4.

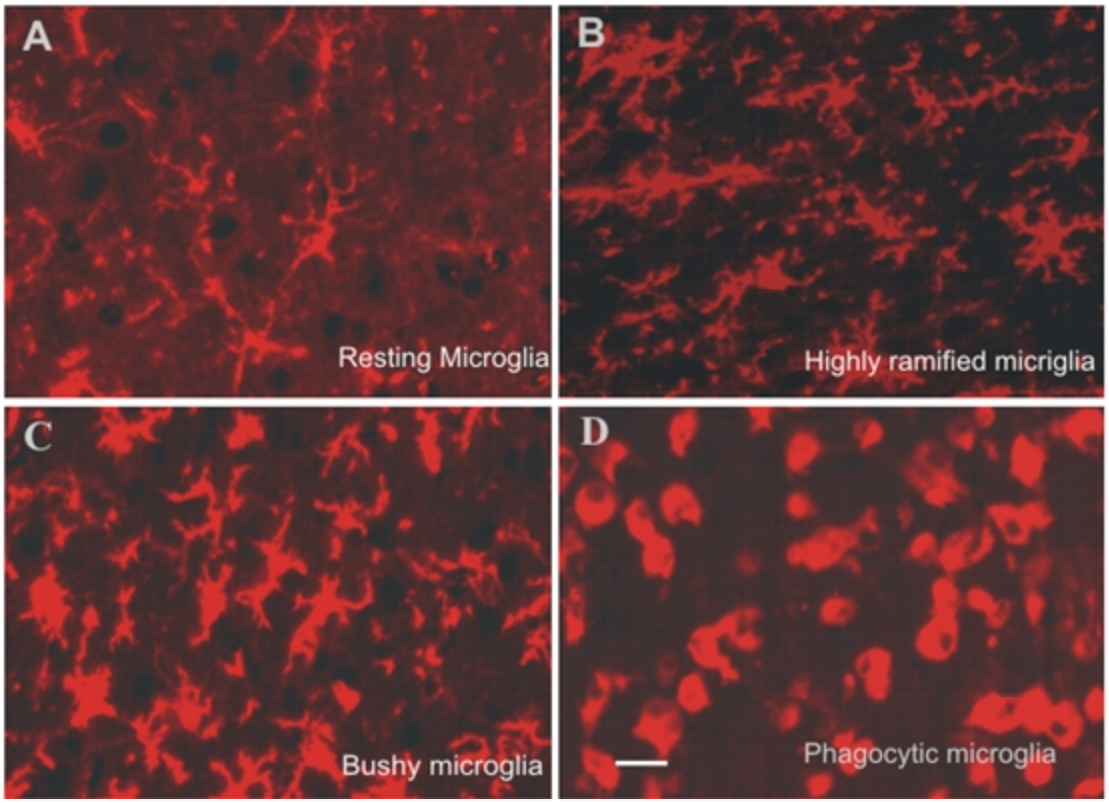

Figure 5-4. The typical morphology of three types/stages of $GSAB_4$+ microglia after PVD II. A: Resting microglia in the cerebral cortex of normal brain, which showed ramified morphology; B-C: Activated microglia: morphological changes of activated microglia include enlarged cell bodies and contraction of processes. Two major morphological types were detected in this model: highly ramified shape (B, enlarged cell body giving rise to ramified tapered processes; day 1 post lesion; peri-infarct) and a bushy shape (C, very large cell body with thick, short processes; day 3 post lesion; peri-infarct) D: Phagocytic microglia demonstrating an amoeboid or round brain macrophage-like morphology (day 6 post lesion; infarct). Scale bar: 20 µm.

In the control group, one day after injury, scattered $GSAB_4$ positive small round cells were present in the affected area, but no resting and activated microglia could be seen there. In the area surrounding the infarct core, bushy and highly ramified cells were seen in increasing numbers. The activation and proliferation of microglia were further increased on day 3. Accumulated round and amoeboid cells were present within the infarct. A dense zone of bushy microglia mingled with amoeboid cells was observed between the infarct and the surrounding area thus forming a transitional zone. Surrounding this transitional zone, most of the microglia were highly ramified. After 6 days, the entire ischemic core was densely covered by round and amoeboid cells. The transitional zone was very narrow compared to day 3. Highly ramified cells mixed with bushy cells were seen immediately surrounding the infarct core. The density of the $GSAB_4$ positive cells in the surrounding area was doubled compared to the contralateral area, from 14,095 ± 438 to 27,088 ± 4,291 cells/mm^3 ($P<0.05$; $n=3$), indicating a robust activation of microglia after PVD II. In the minocycline-treated group, neither the morphology and distribution of the activated types nor their densities were changed 1, 3 and 6 days following ischemia (Fig. 5-5). The density of activated microglia surrounding the infarct core was further quantified on day 6 in the minocycline treated group. Minocycline did not change the density of $GSAB_4$ positive cells in the contralateral brain: 13,798 ± 1,621 cells/mm^3 in the minocycline-treated group and 14,095 ± 438 cells/mm^3 in the control group. The density of $GSAB_4$ positive cells in the area surrounding the infarct showed no significant difference between the minocycline-treated group (23,610 ± 1,067 cells/mm^3) and the untreated group (27,088 ± 4,291 cells/mm^3; Fig 5-5, G) as well. These results indicated that minocycline treatment did not alter the activation of microglial phenotypes.

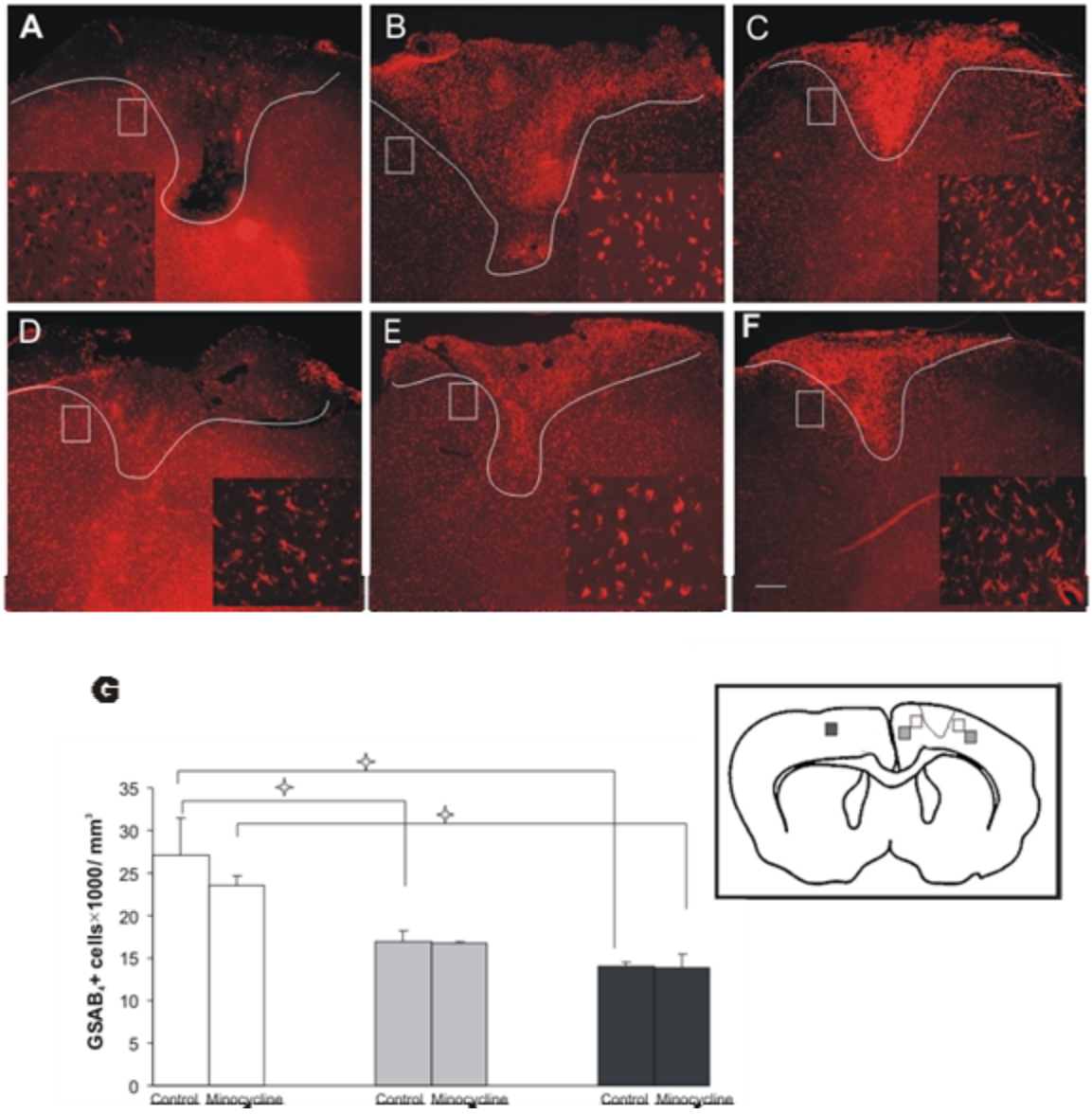

Figure 5-5. Comparison of $GSAB_4$ staining in the infarct and peri-infarct area of control group (A, B, C) and minocycline-treated group (D, E, F) at different time points. A, D: day 1; B, E: day 3 and C, F: day 6. In the minocycline-treated group, neither the morphological activation of microglia nor density was changed 1, 3 or 6 days following ischemia. White outlines delineate the lesion. The small picture insets represent high magnification of the rectangular outlined areas. Scale bar: 300 μm. G: Quantitative comparison of $GSAB_4$+ cells in the different areas surrounding the lesion on day 6 in control group and minocycline-treated group. The inset represents a coronal section with

locations of the ischemic lesion and representative fields used in quantification. The two-way ANOVA was applied to the data for statistical significance. Multiple post hoc comparisons were performed with Bonferonni's multiple comparison post-test. The two-way ANOVA showed only a significant main effect of distance from the lesion on $GSAB_4$+ cell density, $F(2,12)=26.30$, $P<0.0001$). There was no significant main effect of the minocycline treatment. Bonferonni's post-test revealed the cell density was significantly (✧ $P<0.05$, white bar vs. black bar) increased in the areas immediately surrounding the lesion compared with the contralateral area in both control and minocycline-treated groups. Bonferonni's post-test also revealed a significant increase of cell density in the areas immediately surrounding the lesion compared with the remote area (✧ $P<0.05$, white bar vs. grey bar) in the control groups.

5.2.2.2 Infiltration of Leukocytes and T-lymphocytes

Only few infiltrating leukocytes, predominately polymorphonuclear neutrophils (PMNs), determined by myeloperoxidase (MPO) immunoreactivity, were detected in either the contralateral side or the tissue outside the lesion of the ipsilateral hemisphere. The MPO immunoreactive cells were evident in the lesion site at day 1 and day 3 after PVD II (Fig 5-6 A, B) and only occasionally seen in the lesion site at day 6. Quantitative analysis showed that minocycline treatment did not significantly reduce the invasion of PMNs (Fig 5-6 C). Only very few infiltrating T-lymphocytes (CD3 immunoreactive cells) were seen around the border of the lesion site on day 1. At day 3, their numbers had increased, and reaching a peak around day 6. The infiltration of CD3 immunoreactive lymphocytes was not affected by minocycline treatment (data not shown).

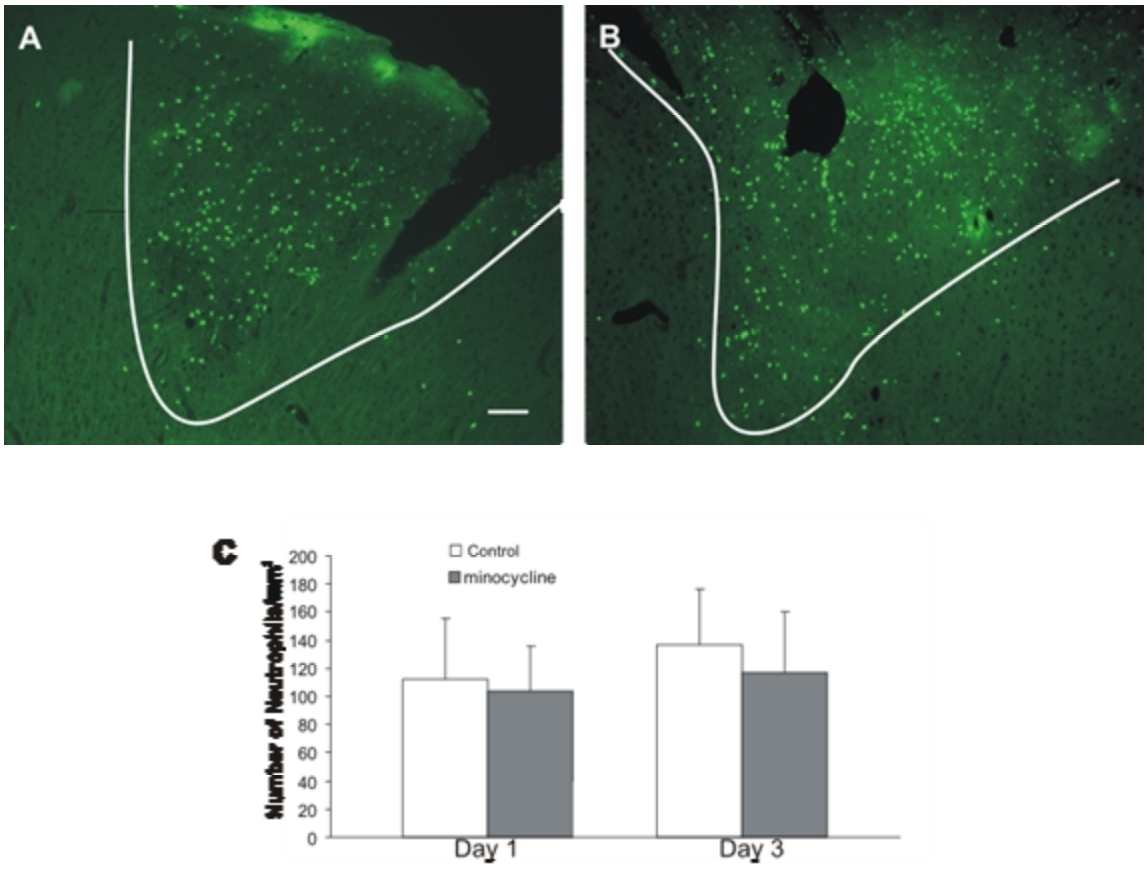

Figure 5-6. Infiltration of neutrophils after PVD II. (A, B) Photomicrographs of myeloperoxidase-immunostained neutrophil infiltration in lesion 1 day (A) and 3 days (B) after PVD II. The white outline indicates the border of the infarct zone. (C) Number of polymorphonuclear neutrophils in the lesion at day 1 and day 3 after PVD II. Myeloperoxidase-positive cells were normalized with the lesion area. Minocycline treatment did not reduce the number of polymorphonuclear neutrophils in the lesion (n=3). Scale bar: 100 μm.

5.2.2.3 Interleukin-1β Protein Expression

The amount of IL-1β in the tissue extract was expressed as ng/g wet weight of the samples. The PVD II resulted in a significant increase in the IL-1β concentration of injured brain tissue compared to the contralateral side (Fig. 5-7). The significant increase of IL-1β was primarily due to the large increase seen in the control groups since the post-test revealed no significant difference between the levels measured in the ischemic lesion vs. the contralateral side in minocycline-treated groups. This suggests the minocycline treatment reduced the IL-1β expression induced by ischemic injury,

although this reduction was not large enough to reach statistical significance. IL-1β concentration was also normalized to the total sample brain protein. Both ways of expressing the data showed similar results.

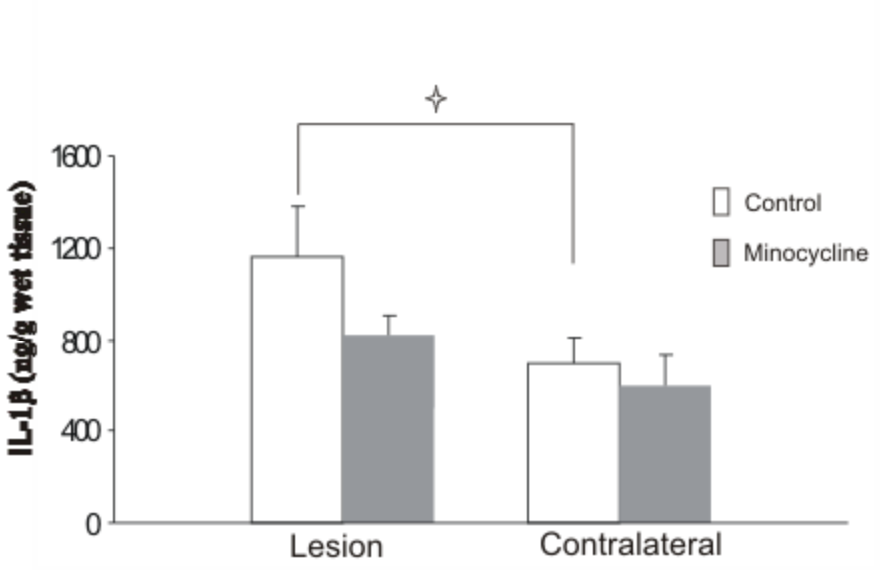

Fig 5-7. ELISA analysis of IL-1β expression in the brain after PVD II. The data are expressed in ng/g wet tissue weight. Two-way ANOVA was applied to the data for statistical significance. Multiple post hoc comparisons were performed with Bonferonni's multiple comparison post-test. The two-way ANOVA only revealed a significant main effect of the ischemia on the IL-1β level, $F(1,24)=6.37$, $P<0.019$; The main effect of minocycline treatment failed to reach statistical significance, $F(1,24)=2.66$, $P=0.12$. The two-way ANOVA revealed no significant interaction between the lesion/no lesion and minocycline/saline variables, $F(1,24)=0.88$, $P=0.36$. Bonferonni's post-test revealed the IL-1β level was significant higher in the ipsilateral side (lesion) than in the contralateral side (non-lesion) in the control group (✧$p<0.05$ white), but not significantly difference between ipsilateral and contralateral side in the minocycline-treated group. The data are shown as mean ± SEM (n=7).

5.2.3 Side Effects of Minocycline Treatment on Adult Rats

There was no mortality in either control or minocycline-treated groups. The PVD II model caused a small (average of 6.7% ±0.2%) body weight loss at day 1

relative to body weight before injury. Afterward, the weight stopped dropping and gradually increased after 3 days, with an average gain of 3% by day 6. On day 1, the body weight loss (control 6.7% ± 0.2% vs minocycline 6.1% ± 0.5) between the two groups was similar. However, on day 3, when the control animals stopped losing weight, the body weights of the minocycline-treated animals kept declining and reached the maximum loss on day 6 (Fig 5-8). In the present study, minocycline treatment (45 mg/kg i.p. twice a day for the first day; 22.5 mg/kg for the subsequent 5 days) prevented the body weight gain that occurred after cortical lesioning between day 3 and 6 ($P<0.05$, Student *t* test). Yellow-colored deposits have been observed on the surface of the liver, and/or on the intestines in some of the minocycline treated animals, varying among animals as judged by visual observation. These yellow deposits in the peritoneal cavity might be an indication of incomplete drug absorption as minocycline is a yellow powder and has poor water solubility. A similar observation has been reported in publications (Fagan et al., 2004b; Szymanska et al., 2006) that also used i.p. administration.

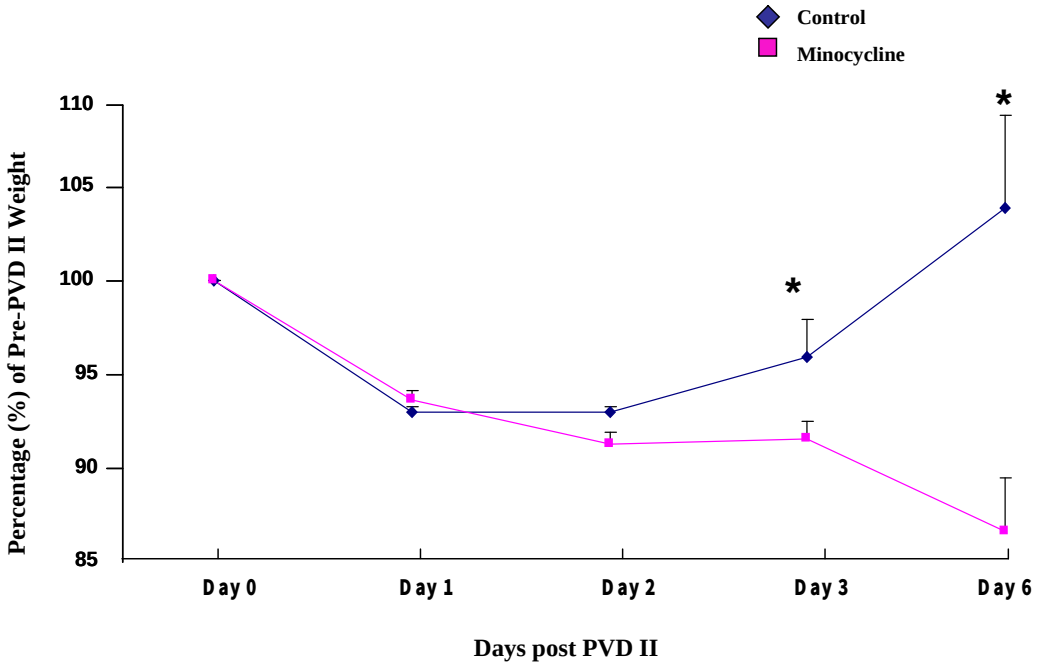

Figure 5-7. Effects of minocycline treatment on body weight following PVD II, represented as a percentage of pre-surgery weight. All rats lose weight on day 1 and day 2 as a consequence of the PVD II. Minocycline treatment impeded the weight gain in the

following days and reached a significant difference between day 3 and day 6. (*P<0.05). All the values in this graph are reported as the mean ± SEM.

5.3 Discussion

In the present study, minocycline treatment showed no effect on the lesion volume. Therefore one has to conclude that there is no neuroprotective effect in this experimental irreversible stroke model. The untreated stroke lesion in control animals transforms normally into an extra-parenchymal fluid-filled cavity surrounded by the glia limitans as a new barrier. Minocycline treatment rescued this area as part of the parenchyma as the space was now occupied by reactive astrocytes. Although no neurons were rescued, this action may still result in beneficial effects as reactive astrocytes are a major source of trophic factors and other neuroprotectants (Pekny and Nilsson, 2005). The mechanism on which the prevention of cavitation is based could not be determined. Microglial activation and infiltration of leukocytes were unaffected by minocycline treatment as judged by the morphology and density of the $GSAB_4$ positive cells, CD3 and MPO positive cells. Although minocycline treatment showed a trend to reduce the expression of IL-1β, it failed to reach statistical significance.

In regards to stroke-like conditions, minocycline has been mainly tested and shown to have neuroprotective effects on the MCAO model, the most common used focal ischemic animal model because of its clinical relevance (Yrjanheikki et al., 1998; Yrjanheikki et al., 1999; Xu et al., 2004; Koistinaho et al., 2005). Ischemic injury in the brain results in neuronal cell death, with characteristics of both necrosis and apoptosis (Lipton, 1999). Apoptosis, which is temporally and spatially different from necrosis in the infarct core, occurs mainly in the surrounding penumbra region (Mergenthaler et al., 2004). Apoptosis is one of the direct targets of minocycline action (Domercq and Matute, 2004) and minocycline acts at the mitochondrial level to reduce the apoptosis of neurons and oligodendrocytes in various neurodegenerative disease models (Lee et al., 2003a; Stirling et al., 2004; Zhu et al., 2002). The class II pial vessel disruption induces a small cortical lesion, which mimics irreversible focal ischemia (Wang and Walz, 2003). Compared to MCAO, it does not create a sizable penumbra of sub-lethal injury in the cortex and striatum (Gotts and Chesselet, 2005), thus fewer neurons are subjected to delayed death, and subsequently fewer neurons are potential targets for treatment (Muir and Grosset, 1999).

Another cause for the lack of effect on lesion volume by minocycline treatment could be the time point of the start of treatment. In the present study, the drug was delivered 1 hour post injury. Indeed, in a study using the permanent MCAO model, it has been shown that if minocycline treatment was initiated before lesioning, the ischemic infarct was dramatically reduced while no effect was observed when the treatment started 2 hours after the onset of the permanent MCAO (Koistinaho et al., 2005). In another study of a transient MCAO model on rat pups, minocycline treatment starting 2 hours after MCA occlusion only reduced the brain injury at 24 hours but not 7 days after lesioning. These authors, too, failed to find a minocycline-induced reduction of microglial activation or expression of local proinflammatory mediators such as IL-1β, IL-18, MCP-1 and CINC-1 (Fox et al., 2005). Minocycline did not inhibit microglia activation in the facial nucleus following crush injury either (Fendrick et al., 2005).

In the present study, treatment was delayed by 1 hour as this is a more realistic scenario for a clinical situation compared to pretreatment or simultaneous treatment with the time of lesioning. Another factor could be that intraperitoneal delivery of minocycline may take up to 4 hours to peak in the systemic circulation (Fagan et al., 2004b). Consistent with their findings (Fagan et al., 2004b), an accumulation of the drug in the liver and intestine was also noted in some of the minocycline-treated animals, which may be associated with a delayed, incomplete and inconsistent absorption of the drug into the bloodstream. Such delays in reaching effective concentrations might be problematic because they may miss the therapeutic window, which is extremely important in acute CNS injury. The minocycline administration protocol used in this study was the same as the one used by Yrjanheikki et al. (1999) in the MCAO model, in which minocycline was successful in rescuing neurons. However, differences in the stroke models, regional brain areas, experimental species, strains and other parameters may require different dosages and treatment protocols in order to produce significant neuroprotective effects (Tsuji et al., 2004). Intravenous injection of minocycline has been shown to be a more consistent and prompt delivery route (Fagan et al., 2004b). Therefore, it might be a more effective treatment following PVD II, if acute neuroprotection is required.

However, despite a lack of effect on the stroke volume by day 6, it was found that minocycline abolished the substantial progressive cavitation that develops in more than 80% of the lesioned animals between day 14 and 21 (Wang and Walz, 2003). The cavity was occupied in minocycline-treated rats by reactive, GFAP+ astrocytes. In addition, the glia limitans, which surrounds the cavity in control animals, was absent in these treated rats. Thus an important effect of minocycline treatment during the first six days after injury was that the loss of brain parenchyma, which appeared quite later, was prevented. Such an effect is new and has not been reported before. Given the importance of lacunar infarctions in human stroke pathology, this finding has relevancy in human treatment with minocycline. In addition, this effect could have important ramifications as the space was now populated by reactive astrocytes as part of the parenchyma. There was no apparent barrier separating these reactive astrocytes from adjacent surviving tissue. As these cells are known to produce neurotrophic factors, they could therefore help salvage neuronal survival, migration and axonal regeneration in adjacent areas.

Progressive cavitation is closely related to the inflammatory response and is based on activation of microglia / macrophages and migration of reactive astrocytes out of the affected area (Fitch et al., 1999). This leads to abandonment by astrocytes leaving this area more vulnerable to inflammatory damage. Therefore it may not come as a surprise that this process is a natural target for minocycline. In the PVD II model, it was found that shortly after injury, PMNs were recruited and infiltrated the lesion area, followed by delayed infiltration of T cells and activated microglia/macrophages (both from hematogenous origin and brain microglia) in the ischemic area and boundary zone. Astrocytes abandon the lesion within the first few days, but at the border they become reactive and divide. Six days after lesioning, an astrocytic boundary, known as *glia limitans* is formed, surrounding the lesion. By day 21 the lesion site is transformed into a fluid-filled cavity (Wang and Walz, 2003; Wang et al., 2004).

In the present stroke model, minocycline treatment did not change any of the patterns of these cell types in the first six days. However, it prevented the formation of the cavity by filling up the space with reactive astrocytes between day 6 and 21. It should be pointed out that minocycline treatment was stopped at day 6, when there was not yet a cavity. Reactive astrocytes most likely migrated back into the lesioned area,

and this migration prevented the formation of a fluid-filled cyst. It is usually persistent macrophage / microglia activation that is responsible for the outward migration of astrocytes (Fitch et al., 1999). Although in this study no direct evidence was found for reduced inflammation after minocycline treatment, it seems most likely that minocycline is preventing cavitation through its anti-inflammatory effect on microglia early in the first six days. Activated microglia/macrophages not only act as scavengers removing tissue debris, but also release numerous agents that are toxic to CNS cells, including inflammatory cytokines and glutamate, which aggravate secondary tissue injury and modulate the astrocyte response by releasing inflammatory cytokines, chemoattractants such as osteopontin (Wang et al., 1998a) and MMPs (Planas et al., 2002). Among these inflammatory cytokines, IL-1β plays an important role in the signaling between microglia and reactive astrocytes (Giulian et al., 1988; Herx and Yong, 2001).

An alterative explanation is that this repopulation was not caused by changes in diffusible microglia-astrocyte signals, but by changes in matrix molecules. Fitch et al. (1999) found that early in the progressive cavitation process, when the lesion is abandoned by astrocytes, but still filled with a high density of microglia / macrophages, there are increased levels of chondroitin sulfate proteoglycans (CSPGs), which prevent repopulation of the cavity by astrocytes. Thus, it may well be that minocycline in the first six days does not change the quantity of microglia activation but specifically down-regulates signals that prevent astrocyte repopulation, one of which might be CSPG.

6. METHODOLOGY DEVELOPMENT: *IN VIVO* LABELING OF SVZ CELLS IN ADULT RATS

6.1 Introduction

It is now well accepted that neurogenesis in the adult rodent brain is retained within two restricted regions: the SVZ of the lateral ventricle and the DG of the hippocampus. SVZ multipotent progenitors give rise to neuroblasts that migrate to the OB via a restricted pathway, the rostral migratory stream. Upon reaching the subependymal zone, which is located in the middle of the OB, the majority of neuroblasts migrate to the granule cell layer while a small fraction of neuroblasts reach the glomerular layer, which is the most superficial layer in the OB, and then differentiate into interneurons in each region (Alvarez-Buylla and Lim, 2004).

In response to ischemic injury in the adult brain, the appearance of new neurons has been observed in normally non-neurogenic regions, such as the neocortex, striatum and hippocampus, by several groups (reviewed in section 1.3.2). The appearance of these new neurons can be due to two mechanisms: 1) local parenchymal precursors might activate and differentiate into new neurons after injury; 2) precursors from normally neurogenic regions, such as the SVZ, might migrate towards the injured parenchyma in response to the ischemic stimulus. Recent studies have suggested that precursors from the SVZ might be the primary source of such newborn neurons in the adult (reviewed in section 1.3.2).

Do SVZ-derived progenitors serve as an endogenous source for replacement associated with brain injury induced by PVD II? To address this issue, one needs a reliable method for labeling large numbers of SVZ precursor cells, thus making it possible to track their migration and differentiation. Several methods have been used to trace SVZ-derived progenitors during the migration process or after differentiation, such as the use of BrdU, fluorescence dyes and retroviral vectors

(Doetsch and Alvarez-Buylla, 1996; De Marchis et al., 2001; Parent et al., 2002; Petreanu and Alvarez-Buylla, 2002; Winner et al., 2002; Saghatelyan et al., 2003).

BrdU, a thymidine analog, is administered intraperitoneally and is incorporated into newly synthesized DNA. An antibody directed against BrdU allows the identification of cells that have already incorporated BrdU, thus providing a marker for all cells that had DNA synthesis in the presence of BrdU (Taupin, 2006b). This will include all the dividing cells along the SVZ-RMS-OB axis. Retroviruses are suitable for identification of mitotic cells because viral integration only occurs when cells undergo complete cell division. RVs normally carry a reporter gene, whose expression requires viral integration into the host genome, and allows direct visualization and analysis of the transfected cells and their progeny. When such a vector is stereotaxically injected into the SVZ, dividing cells such as neural progenitors in this area would be infected. However, it seems the labeling efficiency is lower than with BrdU (Sohur et al., 2006). Lipophilic tracers, such as DiI or cell tracker green, can passively diffuse in between the lipid membrane bilayer of cells, therefore yielding excellent labeling of all neuronal processes. Thus, fluorescent tracers have also been used to labeling SVZ cells with the aid of stereotaxic injection (De Marchis et al., 2001).

The aim of the following experimental section was to develop a reliable and reproducible method for *in vivo* labeling of large numbers of SVZ cells, thus making it possible to track their migration and differentiation. In the following study, three methods were compared: BrdU loading, retrovirus injection and fluorescent tracer injection, to label and trace SVZ-derived progenitors in the normal and injured rat brain.

6.2 Results

6.2.1 BrdU-Labeled Cells in the Normal and PVD II Rat Brains

Three days after intraperitoneal BrdU injection (for protocol see Materials and Methods), the majority of BrdU-labeled cells in normal adult rats were located in the SVZ, the RMS and the hippocampus, all areas where neurogenesis persists into adulthood. In addition, a few BrdU-labeled cells were scattered throughout the corpus callosum and the parenchyma of the neocortex. This probably indicates glial

proliferation, which occurs at a slow rate in these areas. In rats subjected to PVD II, there was a substantial number of BrdU+ cells in addition to those observed in the normal brain: these were inside and around the cortical ischemic lesion two or three days after PVD II (Fig 6-1).

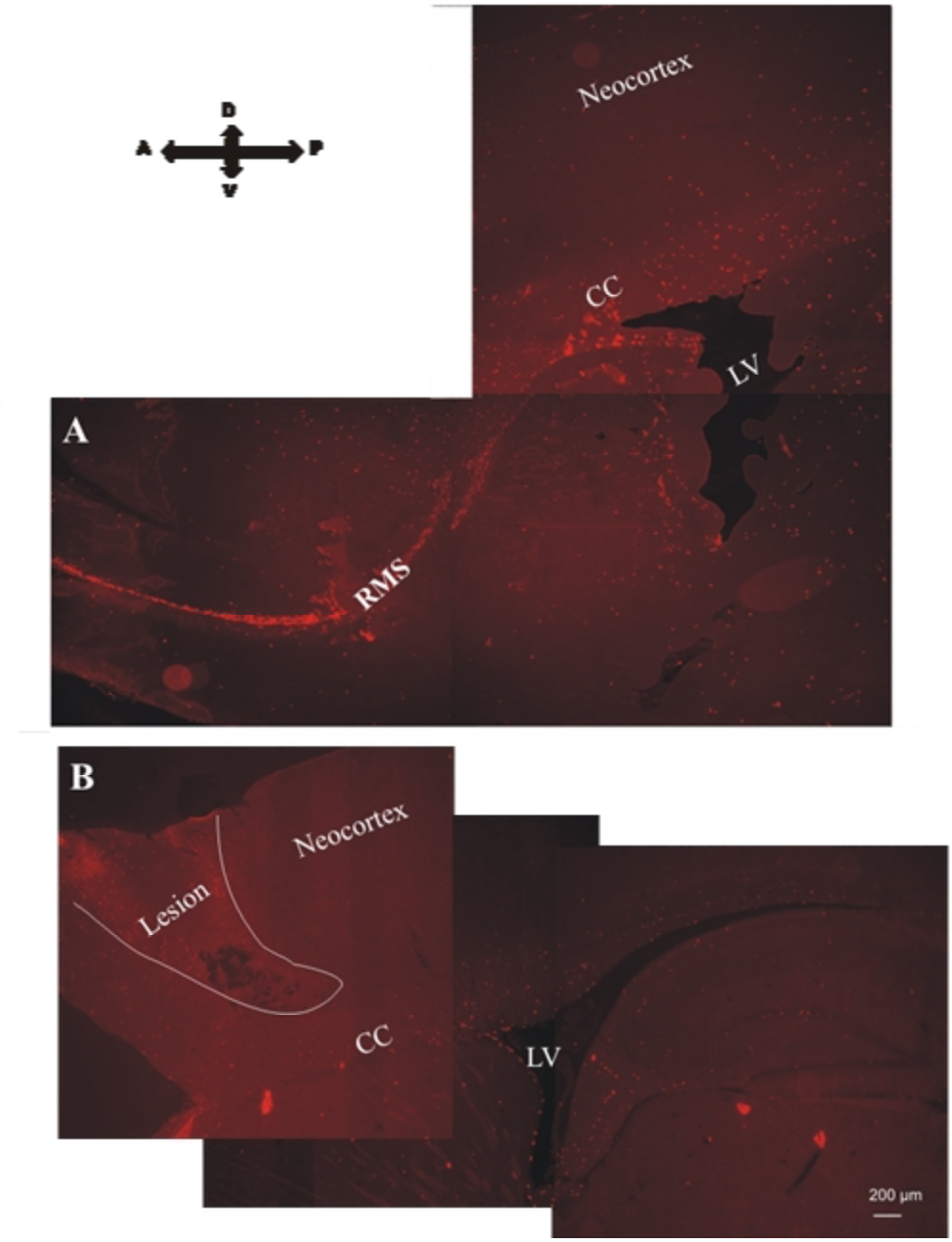

Figure 6-1. Distribution of BrdU+ cells two days after PVD II. A: Parasagittal section, including the whole RMS, demonstrates BrdU labeling throughout almost the entire length of the RMS (densely stained red line). B: The parasagittal section includes the lesion from the same animal. A substantial number of BrdU+ cells were observed in the PVD II lesion. Although the majority of BrdU-labeled cells were located in the SVZ of LV, the RMS and the hippocampus, a few BrdU+ cells were also scattered throughout the CC and the parenchyma of the neocortex. Red dots are the BrdU+ cells. Scale bar: 200 μm. RMS: rostral migratory stream; LV: lateral ventricle; CC: corpus callosum.

6.2.2 Retrovirus Labeled Cells in the Normal and PVD II Rat Brains

RVs will only be taken up by mitotic cells (Craig et al., 1999; Hu and Pathak, 2000). A replication-deficient RV carrying the Lac-Z gene, which produces the marker enzyme β-galactosidase, was utilized to label proliferating neuronal progenitors in the SVZ (Craig et al., 1999). Four or 6 days after intraventricular injection of the RVs, only a few labeled migrating cells were seen along the SVZ-RMS-OB pathway (Fig. 6-2). Surprisingly, there were very few labeled cells in ependymal and subependymal cell layers. Instead, many choroid plexus cells were labeled by β-galactosidase. In addition, scattered β-galactosidase labeled cells were observed elsewhere in the rest of the brain. The density of labeled cells in different brain areas are as follows: choroid plexus > olfactory bulb > striatum > cortex (Fig. 6-2). Except in the choroid plexus, most of the labeled cells had a macrophage-like morphology and were associated with blood vessels. In the PVD II animals, some labeled cells were observed within the lesion, exhibiting a morphological appearance similar to macrophages.

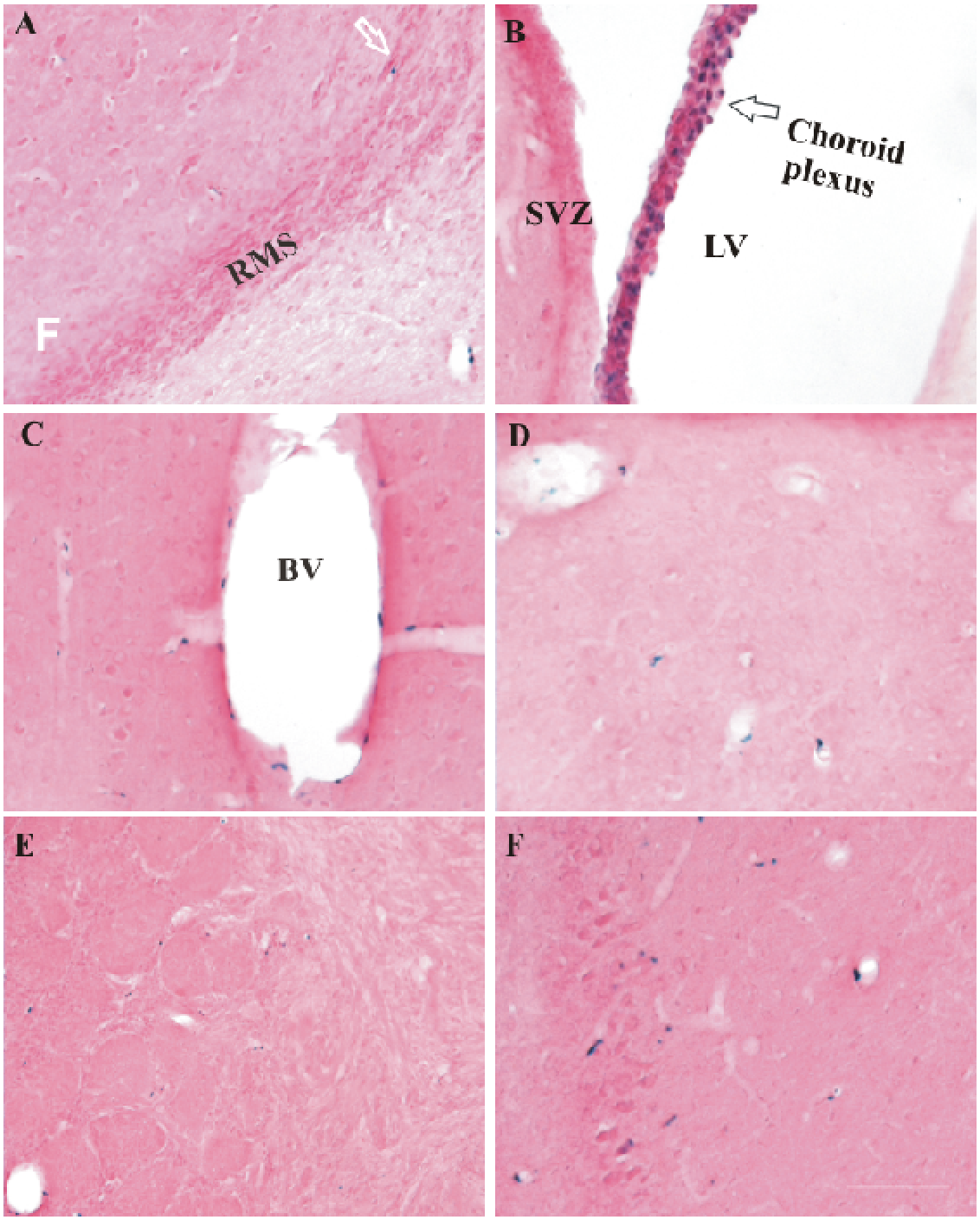

Figure 6-2. Distribution of β-galactosidase positive cells (blue cells) six days after intraventricular injection of RVs, in the RMS (A), choroid plexus (B), cortex (C), striatum (D), OB (E, F). Only a few labeled migrating cells were seen along the SVZ-RMS-OB pathway. The labeled cells can be seen elsewhere in the brain and the order of their density is: choroid plexus (B) > olfactory bulb (E, F) > striatum (D) > neocortex (C). Labeled cells are very often found associated with blood vessels. Scale

bar: 100 μm. BV: blood vessel; RMS: rostral migratory stream; SVZ: subventricular zone.

6.2.3 DiI-Labeled Cells in the Normal and PVD II Rat Brains

Similarly, injection of DiI into the adult brain lateral ventricle resulted in strong labeling of cells in the ependymal layer throughout the ventricular system including the contralateral lateral ventricle. This suggests that injection of DiI into the lateral ventricle results in the movement of DiI throughout the CSF. However, it did not result in DiI-labeled migrating cells in the RMS or olfactory bulb. Taking into consideration the architecture of the SVZ, SVZ cells have little direct contact with the lateral ventricle since it is separated from the lateral ventricle by the ependymal cell layer. Thus, to target SVZ cells, the injection site should be aimed directly at the subventricular area of the lateral ventricle.

In order to position the tip of the needle in the SVZa, three coordinate references to either the bregma skull or pial surface were tested (Table 6-1). Stereotaxic injection of DiI into SVZa resulted in a strong labeling of the lateral ventricle, which suggests that the released DiI was not restricted to the SVZa, but could diffuse into different cell layers of the lateral ventricle. However, in contrast to the injection into the lateral ventricle, strong DiI labeling of the RMS and the core of the OB were observed in all the SVZa injected animals. The higher-magnified view shows that the DiI-labeled migrating cells are organized as chains (Fig 6-3). Although DiI injection into the SVZa resulted in very strong labeling of the RMS and the core of the OB, a major issue encountered in this study was the lack of a difference in the migratory distance of labeled cells between day 5 and day 11 post-injection animals (Table 6-1). No DiI-labeled cells were observed in the granule cell layer of the OB even 11 days after the injection, which contradicts the findings in the literature. It has been suggested that the neuroblast migration from the SVZ to the OB will take 2 to 9 days (Petreanu and Alvarez-Buylla, 2002; Geraerts et al., 2006).

Table 6-1. Cell labeling after DiI microinjection into the SVZa at different stereotaxic coordinates after different survival times.

Coordinate (SVZa)			Survival days		DiI labeled cells		
AP	ML	D		n	RMS	OB core	GCL
0	1.4	4.8	5	1	+++	+++	-
0	1.4	4.6	11	1	+++	+++	-
0	1.5	3.3*	11	1	+++	+++	-
0.5	1.4	4.8	5	1	+++	+++	-

Stereotaxic coordinates are with reference to the bregma (mm). AP, anteroposterior; ML, medial lateral; D, depth from the skull surface; *represents the depth from the dura matter. Sections were visually scored for the density of DiI labeling in the RMS and OB; +++, dense labeling, ++ moderate labeling, + weak labeling, - no labeling. RMS: rostral migratory stream; OB: olfactory bulb; GCL: granule cell layer; SVZa: anterior of subventricular zone.

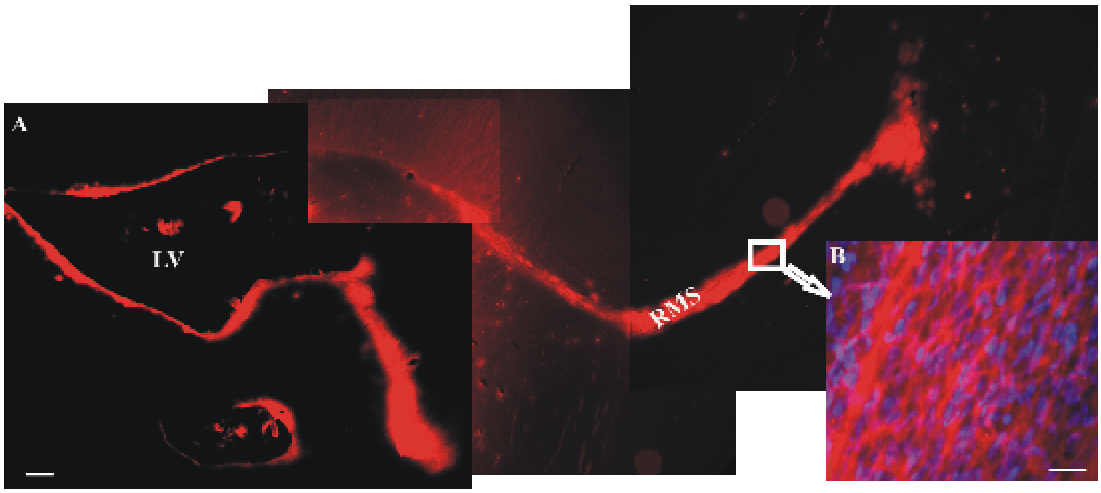

Figure 6-3. DiI labeling after stereotaxic injection into the SVZa. Stereotaxic injection of DiI into the SVZa resulted in strong DiI labeling of the RMS and the wall of the ventricular system (A) in all injected animals. B: The higher-magnified view of RMS (boxed region in A). The nuclei were stained with Hoechst 33243. In contrast, DiI injection into the LV results in heavy labeling of the ependymal layer throughout the

ventricular system only, but very weak or no labeling of the RMS. Scale bar: 200 µm (A); 100 µm (B). LV: lateral ventricle; RMS: rostral migratory stream.

6.2.4 Migration of CFSE-Labeled SVZ Cells in Normal Rats

CFSE is a lipophilic molecule. However, unlike DiI, it is colourless and nonfluorescent until it is transported into cells, where its acetate groups are cleaved by intracellular esterases. To investigate the suitability of CFSE as a label for the SVZ-derived progenitors, 200 nl of 10 mM CFSE were injected into the SVZa and the animals were sacrificed at different time points (1, 3, 5, 7 and 14 days). Since CFSE was injected into the brain tissue (SVZa) instead of ventricles, the injection volume was reduced to 200 nl rather than µl volumes, and the injection speed was limited to 0.1 µl/min with the aid of a microinjector in order to minimize the tissue damage induced by the *in vivo* injection. After injection and sacrifice, parasagittal sections were cut in the cryostat. Preliminary experiments were carried out to test the different concentrations (10 µM, 100 µM, 1 µM, 10 mM) for CFSE, with 10 mM resulting in the strongest cell labeling as indicated by visual observation.

One day after CFSE injection, labeled cells were found mainly in the SVZ and RMS, but not in the core of the OB. Three days later, labeled cells were detected not only in the RMS, but also in the OB, which is in accordance with previously described reports, in which neuroblast migration from the SVZ to the OB occurs within 2 to 9 days (Luskin, 1993; Petreanu and Alvarez-Buylla, 2002). CFSE labeled cells in the RMS showed the typical morphology of migrating neuroblasts, that is an elongated cell body and a leading process usually pointing toward the OB (Fig 6-4). By days 5-7, CFSE labeled cells were observed along the RMS and in the core of the OB. From 7 days on, labeled cells started to appear in the GCL of the OB. By days 10-14, more labeled cells were observed in the GCL and some labeled cells were also seen in the more superficial layers of the OB, such as the glomerular layer. At day 14, the fluorescence intensity was decreased and the fluorescence distribution became uneven, but the labeling was still detectable. In addition, cells in the SVZ were always strongly labeled at any time period examined.

Both ipsilateral SVZ cells and ependymal cells were labeled with CFSE, while contralateral ependymal cells were rarely labeled and no CFSE-labeled cells were found on the pial surface. These findings suggest that with this injection method, CFSE was not transported within the bulk flow of cerebrospinal fluid and did not label the contralateral lateral ventricle as shown by some authors (Ramaswamy et al., 2005). Outside the SVZ-RMS-OB axis, some CFSE-labeled cells were observed in the striatum at all time points. Other than these cells in the striatum, very few CFSE-labeled cells were observed outside of the SVZ-RMS-OB axis. To determine the identity of the labeled cells, immunostaining was performed: CFSE-labeled cells in the SVZ and the RMS were DCX+. A number of DCX+ cells were labeled with CFSE (Fig 6-5). This indicates that a considerable number of migrating neuroblasts was labeled by the CFSE injection into the SVZa.

In conclusion, CFSE labels and stays in SVZ cells through several generations and it can be detected in SVZ progeny for at least 14 days. By injecting CFSE into the anterior of the SVZ, SVZ-derived progenitors and their progeny could be traced. Therefore, this method is a useful tool to study SVZ-derived cell migration and differentiation.

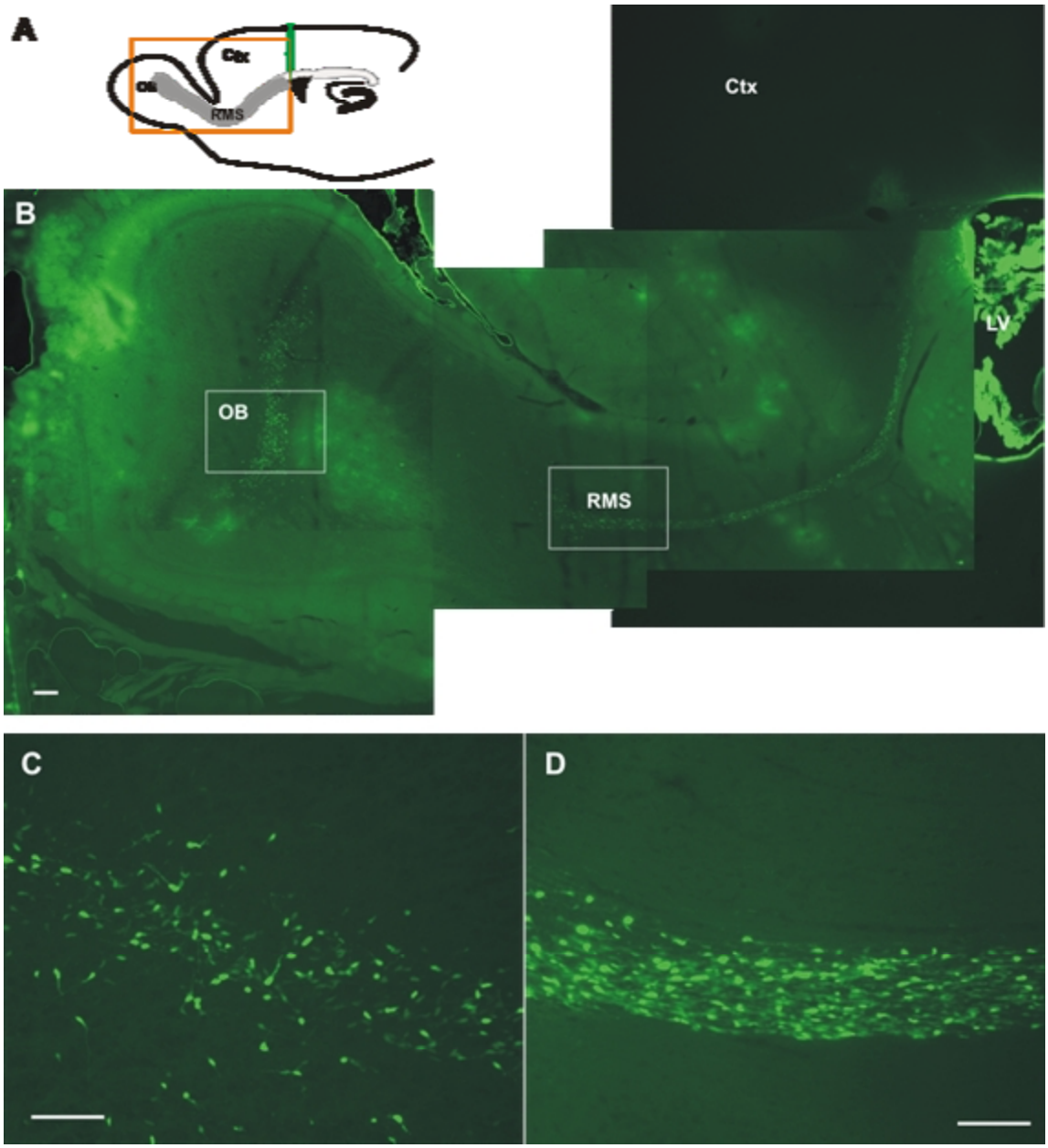

Figure 6-4. Distribution of CFSE-labeled cells in the adult rat brain seven days after CFSE injection into SVZa. A: Schematic drawing with the injection site on the parasagittal brain section. B: Enlargement of the orange box in A, giving an overview of CFSE-labeled cells. C, CFSE-labeled cells in the RMS, enlarged view of the right square outlined area in B. D: CFSE labeled cells in the GCL of OB, enlarged view of the left square outlined area in B. Scale bar: 200 μm. RMS: rostral migratory stream; OB: olfactory bulb; GCL: granule cell layer; Ctx: cortex.

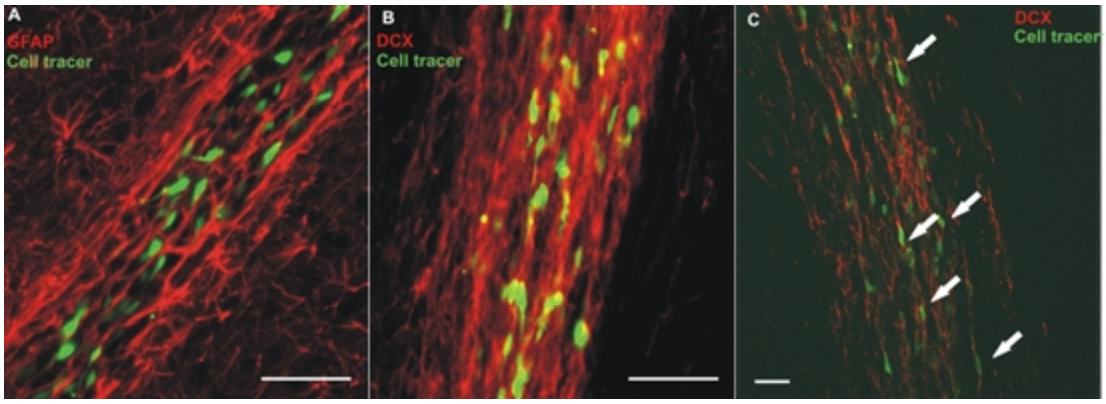

Figure 6-5. Typical appearance of CFSE-labeled cells in the RMS in the parasagittal sections, 3 days after CFSE injection into the SVZa. A: GFAP immunostaining shows that CFSE-labeled cells in the RMS do not express GFAP. These CFSE-labeled cells migrate through a tube-like structure, which is formed by cells expressing GFAP. B: DCX immunostaining shows that all CFSE-labeled cells also express DCX in the RMS. C: Same section viewed with the aid of a confocal microscope, which confirmed the colocalization of DCX and CFSE (white arrows). Scale bar: 50µm.

6.3 Discussion

To date, *in vivo* labeling of SVZ cells of adult brain has been achieved by BrdU administration, retrovirus or fluorescent tracer injection. In this study, I compared these different methods, assessed their effectiveness and conclude that the CFSE injection method into the SVZa outperforms the other two methods, using reproducibility and efficiency of the labeling of adult rodent SVZ precursor cells as criteria.

I have shown that SVZ-derived neuronal progenitors can be labeled by BrdU. BrdU has been the most commonly used method in the studies of neurogenesis. However it has certain disadvantages. It has been reported that high concentrations of BrdU are toxic and that repeated administration is stressful for animals (Rakic, 2002). BrdU only labels the nucleus, therefore the images do not highlight the cytoplasm, dendrites and axons of the labeled cells. Moreover, incorporation of BrdU depends on various factors such as blood flow and vascular permeability, which are affected by the lesions. In order to avoid labeling the proliferating astrocytes, microglia and infiltrated inflammatory cells that are activated by ischemic injury, BrdU was loaded before the induction of the PVD II. Still, substantial numbers of BrdU-labeled cells were observed in the ischemic lesion 3 days after injury, which suggests that cells of hematopoietic origin were labeled and that they infiltrated the lesion. Double staining for a neuronal progenitor cell marker (using DCX or ßIII-tubulin) in combination with immunohistochemistry for BrdU would be able to confirm the neuronal phenotypes of the newly generated (BrdU+) cells. However, I would still not be able to conclude that these cells originated from the SVZ, because BrdU was administrated systemically and therefore it potentially labels all proliferating cells including cells that divide *in situ* in the parenchyma, such as oligodendrocyte precursor cells (OPCs) as well as cells of hematopoietic origin that infiltrate after injury. Stereotaxic injection of BrdU into the SVZa might overcome the above-mentioned problems and therefore provide a useful tool to label SVZ precursor cells (Ohab et al., 2006).

Ventricular injection of the retrovirus resulted in sparse labeling along the SVZ-RMS-OB pathway. A possible explanation is that as the ependymal layers form a physical barrier with the underlying SVZ, only a very limited number of type B cells in

the SVZ are in contact with the ventricular lumen (Doetsch et al., 1997; Doetsch et al., 1999). Subsequent experiments with DiI injection into the lateral ventricle resulted only in heavily labeled ependymal cells throughout the ventricular system, but very weak or no labeling of cells in the RMS. The results therefore confirm this assumption. Indeed, a study by Rogelius et al. (2005) showed that injection of RV into the lateral ventricle of adult rats resulted in the labeling of only a few cells along the SVZ-RMS-OB pathway, whereas injection into the SVZ dramatically improved the labeling efficiency. Consiglio et al. (2004) reported as well that injection of a lentiviral vector into the SVZa but not into the lateral ventricle resulted in labeling of OB neurons. Labeled SVZ cells have been reported using both intraventricular injection (Morshead et al., 1998; Craig et al., 1999) and SVZ injection (Petreanu and Alvarez-Buylla, 2002; Yamada et al., 2004) of RV. However, it is difficult to compare the results of different investigators as transfection efficiency depends largely on the virus concentration, the injected volume of the virus and the choice of promoter (Vercelli et al., 2000). In the present study, the injection of RVs into the lateral ventricle failed to label even ependymal cells, which are slowly dividing cells (Doetsch et al., 1999). Instead, RVs preferentially labeled choroid plexus cells. The reason that the delivery of retrovirus into the lateral ventricle resulted in a selective transfection of choroid plexus cells but not ependymal cells is not entirely clear. It may be due to the RV preferentially labeling fast dividing cells (Rogelius et al., 2005). Surprisingly, scattered β-galactosidase labeled cells were observed everywhere in the brain parenchyma. Most of the labeled cells had a macrophage-like morphology and were associated with both small and large blood vessels. Due to their morphology, close association with the vasculature and their position on the abluminal surface of the vessels, I propose these cells are pericytes or perivascular cells (Thomas, 1999; Allt and Lawrenson, 2001; Betsholtz et al., 2005). Hematopoietic stem cells (HSC) derived from bone marrow have been shown to differentiate into both parenchymal microglia and perivascular cells in the brain and the numbers of these cells increase after cerebral ischemia (Hess et al., 2004; Kokovay et al., 2006). In this study, the RVs might have been transported with the CSF bulk flow, absorbed at the venous sinuses, making their way into the blood circulation, where RVs labeled the bone marrow-derived cells, such as HSC. However, no labeled cells having the highly ramified morphological

characteristic of parenchymal microglia were observed in this case. This might be due to the different differentiating time of the lineage derived from bone marrow. In a study that used transplanted high level hematopoietic reconstitution from a single enhanced green fluorescent protein (EGFP) stem cell into lethally irradiated recipient mice, there were few BM-derived (EGFP+) microglia cells in the brain parenchyma 2 months post-transplantation. However, 4 months later, these cells were abundant in all mice that survived for 4 months or more post-transplantation, whereas BM-derived (EGFP+) pericytes were observed in the brain at both time points (Hess et al., 2004). This suggests that a different period of time may be needed for these HSC-derived cells to engraft as parenchymal microglia and pericytes. However, a further investigation of the nature of these cells is beyond the scope of this project.

Injection of DiI into the anterior of the SVZ resulted in very strong labeling of the RMS and the core of the OB 5 to 11 days after injection. Because of the extremely strong fluorescence in the SVZ and RMS, both with very high cell densities of labeled cells, it is hard to distinguish the individually labeled cells. Moreover, no labeled cells in the GCL of the OB were observed, even 11 days after the injection. Therefore, it is difficult to distinguish if the extremely strong DiI fluorescence of the RMS and core of the OB is the result of a large number of strongly DiI-labeled cells diffusing from the injection site or of leakage from previously labeled cells due to cell membrane damage. Cryostat sectioning was used to process tissue sections in this part of the study. Cryostat sectioning is known to cause damage to cell membranes. If this occurs, it could cause DiI leakage out of labeled cells (Vercelli et al., 2000). As DiI is a lipophilic carbocyanine dye, any permeabilizing reagents, detergents, or high concentrations of organic solvents have the potential to result in degradation of DiI labeling and cause the leakage of some DiI into the extracellular space. This would make it difficult to perform immunohistochemistry experiments, as these require disruption of the phospholipid bilayer. As well, the usage of antifade mounting media that contains glycerol, (such as citifluor) will extract membrane-bound DiI (Terasaki and Jaffe, 1991; Hayaran and Bijlani, 1992; Vercelli et al., 2000). I therefore think that the fading of the dye and fluorescent labeling in the sections is a serious enough issue to interfere with the reliability of this labeling method. In the present experiments immunofluorescent

staining will always have to be applied in order to characterize the phenotype of the DiI labeled cells. Double staining is also needed for quantification and co-localization procedures. It therefore is unavoidable. Taking into consideration all these limitations of DiI, the use of DiI *in vivo* labeling of SVZ cells for this study was not implemented.

CFSE was chosen for this study because it offers several advantages over DiI. Its succinimidyl ester group reacts covalently with the free amino groups of intracellular macromolecules, which enhance its retention time within cells and therefore its ability to be retained intracellularly throughout the aldehyde fixation and immunostaining procedures. Another advantage of CFSE is that it is colorless until it is transported into cells, where its acetate groups are cleaved by intracellular esterases and it is only then that it becomes a highly fluorescent molecule. Therefore, excess unconjugated reagent will passively diffuse through the extracellular space and will be diluted, but it will not be fluorescent. Due to these properties, CFSE-labeled lymphocytes have been successfully tracked *in vivo* up to 8 weeks after injection into mice (Weston and Parish, 1990). CFSE has predominantly been used in lymphocyte proliferation and migration studies and it has also been used to track transplanted Schwann cells (Li et al., 2003) and neuronal cells *in vivo* (Paramore et al., 1992). It has also been shown that the fluorescent signal diffuses evenly throughout the cytoplasm of the labeled cells and is evenly divided between daughter cells with high fidelity and without leakage (Li et al., 2003).

In this study, the effectiveness of an injection of CFSE into the SVZa of adult rats to label migrating SVZ cells was assessed. The time of appearance and the phenotype of SVZ cells in the RMS and OB were consistent with previous studies using different approaches (Petreanu and Alvarez-Buylla, 2002). The time required for newly generated SVZ neuroblasts to reach the OB is 2 to 9 days (Luskin, 1993; Petreanu and Alvarez-Buylla, 2002). In the present study, within that time frame, most labeled cells were located in the OB, distributed in different layers. Unlike RV-based labeling that will only label dividing cells, preferentially fast dividing cells, CFSE will label all SVZ cells. Although no quantification was done, it seems the number of labeled cells in the RMS decreased over time, as the labeled cells were found to migrate further into the OB. However, cells in the SVZ were always well-labeled. This disappearance of CFSE-labeled cells from the RMS indicates that the primary cell types labeled by the

CFSE injection into the SVZa in this study are the fast dividing precursors (type C) and neuroblasts (type A). Very few stem cells (type B) were labeled. An alternative explanation is that the neural stem cells (type B) were labeled and the fluorescence was diluted out when the cells differentiated into neuroblasts and immature neurons due to the frequent cell division. This also highlights some of the limitations of using vital fluorescent dyes to mark the ontogeny of cells *in vivo*.

Compared with DiI, CFSE is able to be retained throughout fixation and permeabilization procedures. In this study, it has been demonstrated that cells within the SVZ can be labeled and followed over 14 days after injection of CFSE into the SVZa.

7. APPEARANCE OF MIGRATING NEUROBLASTS IN THE ISCHEMIC PENUMBRA OF THE PVD II-INDUCED LESION

7.1 Introduction

Adult neurogenesis is a phenomenon that has received a lot of attention in the last decade. As reviewed in the Introduction (section 1.3.2), although adult neurogenesis in the mammalian CNS is a robust and reproducible occurrence, four qualifications have to be considered. 1) Adult neurogenesis is species-dependent with what appears to be a gradual restriction during evolution (Bhardwaj et al. 2006). 2) While there is no doubt that this phenomenon occurs in the subventricular zone, olfactory bulb and dentate gyrus of many species, especially rodents, its occurrence in other brain areas is controversial (Bhardwaj et al., 2006). 3) Adult neurogenesis can be enhanced and induced by factors in the environment like behavior patterns associated with learning, as well as by injury (e.g. ischemia, hemorrhage, etc.) or drug treatment (Lindsey and Tropepe 2006). 4) It has also to be kept in mind that many newly generated neurons may have a transient appearance and may never turn into mature cells, much less into full-fledged participants of neural circuits (Lledo et al. 2006).

Most of the studies on post-stroke neurogenesis have used stroke models involving large vessel occlusion, resulting in massive lesions, such as MCAO. The PVD II model is a modified cortical devascularizing model that is induced by the disruption of only the medium sized pial vessels on a 5 mm diameter cortical surface. This creates a small cone-shaped cortical lesion, restricted mainly to the frontal cortex, involving mostly the primary motor cortex and sometimes the hindlimb sensorimotor cortex as well. The tip never reaches deep enough to touch the corpus callosum (Wang and Walz, 2003). After two weeks, cavitation develops at the site of the lesion.

This stroke model therefore has features resembling the lacunar infarctions observed in humans as a result of small vessel occlusion and silent strokes. Reactive astrocytes surround the lesion, and those in the space between the base of the lesion and the corpus callosum are highly reactive, expressing a high density of vimentin (Wang et al., 2004). This area is strategically situated along a hypothetical pathway, SVZ – RMS - corpus callosum – lesion. One function of these vimentin+ reactive astrocytes could be to serve as a guiderail for the migration of neuroblasts or other newly created precursor cells. Indeed, it was shown here that DCX+ cells appear with the morphology of migrating neuroblasts. Although these DCX+ cells were seen both in the portion of the ischemic penumbra containing vimentin+ astrocytes and in the adjacent part of the corpus callosum, I was not able to confirm that these cells arose from the SVZ/RMS pathway.

7.2 Results

7.2.1 No DCX+ Cells in the Neocortex of Control Rats

Control rats include normal rats that had no surgery, and sham rats, which underwent the whole pial vessel disruption procedure except the disruption of the class II vessels. As expected, the strongest DCX immunoreactivity in normal and sham rats was found in the lateral and dorsal SVZ of the lateral ventricle, the RMS, the accessory olfactory bulb, and the dentate gyrus of the hippocampus (Fig. 7-1 A, F, G). DCX+ cells in the RMS assembled into chains and showed the characteristic morphology of migrating neurons: an ovoid cell body with a leading process (Fig. 7-1 B). Isolated or clusters of DCX+ cells were also seen in the corpus callosum, with their morphology resembling migrating neurons (Fig. 7-1 E), and in the striatum of these sham and normal rats (Fig 7-1 C, D). The characteristic morphology of DCX+ cells in the striatum appeared more like differentiated neurons with long branched processes (Fig. 7-1 D). Numerous DCX+ cells in the RMS were double-labeled with Ki67, which is a marker for dividing cells (Lu et al., 2005). The expression of Ki67 by the DCX+ cells indicates they are proliferating as they migrate along the SVZ/RMS as shown previously by Komitova et al. (2005). DCX immunostaining of parasagittal sections of both normal

and sham rats did not reveal any DCX+ cells in the neocortex. In addition, there were no DCX+ cells in the cortex of the contralateral hemisphere of rats that underwent PVD II at any time period investigated in this study.

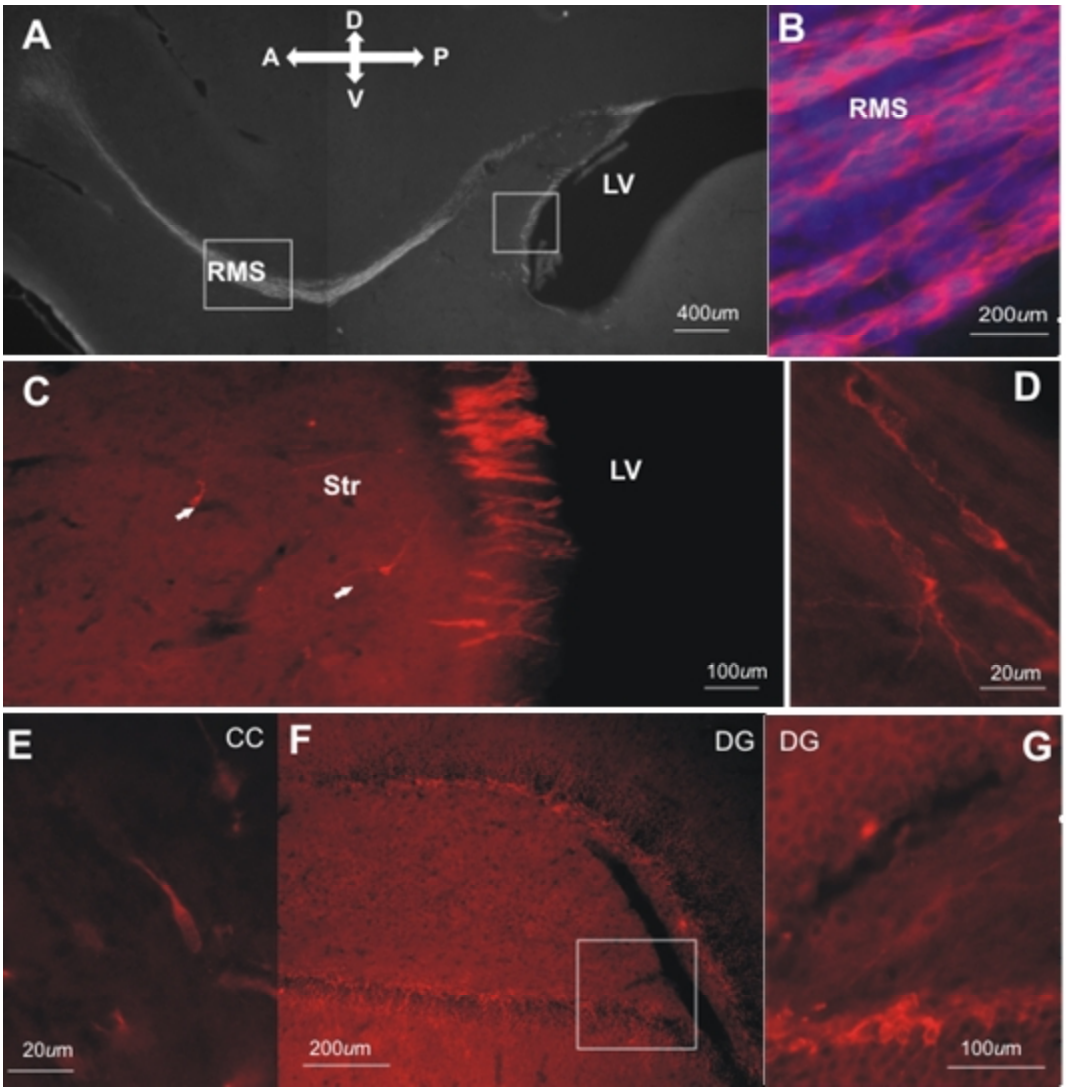

Figure 7-1. Distribution of DCX+ cells in the normal adult rat brain. A: Overview of a parasagittal section shows intense immunostaining in the dorsal and anterior SVZ of the lateral ventricle, RMS and the accessory OB. B, C: Higher magnified views of the rectangular crop areas in A. B, Enlarged view of the RMS. The Hoechst counterstained DCX+ neuroblasts are densely packed and chain-migrating in the RMS. C: Enlarged view of the striatum and striatal SVZ. Scattered DCX+ cells (arrows) in the vicinity of the SVZ. D: Morphology of typical DCX+ cells in the striatum. E: Morphology of the typical DCX+ cells in the CC. F: DCX immunoreactivity in the DG of the

hippocampus. G: Higher magnified view of the rectangular crop area in G. Scale bar: 400 µm (A); 200 µm(B, F), 100 µm (C, G); 20 µm(D,E). RMS: rostral migratory stream; OB: olfactory bulb; LV: lateral ventricle; Str: striatum. DG: dentate gyrus; CC: corpus callosum.

7.2.2 DCX+ cells in the Neocortex and Corpus Callosum after the PVD II Lesion

In the present study, adult rats were sacrificed 1 (n=5), 3 (n=3), 5 (n=5), 10 (n=5) and 14 (n=4) days after pial vessel disruption. Unlike what was seen in the normal and sham rats, DCX+ cells were located in the neocortex between the PVD II-induced lesion and the CC in 1 out of 5 rats of the day 1 post injury group, 2 out of 3 rats in the day 3 post injury group, 2 out of 5 rats in the day 5 post injury group, 4 out of 5 rats in the day 10 post injury group and 3 out of 4 rats in the day 14 post injury group. These DCX+ cells in the neocortex had a morphology resembling differentiated post migratory neurons with long branched processes (Fig. 7-2 C, D, E). A larger number of DCX+ cells were observed in the corpus callosum of PVD II lesioned rats and these cells were more likely to exhibit a migratory morphology with leading and trailing processes (Fig. 7-2 F).

The number of DCX+ cells in the neocortex and corpus callosum underneath the PVD II lesion was quantified in all groups. The one-way ANOVA revealed a significant increase of the number of DCX+ cells in the corpus callosum on day 5, 10 and 14 as compared to the number in the normal rats (n=3) and day 1 post injury. The one-way ANOVA did not reveal a significant effect of the time post-infarct for the number of DCX+ cells in the neocortex (Fig 7-3). However, in contrast there were no DCX+ cells in the neocortex of normal rats (see above) and sham rats; the DCX+ cells only appeared in the neocortex after PVD II and were maintained till 14 days after PVD II lesion (Fig. 7-3). By twenty-one days, the DCX+ cells were still present in the ischemic penumbra of the neocortex in 1 out of 3 animals. However, by 21 days post lesion, the numbers of DCX+ cells in both corpus callosum and neocortex appeared to decrease.

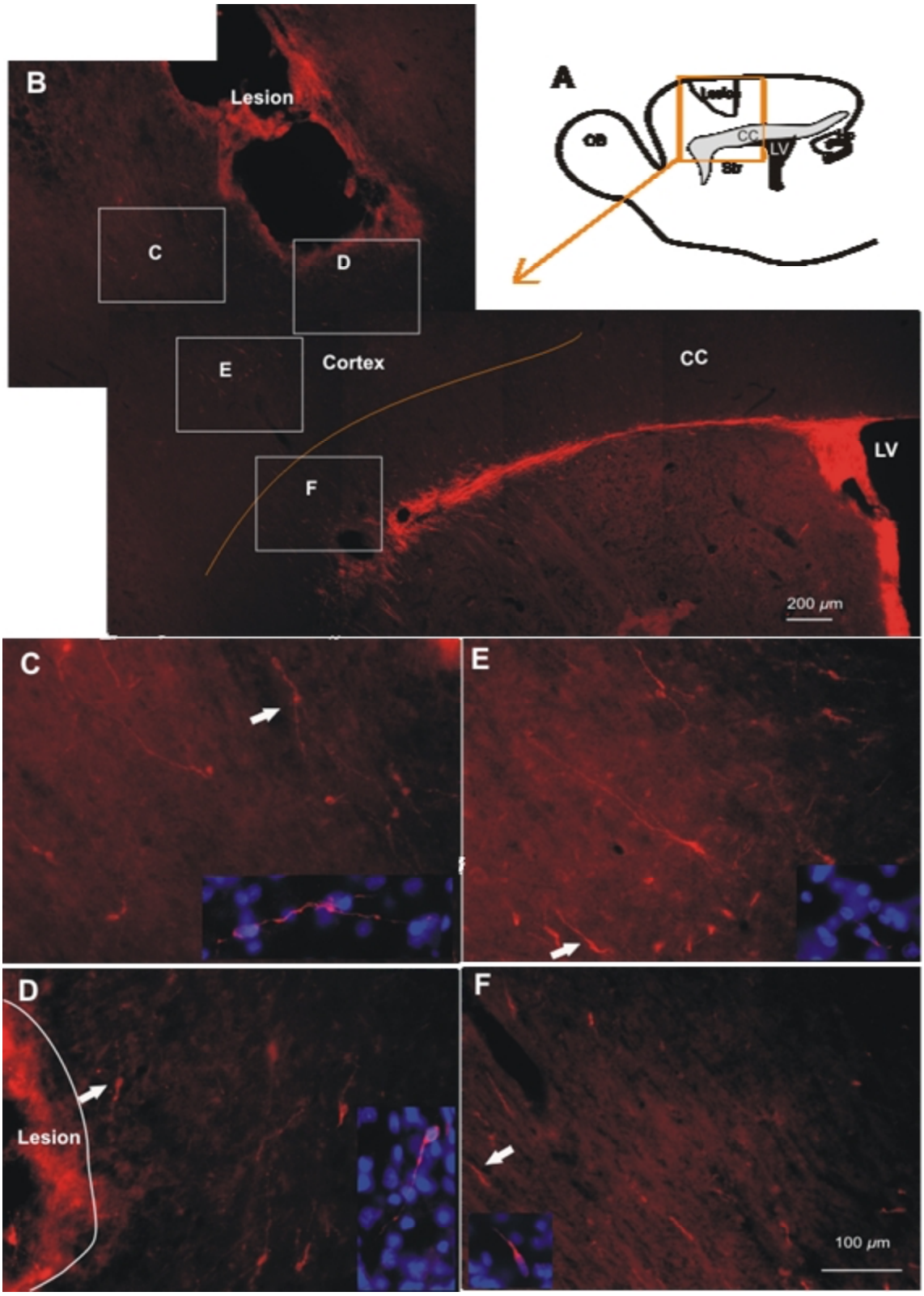

Figure 7-2. Distribution of DCX+ cells 14 days after PVD II. A: Schematic drawing of a representative parasagittal plane in an adult rat brain with the highest density of DCX+ cells. B: DCX+ cells were observed between the RMS and the lesion in both neocortex

and corpus callosum (CC). The area, which is represented by this overview picture, is given in the orange box in the drawing in A. C, D, E, F: Higher magnification of the rectangular areas c, d, e, f in B. They represent white matter (f) and the neocortex surrounding the lesion (c, d, e). Inserted pictures are the enlarged view of DCX+ cell (white arrow) merged with nuclei labeling (Hoechst, blue). The DCX+ cells in the neocortex exhibit a morphology more like differentiated post-migratory neurons (arrows in C, D and E) and DCX+ cells underlying white matter exhibit a migratory morphology with leading and trailing processes (arrow in F). Scale bar: 200 μm (B), 100 μm (C, D, E, F). CC: corpus callosum. OB: olfactory bulb; LV: lateral ventricle; Str: Striatum; Hp: hippocampus.

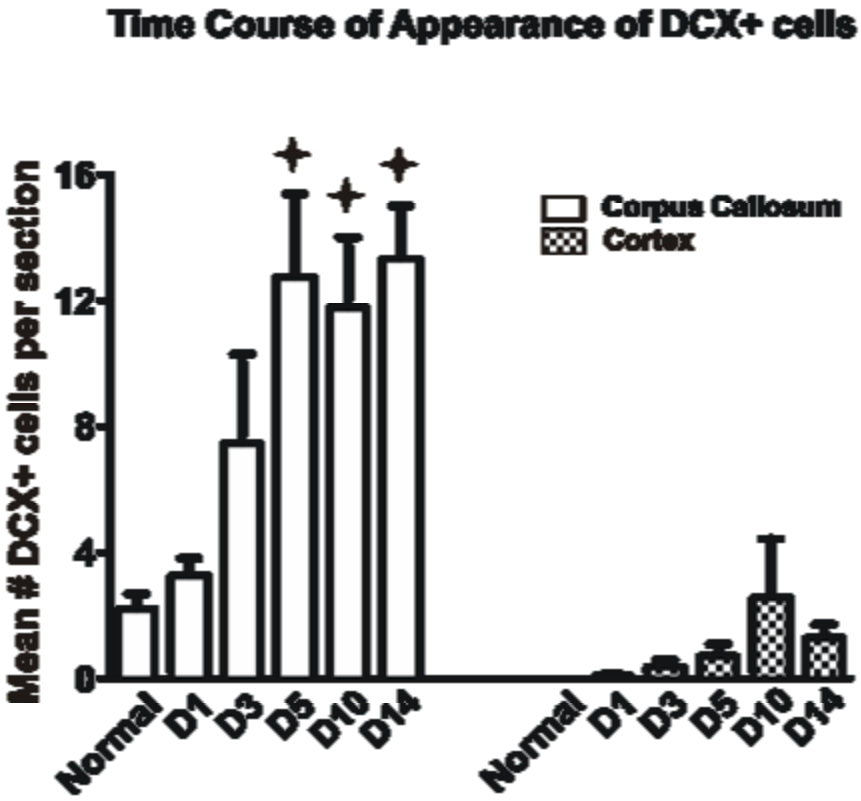

Figure 7-3. Quantification of DCX+ cells in the neocortex and corpus callosum underneath the lesion per 40 *u*m-thick section at different time points after PVD II. The one-way ANOVA was applied to the data, with the data for the corpus callosum and neocortex being analyzed separately for statistical significance. Multiple post hoc comparisons were performed with Bonferonni's multiple comparison post-test. The one-way ANOVA showed a significant main effect of the time post-infarct for the number of DCX+ cells in the corpus callosum, $F(5, 19)=5.622$, $^*P < 0.002$). However, the main effect of the time post-infarct was nonsignificant for the number of DCX+ cells in the neocortex, $F(5,19)=1.064$, $P=0.41$). Bonferonni's post-test revealed the number of DCX+ cells in the corpus callosum was significantly higher ($^*p<0.05$) in the post-infarct Day5, Day10 and Day14 rats than in either Day1 or in normal animals.

7.2.3 Further Characterization of the DCX + Cells

DCX, a microtubule-associated protein, is required for normal neuronal migration in the developing CNS and it is expressed in both radially and tangentially migrating neuroblasts. In contrast to the frequent colocalization of DCX and Ki67 in SVZ and RMS cells, the DCX+ cells underlying the lesion were not colabeled with Ki67, which suggests they were postmitotic (data not shown). Not a single DCX+ cell was observed that coexpressed markers of glia precursors or mature glia, NG-2, vimentin and GFAP. However, some of the DCX+ cells were immunoreactive for βIII-tubulin (Fig 7-4), another marker of immature neurons, which further confirmed their neuronal lineage. Thus, the appearance of DCX can be taken as a sign of immature, migrating cells of the neuronal lineage.

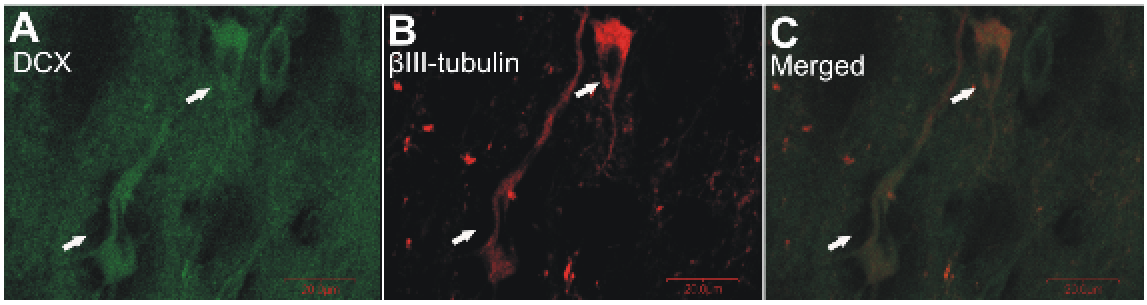

Figure 7-4. High-power confocal images showing a subset of DCX+ cells express βIII-tubulin. Cells double labeled (arrow) for DCX (green, A), βIII-tubulin (red, B), and overlap (orange, C) in the neocortex surrounding the lesion 5 days after PVD II. Scale bar: 20 μm.

7.2.4 *In Vivo* Labeling of Migrating Neuroblasts in the Subventricular Zone in Control Rats

The appearance of DCX+ cells in the neocortex is an indication that neuroblasts are trying to replace dead neurons. I hypothesize that these DCX+ neuroblasts were recruited in response to the ischemic injury from the SVZ and RMS into the neocortex

near the lesion. In order to test this hypothesis, SVZ cells of adult rats were labeled by stereotaxic injection of CFSE into the SVZa. The temporal and spatial distribution of CFSE-labeled SVZ cells and the character of labeled cells in the sham rats (CFSE injection followed by sham PVD II procedure), are similar to the distribution in normal rats (for details of distribution and migration of CFSE-labeled cells see section 6.2.4).

7.2.5 CFSE-Labeled Cells in PVD II Rats

The fluorescent cell tracker CFSE was injected unilaterally into the SVZa before the induction of the cortical ischemic lesion by disrupting the class II pial vessels. Rats were sacrificed 1(n=6), 3 (n=6), 5 (n=7), 7 (n=5), 10 (n=6) and 14 (n=8) days after the surgery. The successful labeling of SVZ cells in each animal was confirmed by the strong labeling of CFSE labeled cells in the SVZ, in the RMS and in the OB (data not shown). Although many CFSE-labeled cells were observed in the RMS and in the OB, there were no CFSE-labeled cells observed in either the corpus callosum or the ischemic penumbra underlying the lesion.

To test the possibility that neuroblasts born after the PVD II-induced injury were the ones preferentially being recruited to migrate towards the lesion, CFSE was injected into the SVZa 2, 3 and 5 days after PVD II and the animals were sacrificed 10 days (n=3) or 14 days (n=3) after making the lesion. There were still no CFSE-labeled cells located in either ischemic penumbra or the corpus callosum underneath the lesion.

7.3 Discussion

A cortical ischemic injury is induced by disrupting the pial vessel II on the sensorimotor cortex of adult Wistar rats. In response to this injury, DCX-expressing cells were present in the neocortex and corpus callosum underneath the lesion up to 14 days after injury. In this study, DCX was used as the principal marker of the migrating neuroblasts and immature neurons (Francis et al., 1999; Nacher et al., 2001). DCX, a microtubule-associated phosphoprotein, is required for normal neuronal migration in the developing CNS and is expressed in the migrating neuroblasts in both developing and adult brain. In the adult brain, DCX expression is mainly retained within the two areas of

continuous neurogenesis. It has been suggested that DCX is a reliable and suitable marker for adult neurogenesis (Brown et al., 2003; Couillard-Despres et al., 2005) and it is transiently expressed in newly generated neurons (Ming and Song, 2005). Furthermore, these DCX+ cells displayed the typical morphology of migrating neuroblasts in the white matter and differentiated neurons in the neocortex (Nacher et al., 2001; Brown et al., 2003) and they do not express markers of glia cells, such as GFAP and NG2, but another marker of immature neurons, βIII-tubulin. Therefore, based on both morphological and immunochemical characters, the appearance of DCX+ neuroblasts in the neocortex is an attempt of the brain to replace the dead neurons in response to ischemic injury. It is an indication of a repair process in the adult brain in response to the ischemic injury, although the numbers suggest the density of neuroblasts is at a low level.

To date, post-stroke neurogenesis has been well studied, mostly in the massive ischemic injury model induced by occlusion of MCA, and accumulating evidence suggests that focal ischemic injury can induce neurogenesis in peri-infarct striatum (Arvidsson et al., 2002; Parent et al., 2002; Jin et al., 2003; Zhang et al., 2004; Nygren et al., 2006a; Thored et al., 2006; Yamashita et al., 2006) and/or neocortex (Gu et al., 2000; Jiang et al., 2001; Jin et al., 2003; Ohab et al., 2006). Within the first two weeks, newborn immature neurons as indicated by the expression of neuronal lineage cell markers such as DCX or βIII-tubulin were observed in tissue surrounding the infarct area (Arvidsson et al., 2002; Parent et al., 2002; Jin et al., 2003; Zhang et al., 2004; Nygren et al., 2006a; Yamashita et al., 2006). A few weeks later, a portion of the newly generated cells expressed the markers for mature neurons, such as NeuN and region-specific mature neuronal markers, such as DARPP-42 and calbindin (Arvidsson et al., 2002; Parent et al., 2002; Yamashita et al., 2006). Interestingly, using different variations of the MCAO model, a model mimicking focal ischemia and inducing an excessive infarct in both neocortex and striatum, some studies found post-stroke neurogenesis in the injured cortex (Jiang et al., 2001; Jin et al., 2003). Other studies failed to detect cortical neurogenesis (Arvidsson et al., 2002; Parent et al., 2002; Zhang et al., 2004; Yamashita et al., 2006). However, all of these studies found moderate levels of post-stroke neurogenesis in the striatum. A recent study has shown substantial

cortical neurogenesis in the peri-infarct cortex (Ohab et al., 2006). In this study, with stereological quantification, they found around 2,000 DCX+ cells in the peri-infarct cortex per animal at day 3 after stroke, increasing to more than 10,000 DCX+ cells per animal at day 7. In the present study, the number of induced neuroblasts (DCX+cells) post-PVD II is much lower (estimated at around 150 DCX+ cells in the injured neocortex per animal) as compared to the number of DCX-expressing cells in the study by Ohab (2006). In that study, the focal ischemic injury was induced by permanent occlusion of the distal middle cerebral artery and transient occlusion of the bilateral common carotid in the mouse, and was mainly located at the somatosensory barrel field cortex (Ohab et al., 2006). As mentioned before, the PVD II model induces a smaller cortical ischemic injury as compared to other cortical ischemic models and the lesion is mainly located in the primary motor cortex. Taking these data together, it is highly likely that the nature of the injury, the location and extent/size of the ischemic injury may influence the degree of the signal(s) necessary to recruit migration of neuroblasts and induce neuronal subtype differentiation. Indeed, it has been shown that the number of the immature neurons and newly generated neurons in the striatum correlated significantly with the volume of the striatal injury (Thored et al., 2006).

This study did not attempt to determine the long-term survival of these DCX-expressing neuroblasts. Therefore the ultimate fate of these DCX+ cells is unclear. Long-term survival studies suggest that the majority of the newly generated neuroblasts in the damaged area undergo programmed cell death, while a small portion survive for many months, differentiate into neurons expressing mature neuron markers and regional specific neuron markers (Arvidsson et al., 2002; Ohab et al., 2006; Thored et al., 2006), and form synapses in the damaged area (Yamashita et al., 2006). This is an indication that these cells may be functional mature neurons. However, functional analysis, such as the use of electrophysiology to determine the neuronal properties of these newborn neurons was not undertaken.

The appearance of DCX+ cells in the neocortex and corpus callosum of adult rats after a cortical ischemic injury raises the question of the cellular origin of these induced DCX+ neuroblasts. Do they arise from local parenchymal precursors or precursors from normally neurogenic regions, such as SVZ, which might migrate long distances into the

injured neocortex in response to the ischemic stimulus? By directly labeling SVZ cells with DiI or a viral vector, SVZ neuroblasts have been shown to migrate into the damaged striatum and/or cortex in response to ischemic injury (Jin et al., 2003; Ohab et al., 2006; Yamashita et al., 2006) and traumatic injury (Ramaswamy et al., 2005). After PVD II, DCX + cells mainly located in both the neocortex and corpus callosum between the injury and SVZ area. These DCX+ cells display a differential morphology. It seems that in the white matter, DCX+ cells display the form typical of migrating neuroblasts, i.e. elongated nuclei with leading processes (Nacher et al., 2001; Brown et al., 2003). In the neocortex, DCX+ cells have a morphology more like a differentiated cell: a more rounded cell body with long and branched processes (Nacher et al., 2001). Time course quantification of DCX+ cells showed that the stroke-like injury first induced a peak of DCX+ cells in the subcortical white matter, and then in the peri-infarct cortex. These results suggest that these DCX+ cells migrate from the direction of the corpus callosum to the neocortex. However, the orientation of these DCX+ cells was not necessarily consistent with migration away from the corpus callosum toward the ischemic injury. I hypothesized that these DCX+ cells are originating from the SVZ precursor cells, the biggest neural progenitor pool of the adult brain. In response to PVD II, the SVZ neuroblasts may migrate out of the RMS, through the corpus callosum into the neocortex towards the lesion. However, *in vivo* labeling of SVZ cells with CFSE resulted in no CFSE-labeled cells outside the SVZ-RMS-OB pathway. This suggests that these DCX+ cells are not originally from the subventricular zone of the lateral ventricle. One possible source is that precursor cells might be residing in the corpus callosum. Studies suggest that OPCs may possess a wider differentiation potential than previously assumed and thus may be considered a multipotent stem cell (Kondo and Raff, 2000; Belachew et al., 2003). Resident glial precursors isolated from human subcortical white matter appear to be multipotential cells that are capable of undergoing not only gliogenesis but also neurogenesis *in vitro*, and following transplantation *in vivo* (Nunes et al., 2003). Following transplantation to the adult rat hippocampus, cortical OPCs differentiated into cells expressing DCX and NeuN (Gaughwin et al., 2006). Although I was not able to show that these DCX cells coexpressed glial antigen 2 (NG2), a marker for OPCs, it

could very well be that these OPCs lost the expression of NG2 as they began differentiating into the neuronal lineage cells.

Another possible source is bone marrow-derived cells. It has been reported that migrating neuroblasts cluster in the peri-infarct area in the vicinity of blood vessels (Zhang et al., 2001; Thored et al., 2006; Yamashita et al., 2006). This close association suggests that these cells were recruited either from local multipotent precursors cells, or from the infiltration of blood-borne cells (Lledo et al., 2006). Bone marrow contains a wide variety of stem and progenitor cells, such as hematopoietic stem cells, that can mobilize into ischemic sites (Rafii and Lyden, 2003). After cerebral ischemia, bone marrow-derived cells rapidly infiltrate the brain. There they give rise primarily to microglia and endothelial cells. There are also reports that they give rise to a limited number of cells with neuronal markers (Hess et al., 2002; Cogle et al., 2004; Hess et al., 2004). In the present study, injections of 200 nl CFSE into the SVZa resulted in no labeling of the contralateral lateral ventricle, which suggests that by using this injection method, CFSE was not transported with the bulk flow of cerebral spinal fluid as shown by some authors (Ramaswamy et al., 2005). Therefore, CFSE should not be able to label any blood born cells in this study. If these DCX+ cells indeed arise from bone marrow-derived cells, this CFSE-labeling method would not result in the appearance of labeled cells in the peri-infarct area.

Recent studies using transgenic targeting strategies (Cre-loxP recombination system) to specifically label SVZ cells, have provided direct evidence that stroke can induce the migration of SVZ neuroblasts into the damaged striatum (Yamashita et al., 2006) and cortex (Ohab et al., 2006). The GFAP-expressing cells are the primary progenitors of these migrating neuroblasts, although it can not be ruled out that some of the newborn neurons may be generated locally. In a study of the fates of newborn neurons in an induced synchronous apoptotic degeneration model of corticothalamic projection neurons, it was suggested, but not proven, that newborn neurons appear to originate from precursors located within the neocortex. A second population appeared to originate in or near the subventricular zone (Magavi et al., 2000). In the present study, as suggested by the number of DCX+ cells, the number of migrating neuroblasts/immature neurons after PVD II are fairly low and this makes it difficult to study the origin and

precise phenotypes of these cells. The low level of cortical neuroblasts in these experiments as compared to other studies (Ohab et al., 2006; Yamashita et al., 2006) could be caused by the large ischemic lesion in the striatum and/or cortex, which may attract new neurons formed in the SVZ more efficiently, as compared with the small distant cortical lesion produced in this study. It is also important to underscore that the approaches used in this study to trace SVZ cells have detection limits. As a lipophilic dye, CFSE may be diluted over time by cell divisions. As well, the one-time injection of CFSE into SVZ may only label a portion of the SVZ cells. Therefore I can not rule out the possibility that there is a very small stream of neuroblasts that migrate out of the RMS in response to cortical ischemic injury. If these DCX+ cells are indeed derived by migration from the SVZ, the tracing of such a low number of cells can only be achieved by genetically tagging all the SVZ neural progenitors.

Stroke is a leading cause of death and disability and it is a diverse disease in terms of causes, manifestations, severity and anatomic sites. In response to PVD II, a model mimicking small vessel stroke, DCX+ neuroblasts appear in the neocortex and corpus callosum of adult rats up to 14 days post injury. These results demonstrate that endogenous neural precursors can be induced to differentiate into neocortical neuronal lineage cells in the neocortex, a non-neurogenic region of the adult rodent brain. Regeneration of the lost neurons is critical for functional improvement. These results suggest that progenitor cells of the rodent adult brain can be triggered to produce new cortical neurons in response to small vessel stroke, although this neurogenic response might be low and transient. This opens up the possibility of a therapeutic approach to enhance the generation and survival of these new neurons and their incorporation into reorganizing neural circuits. A precise understanding of the mechanism of neuronal regeneration is necessary in order to design novel strategies to enhance these processes. *In vivo* labeling of SVZ cells with CFSE resulted in no CFSE labeled cells outside the SVZ-RMS-OB pathway. This finding does not support the notion that these DCX+ cells are neuroblasts migrating from the subventricular zone of the lateral ventricle. An alternative is that they might be derived from local precursors, either from the corpus callosum or the neocortex itself. However, the number of induced neuroblasts (DCX+ cells) post-injury is low. Therefore, it is possible that there is indeed a very small stream

of neuroblasts migrating out of the RMS in response to the cortical injury, as this may not be detected by the current *in vivo* SVZ cell-labeling technique.

8. GENERAL DISCUSSION

8.1 PVD II, a Model to Mimic Small Vessel Stroke

Stroke is a disease caused by blood vessel dysfunction. It is the third leading cause of death in North America (Fatahzadeh and Glick, 2006). To date, most commonly used stroke models involve the occlusion of larger arteries and induce massive lesions (Carmichael, 2005). However, approximately 25% of first human strokes are caused by small vessel ischemia (Lammie et al., 1998; Greenberg, 2006). In Japan, over 50% of ischemic strokes are the result of small vessel ischemia (Greenberg, 2006; Kitamura et al., 2006) and they are also more common in China than in the western countries (Davis et al., 1990). It is now generally acknowledged that small vessel ischemia can eventually lead to lacunar infarctions (Lammie, 2000). However, stroke based on small-vessel disease has been underrepresented in stroke models. There are no satisfactory animal models for lacunar infarction, which would allow for systematic study of the genesis and properties of lacunes. Consequently small vessel disease and resulting lacunar infarction have not been well studied in experimental models (Greenberg, 2006).

The original pial vessel disruption model involves the stripping of all vessels in an area of the cortex. This results in a large rectangular lesion involving subcortical structures, such as corpus callosum, and also creates hemorrhage (Farr and Wishaw, 2002; Gonzalez and Kolb, 2003). It therefore resembles more a situation caused by neurotrauma rather than ischemia. In this thesis, this model is modified by focusing on a smaller surface area (5 mm diameter circle) and disrupting only medium size vessels. This modification prevents hemorrhage and results in a highly consistent and reproducible cortical injury, cone-shaped and exclusively located in the cerebral cortex. In

comparison with other cortical ischemic injury models, the lesion induced by PVD II is much smaller in size (around 1 mm^3). In the third week a cavity develops in the area of the lesion, devoid of cells and surrounded by a glia limitans consisting of reactive astrocytes. The PVD II model resembles human lacunar infarctions in size and structure, as fluid-filled cavities are a hallmark of human lacunar infarction (Wardlaw, 2004).

There are, however, two disadvantages associated with this model. First, the disruption of the vessels is irreversible. However, reperfusion is not an issue in the genesis and pathology of lacunar infarctions. The second and more serious problem of course is that this cavity is located in the gray matter of the cerebral cortex. Human lacunes are only in exceptional cases located in this brain area and are most commonly found in the deep subcortical areas, such as the putamen, caudate, thalamus and pons. However, they do occur occasionally in the cerebral cortex (Chester et al., 1978), making it likely that the same general mechanisms may apply to the genesis and properties of these cavities in the cerebral cortex as they would in those situated in deeper layers. This must be verified in the future.

The advantages of this easy-to-use model, its reliability and reproducibility, even when used by different investigators, far outweigh these disadvantages, at least at this stage of investigation. Thus, one may be confident that the cone-shaped lesion with a volume of approximately 1-mm^3, which turns into a fluid-filled cavity in the third week (Wang and Walz, 2003) is a realistic approximation of human small-vessel disease.

8.2 Minocycline

The search for potential therapeutic approaches for the treatment of stroke, led to the investigation of two potential mechanisms: reduction of inflammation with minocycline treatment and neurogenesis of endogenous progenitor cells. Minocycline has neuroprotective properties in different animal models of acute CNS injury and chronic neurological diseases due to its anti-inflammatory and anti-apoptotic actions (Domercq and Matute, 2004; Stirling et al., 2005). In the present study, minocycline treatment was started after the induction of PVD II and continued for six days. It prevented the genesis of a cavity. With minocycline treatment the lesion volume is not changed, but the area that normally consists of the cavity and the surrounding glia

limitans is now not separated from the parenchyma by a wall (the *glia limitans*), but remains part of the parenchyma. It is completely filled with reactive astrocytes. Progressive cavitation is closely related to the inflammatory response and is based on activation of microglia/macrophages and migration of reactive astrocytes out of the affected area (Fitch et al., 1999). This leads to abandonment by astrocytes and therefore leaves this area more vulnerable to inflammatory damage. Therefore, it may not come as a surprise that this process is a natural target for minocycline as minocycline is generally assumed to interfere with inflammation and microglial properties. In the PVD II, it was found that shortly after injury, the PMNs were recruited and infiltrated in the lesion area, followed by delayed infiltration of T cells and activated microglia / macrophages (both of hematopoietic origin and brain microglia) in the ischemic area and boundary zone. Six days after lesioning, an astrocytic boundary, known as glia limitans, started to form around the lesion. The formation of this border must be prevented by minocycline. Therefore reactive astrocytes can migrate back into the lesioned area and this migration prevented the formation of a fluid-filled cyst. It is usually persistent macrophage/microglia activation that is responsible for the outward migration of astrocytes first of all (Fitch et al., 1999). Activated microglia/macrophages not only act as scavengers removing tissue debris, but also release numerous agents that are toxic to CNS cells, including inflammatory cytokines and glutamate, which aggravate secondary tissue injury and modulate the astrocyte response by releasing inflammatory cytokines, such as IL-1β and chemoattractants, such as osteopontin and MMPs. Although no direct evidence for reduced inflammation after minocycline treatment was found in this study, it seems most likely that minocycline is preventing cavitation through its anti-inflammatory effect on microglia early during the first 6 days.

8.3 Appearance of Cortical Neuroblasts in Response to the PVD II Model

I investigated if, in response to PVD II, there is an induction of neurogenesis by endogenous precursors, which could potentially be harnessed for post-stroke treatment. In response to this injury, DCX-expressing neuroblasts were present in the neocortex and corpus callosum underneath the lesion up to 14 days after injury. Using both

morphological and immunocytochemical criteria, I am confident that these DCX-expressing cells are migrating neuroblasts/immature neurons and that they are present in the ischemic neocortex, a non-neurogenetic area in the normal adult brain. As I found no evidence for a migratory route out of the SVZ-RMS-OB axis towards the lesioned cerebral cortex, it seems likely that these cells are generated locally in the cerebral cortex. Therefore these results support the view that the adult cortex is capable of neuronal regeneration in response to ischemic injury. This evidence of neurogenic upregulation in the damaged ischemic brain is of potential interest for the development of therapeutic strategies that exploit naturally existing responses. However, it is important for me to remain critical and cautious in the interpretation of the phenomenon of post-stroke cortical neurogenesis. In this thesis, no experiments with regard to the fate of these DCX+ cells were performed, and therefore there is no evidence that these DCX+ cells in the neocortex survive and become functional mature neurons after PVD II. However, these results do suggest that it may be possible to manipulate endogenous neural precursors *in situ* to undergo neurogenesis in the adult brain. Whether this endogenous post-stroke neurogenesis can improve functional recovery after stroke is unresolved. Attempts at endogenous repair might require exogenous support to increase the number of neurons generated in the injured area. Elucidation of relevant molecular targets is necessary for the development of future neuronal replacement therapy after a stroke that does not require transplantation of exogenous cells.

8.4 The Origin of the Induced Cortical Neuroblasts

In this study, *in vivo* labeling of SVZ cells with CFSE did not result in the appearance of any CFSE-labeled cells outside the SVZ-RMS-OB axis in response to PVD II. This finding does therefore not support the view that these DCX+ neuroblasts migrated from the SVZ of the lateral ventricle in response to the ischemic injury. However, due to the technical limitations, I can not completely rule out such a conclusion unless the method used for tracing migration would result in the permanent labeling of all the SVZ cells and their progeny. Doing this by taking advantage of the Cre-loxP system in transgenic mice, which resulted in region- and cell-type-specific cell labeling and long-term tracing of SVZ cells, recent studies (Ohab et al., 2006;

Yamashita et al., 2006) have shown that SVZ GFAP-expressing precursor cells are the primary source of new neurons in the ischemic brain. It would be interesting to apply the PVD II model to these Cre-transgenetic mice. This may help to elucidate the origin of the DCX+ neuroblasts. The other possible origin of these DCX + neuroblasts in the present study could be the local parenchymal precursors of the corpus callosum or cerebral cortex. Multipotent neural progenitors have now been isolated from various non-neurogenic regions of the adult mammalian CNS (reviewed in section 1.3.2.1.3). Resident glial precursors isolated from human subcortical white matter appear to be multipotential cells capable of undergoing gliogenesis as well as neurogenesis *in vitro* following transplantation (Nunes et al., 2003). Intraventricular infusion of specific growth factors, such as EGF, an effective mitogen, may help to elucidate the cell origin. When growth factors are infused into the lateral ventricle, they do not diffuse very far into the parenchyma of the brain. Therefore, their first molecular targets have to be neural precursors in the SVZ. Thus, if such an intraventricular growth factor infusion affects the number of DCX+ neuroblasts after PVD II, it would provide valuable evidence that SVZ precursors contribute to these DCX+ cells. If intraventricular infusion had no effect on the numbers, it would suggest that these cells are derived from parenchymal precursors. Identifying the origin of these post-PVD II DCX+ neuroblasts would be particularly relevant to the possibility of manipulating endogenous precursors for therapeutic purposes.

8.5 Future Direction

The mammalian brain is known to have limited ability to regenerate after injury. The presence of DCX+ neuroblasts after a PVD II lesion raises some questions: e.g., is this an attempt of the brain to regenerate new cortical neurons to replace the dead ones induced by ischemic injury? To answer this question, it would be important to follow the maturation of these DCX+ cells and their ultimate fate. Further research should also focus on understanding the crucial signals for proliferation, survival and differentiation of the endogenous precursors. This may lead to development of a method to manipulate the low level of post-stroke neurogenesis to a therapeutically useful level.

Post-stroke inflammation is a complex phenomenon that involves many different inflammatory cells in the CNS, and plays an important role in cell survival and tissue remodeling. It has been suggested that inflammation is detrimental to neurogenesis (Ekdahl et al., 2003). Blocking inflammation by minocycline has been shown to increase the survival of new hippocampal neurons after focal ischemia (Liu et al., 2007). On the other hand, it has also been reported that inflammation at the injury site plays an important role in attracting the neural precursor cells, which then migrate toward damaged areas of the brain, possibly through some chemokines (Belmadani et al., 2006). Therefore, it would be particularly interesting to combine the two pieces of work in this thesis to examine the effect of inflammation on the expression of DCX+ after PVD II lesion. These experiments may shed light on the therapeutic potential of anti-inflammatory therapy on brain repair after ischemia.

9. CONCLUSION

In this study, a new rat stroke model was introduced, a modification of the original pial vessel disruption model, but with vastly different properties. It always leads to the development of a fluid-filled encapsulated cyst as a result of exclusive disruption of medium-sized vessels. I therefore make an argument that this model, albeit situated in the cerebral cortex, can be used to study cavitation. I also argue that this cavitation is a model of the genesis of lacunar infarctions. This model should therefore be useful in the study of the genesis of lacunes as a result of ischemia in small vessels. It should be useful in the development of pharmacological strategies with the aim to prevent formation of lacunar infarctions.

I find evidence for inflammation as a major contributor to cavitation after PVD II, especially for microglia-astrocyte interaction. Minocycline interferes with these interactions, therefore it may facilitate the repopulation of the lesion by reactive astrocytes and prevent formation of a cavity and a glial limitan. Although I did not find direct evidence for reduced inflammation at the cellular level after minocycline treatment, it seems likely minocyline acts on the signaling between microglia and reactive astrocytes.

I found evidence that endogenous neural precursors may serve as a source of new neurons after small vessel strokes. In response to PVD II, cells which express DCX and immature neuronal markers, and exhibit the morphology of neuroblasts and post-migrating neurons, appear in the neocortex and corpus callosum. These are non-neurogenetic areas in the normal adult brain. The presence of these migrating neuroblasts / immature neurons, is an indication that endogenous precursors attempt to become neurons in the vicinity of the cortical ischemic injury. Results from these *in vivo* labeling experiments suggested that these post-stroke induced neuroblasts / immature neurons are not originating from the SVZ, but might be generated from local precursors

in the neocortex or corpus callosum. However, as the number of induced neuroblasts (DCX+ cells) is low, we can not rule out the possibility that these cells are indeed from SVZ-RMS axis and that we failed to detect this small stream of emigration due to limitations of our tracing technique. I tested various tracing procedures and the CFSE-labeling approach seemed to be suited best for the purposes of the present study.

Taken together, I have developed a new animal model that can be used with high reliability and low variation to create lacunar infarction – like injuries. It therefore can serve as a model of small vessel disease, a highly undeveloped area of research. The findings that minocycline treatment *after* stroke prevents these lacunes and that neuroblasts appear near the lesion in the neocortex opens up new targets for post-stroke treatment.

10. REFENCES

Adkins-Muir DL, Jones TA (2003) Cortical electrical stimulation combined with rehabilitative training: enhanced functional recovery and dendritic plasticity following focal cortical ischemia in rats. Neurol Res 25:780-788.

Allt G, Lawrenson JG (2001) Pericytes: cell biology and pathology. Cells Tissues Organs 169:1-11.

Aloisi F (1999) The role of microglia and astrocytes in CNS immune surveillance and immunopathology. Adv Exp Med Biol 468:123-133.

Altman J (1963) Autoradiographic investigation of cell proliferation in the brains of rats and cats. Anat Rec 145:573-591.

Alvarez-Buylla A, Lim DA (2004) For the long run: maintaining germinal niches in the adult brain. Neuron 41:683-686.

Alvarez-Buylla A, Garcia-Verdugo JM, Tramontin AD (2001) A unified hypothesis on the lineage of neural stem cells. Nat Rev Neurosci 2:287-293.

Arboix A, Marti-Vilalta JL (2004) New concepts in lacunar stroke etiology: the constellation of small-vessel arterial disease. Cerebrovasc Dis 17 Suppl 1:58-62.

Aronowski J, Labiche LA (2003) Perspectives on reperfusion-induced damage in rodent models of experimental focal ischemia and role of gamma-protein kinase C. ILAR J 44:105-109.

Arvidsson A, Kokaia Z, Lindvall O (2001) N-methyl-D-aspartate receptor-mediated increase of neurogenesis in adult rat dentate gyrus following stroke. Eur J Neurosci 14:10-18.

Arvidsson A, Collin T, Kirik D, Kokaia Z, Lindvall O (2002) Neuronal replacement from endogenous precursors in the adult brain after stroke. Nat Med 8:963-970.

Arvin B, Neville LF, Barone FC, Feuerstein GZ (1996) The role of inflammation and cytokines in brain injury. Neurosci Biobehav Rev 20:445-452.

Arvin KL, Han BH, Du Y, Lin SZ, Paul SM, Holtzman DM (2002) Minocycline markedly protects the neonatal brain against hypoxic-ischemic injury. Ann Neurol 52:54-61.

Back T, Hemmen T, Schuler OG (2004) Lesion evolution in cerebral ischemia. J Neurol 251:388-397.

Bamford J, Sandercock P, Jones L, Warlow C (1987) The natural history of lacunar infarction: the Oxfordshire Community Stroke Project. Stroke 18:545-551.

Bar T (1980) The vascular system of the cerebral cortex. Adv Anat Embryol Cell Biol 59:I-VI,1-62.

Barone FC, Feuerstein GZ (1999) Inflammatory mediators and stroke: New opportunities for novel therapeutics. J Cerebral Blood Flow Metab 19:819-834.

Bauer S, Hay M, Amilhon B, Jean A, Moyse E (2005) In vivo neurogenesis in the dorsal vagal complex of the adult rat brainstem. Neuroscience 130:75-90.

Bedard A, Parent A (2004) Evidence of newly generated neurons in the human olfactory bulb. Brain Res Dev Brain Res 151:159-168.

Belachew S, Chittajallu R, Aguirre AA, Yuan X, Kirby M, Anderson S, Gallo V (2003) Postnatal NG2 proteoglycan-expressing progenitor cells are intrinsically multipotent and generate functional neurons. J Cell Biol 161:169-186.

Belmadani A, Tran PB, Ren D, Miller RJ (2006) Chemokines regulate the migration of neural progenitors to sites of neuroinflammation. J Neurosci 26:3182-3191.
Bernier PJ, Bedard A, Vinet J, Levesque M, Parent A (2002) Newly generated neurons in the amygdala and adjoining cortex of adult primates. Proc Natl Acad Sci U S A 99:11464-11469.
Betsholtz C, Lindblom P, Gerhardt H (2005) Role of pericytes in vascular morphogenesis. Exs:115-125.
Bhardwaj RD, Curtis MA, Spalding KL, Buchholz BA, Fink D, Bjork-Eriksson T, Nordborg C, Gage FH, Druid H, Eriksson PS, Frisen J (2006) Neocortical neurogenesis in humans is restricted to development. Proc Natl Acad Sci U S A 103:12564-12568.
Boenisch T (2001) Formalin-fixed and heat-retrieved tissue antigens: a comparison of their immunoreactivity in experimental antibody diluents. Appl Immunohistochem Mol Morphol 9:176-179.
Braun JS, Jander S, Schroeter M, Witte OW, Stoll G (1996) Spatiotemporal relationship of apoptotic cell death to lymphomonocytic infiltration in photochemically induced focal ischemia of the rat cerebral cortex. Acta Neuropathol (Berl) 92:255-263.
Brazel CY, Romanko MJ, Rothstein RP, Levison SW (2003) Roles of the mammalian subventricular zone in brain development. Prog Neurobiol 69:49.
Breedveld FC, Dijkmans BA, Mattie H (1990) Minocycline treatment for rheumatoid arthritis: an open dose finding study. J Rheumatol 17:43-46.
Brown JP, Couillard-Despres S, Cooper-Kuhn CM, Winkler J, Aigner L, Kuhn HG (2003) Transient expression of doublecortin during adult neurogenesis. J Comp Neurol 467:1-10.
Brundula V, Rewcastle NB, Metz LM, Bernard CC, Yong VW (2002) Targeting leukocyte MMPs and transmigration: minocycline as a potential therapy for multiple sclerosis. Brain 125:1297-1308.
Calza L, Giardino L, Pozza M, Bettelli C, Micera A, Aloe L (1998) Proliferation and phenotype regulation in the subventricular zone during experimental allergic encephalomyelitis: in vivo evidence of a role for nerve growth factor. Proc Natl Acad Sci U S A 95:3209-3214.
Cameron HA, McKay RD (2001) Adult neurogenesis produces a large pool of new granule cells in the dentate gyrus. J Comp Neurol 435:406-417.
Carleton A, Petreanu LT, Lansford R, Alvarez-Buylla A, Lledo PM (2003) Becoming a new neuron in the adult olfactory bulb. Nat Neurosci 6:507-518.
Carmichael ST (2005) Rodent models of focal stroke: size, mechanism, and purpose. NeuroRx 2:396-409.
Chen H, Chopp M, Schultz L, Bodzin G, Garcia JH (1993) Sequential neuronal and astrocytic changes after transient middle cerebral artery occlusion in the rat. J Neurol Sci 118:109-106.
Chen J, Magavi SS, Macklis JD (2004) Neurogenesis of corticospinal motor neurons extending spinal projections in adult mice. Proc Natl Acad Sci U S A 101:16357-16362.
Chen M, Ona VO, Li M, Ferrante RJ, Fink KB, Zhu S, Bian J, Guo L, Farrell LA, Hersch SM, Hobbs W, Vonsattel JP, Cha JH, Friedlander RM (2000)

Minocycline inhibits caspase-1 and caspase-3 expression and delays mortality in a transgenic mouse model of Huntington disease. Nat Med 6:797-801.
Chen Y, Swanson RA (2003) Astrocytes and brain injury. J Cereb Blood Flow Metab 23:137-149.
Chester EM, Agamanolis DP, Banker BQ, Victor M (1978) Hypertensive encephalopathy: a clinicopathologic study of 20 cases. Neurology 28:928-939.
Chiasson BJ, Tropepe V, Morshead CM, van der Kooy D (1999) Adult mammalian forebrain ependymal and subependymal cells demonstrate proliferative potential, but only subependymal cells have neural stem cell characteristics. J Neurosci 19:4462-4471.
Choi DW (1996) Ischemia-induced neuronal apoptosis. Curr Opin Neurobiol 6:667-672.
Cogle CR, Yachnis AT, Laywell ED, Zander DS, Wingard JR, Steindler DA, Scott EW (2004) Bone marrow transdifferentiation in brain after transplantation: a retrospective study. Lancet 363:1432-1437.
Conner JM, Hoener MC, Varon S (1998) Partial cortical devascularization results in elevations of cortical nerve growth factor and increases nerve growth factor protein within basal forebrain cholinergic neurons. Neuroscience 83:1003-1011.
Consiglio A, Gritti A, Dolcetta D, Follenzi A, Bordignon C, Gage FH, Vescovi AL, Naldini L (2004) Robust in vivo gene transfer into adult mammalian neural stem cells by lentiviral vectors. Proc Natl Acad Sci U S A 101:14835-14840.
Cooper O, Isacson O (2004) Intrastriatal transforming growth factor alpha delivery to a model of Parkinson's disease induces proliferation and migration of endogenous adult neural progenitor cells without differentiation into dopaminergic neurons. J Neurosci 24:8924-8931.
Costa S, Planchenault T, Charriere-Bertrand C, Mouchel Y, Fages C, Juliano S, Lefrancois T, Barlovatz-Meimon G, Tardy M (2002) Astroglial permissivity for neuritic outgrowth in neuron-astrocyte cocultures depends on regulation of laminin bioavailability. Glia 37:105-113.
Couillard-Despres S, Winner B, Schaubeck S, Aigner R, Vroemen M, Weidner N, Bogdahn U, Winkler J, Kuhn HG, Aigner L (2005) Doublecortin expression levels in adult brain reflect neurogenesis. Eur J Neurosci 21:1-14.
Craig CG, D'sa R, Morshead CM, Roach A, van der Kooy D (1999) Migrational analysis of the constitutively proliferating subependyma population in adult mouse forebrain. Neuroscience 93:1197-1206.
Danton GH, Dietrich WD (2003) Inflammatory mechanisms after ischemia and stroke. J Neuropathol Exp Neurol 62:127-136.
Davis LE, Xie JG, Zou AH, Wang JY, Liu YJ, Go TX, Cai Y (1990) Deep cerebral infarcts in the People's Republic of China. Stroke 21:394-396.
Dayer AG, Cleaver KM, Abouantoun T, Cameron HA (2005) New GABAergic interneurons in the adult neocortex and striatum are generated from different precursors. J Cell Biol 168:415-427.
De Marchis S, Fasolo A, Shipley M, Puche A (2001) Unique neuronal tracers show migration and differentiation of SVZ progenitors in organotypic slices. J Neurobiol 49:326-338.
del Zoppo G, Ginis I, Hallenbeck JM, Iadecola C, Wang XK, Feuerstein GZ (2000) Inflammation and stroke: Putative role for cytokines, adhesion molecules and iNOS in brain response to ischemia. Brain Pathol 10:95-112.

Dempsey RJ, Sailor KA, Bowen KK, Tureyen K, Vemuganti R (2003) Stroke-induced progenitor cell proliferation in adult spontaneously hypertensive rat brain: effect of exogenous IGF-1 and GDNF. J Neurochem 87:586-597.
Dietrich WD, Watson BD, Busto R, Ginsberg MD, Bethea JR (1987a) Photochemically induced cerebral infarction. I. Early microvascular alterations. Acta Neuropathol (Berl) 72:315-325.
Dietrich WD, Busto R, Watson BD, Scheinberg P, Ginsberg MD (1987b) Photochemically induced cerebral infarction. II. Edema and blood-brain barrier disruption. Acta Neuropathol (Berl) 72:326-334.
Diguet E, Rouland R, Tison F (2003) Minocycline is not beneficial in a phenotypic mouse model of Huntington's disease. Ann Neurol 54:841-842.
Diguet E, Gross CE, Tison F, Bezard E (2004a) Rise and fall of minocycline in neuroprotection: need to promote publication of negative results. Exp Neurol 189:1-4.
Diguet E, Fernagut PO, Wei X, Du Y, Rouland R, Gross C, Bezard E, Tison F (2004b) Deleterious effects of minocycline in animal models of Parkinson's disease and Huntington's disease. Eur J Neurosci 19:3266-3276.
Dirnagl U, Iadecola C, Moskowitz MA (1999) Pathobiology of ischaemic stroke: an integrated view. Trends Neurosci 22:391-397.
Doetsch F, Alvarez-Buylla A (1996) Network of tangential pathways for neuronal migration in adult mammalian brain. Proc Natl Acad Sci U S A 93:14895-14900.
Doetsch F, Garcia-Verdugo JM, Alvarez-Buylla A (1997) Cellular composition and three-dimensional organization of the subventricular germinal zone in the adult mammalian brain. J Neurosci 17:5046-5061.
Doetsch F, Caille I, Lim DA, Garcia-Verdugo JM, Alvarez-Buylla A (1999) Subventricular zone astrocytes are neural stem cells in the adult mammalian brain. Cell 97:703-716.
Domercq M, Matute C (2004) Neuroprotection by tetracyclines. Trends Pharmacol Sci 25:609-612.
Dreier JP, Kleeberg J, Petzold G, Priller J, Windmuller O, Orzechowski HD, Lindauer U, Heinemann U, Einhaupl KM, Dirnagl U (2002) Endothelin-1 potently induces Leao's cortical spreading depression in vivo in the rat: a model for an endothelial trigger of migrainous aura? Brain 125:102-112.
Du Y, Ma Z, Lin S, Dodel RC, Gao F, Bales KR, Triarhou LC, Chernet E, Perry KW, Nelson DL, Luecke S, Phebus LA, Bymaster FP, Paul SM (2001) Minocycline prevents nigrostriatal dopaminergic neurodegeneration in the MPTP model of Parkinson's disease. Proc Natl Acad Sci U S A 98:14669-14674.
Ekdahl CT, Claasen JH, Bonde S, Kokaia Z, Lindvall O (2003) Inflammation is detrimental for neurogenesis in adult brain. Proc Natl Acad Sci U S A 100:13632-13637.
Emsley JG, Mitchell BD, Kempermann G, Macklis JD (2005) Adult neurogenesis and repair of the adult CNS with neural progenitors, precursors, and stem cells. Prog Neurobiol 75:321-341.
Eriksson PS, Perfilieva E, Bjork-Eriksson T, Alborn AM, Nordborg C, Peterson DA, Gage FH (1998) Neurogenesis in the adult human hippocampus. Nat Med 4:1313-1317.

Fagan SC, Hess DC, Hohnadel EJ, Pollock DM, Ergul A (2004a) Targets for vascular protection after acute ischemic stroke. Stroke 35:2220-2225.
Fagan SC, Edwards DJ, Borlongan CV, Xu L, Arora A, Feuerstein G, Hess DC (2004b) Optimal delivery of minocycline to the brain: implication for human studies of acute neuroprotection. Exp Neurol 186:248-251.
Farber K, Kettenmann H (2005) Physiology of microglial cells. Brain Res Brain Res Rev 48:133-143.
Farr TD, Whishaw IQ (2002) Quantitative and qualitative impairments in skilled reaching in the mouse (Mus musculus) after a focal motor cortex stroke. Stroke 33:1869-1875.
Fatahzadeh M, Glick M (2006) Stroke: epidemiology, classification, risk factors, complications, diagnosis, prevention, and medical and dental management. Oral Surg Oral Med Oral Pathol Oral Radiol Endod 102:180-191.
Fawcett JW, Asher RA (1999) The glial scar and central nervous system repair. Brain Res Bull 49:377-391.
Fedoroff S, Berezovskaya O, Maysinger D (1997) Role of colony stimulating factor-1 in brain damage caused by ischemia. Neurosci Biobehav Rev 21:187-191.
Felberg RA, Naidech AM (2003) The 5 Ps of acute ischemic stroke treatment: parenchyma, pipes, perfusion, penumbra, and prevention of complications. South Med J 96:336-342.
Fendrick SE, Miller KR, Streit WJ (2005) Minocycline does not inhibit microglia proliferation or neuronal regeneration in the facial nucleus following crush injury. Neurosci Lett 385:220-223.
Ferrer I, Planas AM (2003) Signaling of cell death and cell survival following focal cerebral ischemia: life and death struggle in the penumbra. J Neuropathol Exp Neurol 62:329-339.
Ferretti P (2004) Neural stem cell plasticity: recruitment of endogenous populations for regeneration. Curr Neurovasc Res 1:215-229.
Fidler PS, Schuette K, Asher RA, Dobbertin A, Thornton SR, Calle-Patino Y, Muir E, Levine JM, Geller HM, Rogers JH, Faissner A, Fawcett JW (1999) Comparing astrocytic cell lines that are inhibitory or permissive for axon growth: the major axon-inhibitory proteoglycan is NG2. J Neurosci 19:8778-8788.
Fisher M, Garcia JH (1996) Evolving stroke and the ischemic penumbra. Neurology 47:884-888.
Fitch MT, Doller C, Combs CK, Landreth GE, Silver J (1999) Cellular and molecular mechanisms of glial scarring and progressive cavitation: in vivo and in vitro analysis of inflammation-induced secondary injury after CNS trauma. J Neurosci 19:8182-8198.
Fox C, Dingman A, Derugin N, Wendland MF, Manabat C, Ji S, Ferriero DM, Vexler ZS (2005) Minocycline confers early but transient protection in the immature brain following focal cerebral ischemia-reperfusion. J Cereb Blood Flow Metab 25:1138-1149.
Francis F, Koulakoff A, Boucher D, Chafey P, Schaar B, Vinet MC, Friocourt G, McDonnell N, Reiner O, Kahn A, McConnell SK, Berwald-Netter Y, Denoulet P, Chelly J (1999) Doublecortin is a developmentally regulated, microtubule-associated protein expressed in migrating and differentiating neurons. Neuron 23:247-256.

Friedlander RM (2003) Apoptosis and caspases in neurodegenerative diseases. N Engl J Med 348:1365-1375.
Frielingsdorf H, Schwarz K, Brundin P, Mohapel P (2004) No evidence for new dopaminergic neurons in the adult mammalian substantia nigra. Proc Natl Acad Sci U S A 101:10177-10182.
Frizzell JP (2005) Acute stroke: pathophysiology, diagnosis, and treatment. AACN Clin Issues 16:597-598.
Funnell WR, Maysinger D, Cuello AC (1990) Three-dimensional reconstruction and quantitative evaluation of devascularizing cortical lesions in the rat. J Neurosci Methods 35:147-156.
Fuxe K, Bjelke B, Andbjer B, Grahn H, Rimondini R, Agnati LF (1997) Endothelin-1 induced lesions of the frontoparietal cortex of the rat. A possible model of focal cortical ischemia. Neuroreport 8:2623-2629.
Gage FH (2000) Mammalian neural stem cells. Science 287:1433-1438.
Garcia AD, Doan NB, Imura T, Bush TG, Sofroniew MV (2004) GFAP-expressing progenitors are the principal source of constitutive neurogenesis in adult mouse forebrain. Nat Neurosci 7:1233-1241.
Gartshore G, Patterson J, Macrae IM (1997) Influence of ischemia and reperfusion on the course of brain tissue swelling and blood-brain barrier permeability in a rodent model of transient focal cerebral ischemia. Exp Neurol 147:353-360.
Gaughwin PM, Caldwell MA, Anderson JM, Schwiening CJ, Fawcett JW, Compston DA, Chandran S (2006) Astrocytes promote neurogenesis from oligodendrocyte precursor cells. Eur J Neurosci 23:945-956.
Geraerts M, Eggermont K, Hernandez-Acosta P, Garcia-Verdugo JM, Baekelandt V, Debyser Z (2006) Lentiviral vectors mediate efficient and stable gene transfer in adult neural stem cells in vivo. Hum Gene Ther 17:635-650.
Ginsberg MD, Busto R (1989) Rodent models of cerebral ischemia. Stroke 20:1627-1642.
Giulian D, Woodward J, Young DG, Krebs JF, Lachman LB (1988) Interleukin-1 injected into mammalian brain stimulates astrogliosis and neovascularization. J Neurosci 8:2485-2490.
Gonzalez CL, Kolb B (2003) A comparison of different models of stroke on behaviour and brain morphology. Eur J Neurosci 18:1950-1962.
Gottlieb DI (2002) Large-scale sources of neural stem cells. Annu Rev Neurosci 25:381-407.
Gotts JE, Chesselet MF (2005) Migration and fate of newly born cells after focal cortical ischemia in adult rats. J Neurosci Res 80:160-171.
Gould E, Reeves AJ, Graziano MS, Gross CG (1999) Neurogenesis in the neocortex of adult primates. Science 286:548-552.
Gould E, Vail N, Wagers M, Gross CG (2001) Adult-generated hippocampal and neocortical neurons in macaques have a transient existence. Proc Natl Acad Sci U S A 98:10910-10917.
Greenberg SM (2006) Small vessels, big problems. N Engl J Med 354:1451-1453.
Gu W, Brannstrom T, Wester P (2000) Cortical neurogenesis in adult rats after reversible photothrombotic stroke. J Cereb Blood Flow Metab 20:1166-1173.

Hama H, Kasuya Y, Sakurai T, Yamada G, Suzuki N, Masaki T, Goto K (1997) Role of endothelin-1 in astrocyte responses after acute brain damage. J Neurosci Res 47:590-602.
Harrison DC, Davis RP, Bond BC, Campbell CA, James MF, Parsons AA, Philpott KL (2001) Caspase mRNA expression in a rat model of focal cerebral ischemia. Brain Res Mol Brain Res 89:133-146.
Hayaran A, Bijlani V (1992) Polyacrylamide as an infiltrating and embedding medium for vibratome sectioning of human fetal cerebellum containing DiI-filled axons. J Neurosci Methods 42:65-68.
Hermann DM, Kilic E, Hata R, Hossmann KA, Mies G (2001) Relationship between metabolic dysfunctions, gene responses and delayed cell death after mild focal cerebral ischemia in mice. Neuroscience 104:947-955.
Herx LM, Yong VW (2001) Interleukin-1 beta is required for the early evolution of reactive astrogliosis following CNS lesion. J Neuropathol Exp Neurol 60:961-971.
Hess DC, Hill WD, Martin-Studdard A, Carothers J, Brailer J, Carroll J (2002) Blood into brain after stroke. Trends Mol Med 8:452-453.
Hess DC, Abe T, Hill WD, Studdard AM, Carothers J, Masuya M, Fleming PA, Drake CJ, Ogawa M (2004) Hematopoietic origin of microglial and perivascular cells in brain. Exp Neurol 186:134-144.
Hewett SJ, Csernansky CA, Choi DW (1994) Selective potentiation of NMDA-induced neuronal injury following induction of astrocytic iNOS. Neuron 13:487-494.
Holmqvist BI, Ostholm T, Ekstrom P (1992) DiI tracing in combination with immunocytochemistry for analysis of connectivities and chemoarchitectonics of specific neural systems in a teleost, the Atlantic salmon. J Neurosci Methods 42:45-63.
Horn J, Limburg M (2001) Calcium antagonists for ischemic stroke: a systematic review. Stroke 32:570-576.
Hossmann KA (2006) Pathophysiology and therapy of experimental stroke. Cell Mol Neurobiol 26:1055-1081.
Hu WS, Pathak VK (2000) Design of retroviral vectors and helper cells for gene therapy. Pharmacol Rev 52:493-511.
Huang J, Upadhyay UM, Tamargo RJ (2006) Inflammation in stroke and focal cerebral ischemia. Surg Neurol 66:232-245.
Hughes PM, Anthony DC, Ruddin M, Botham MS, Rankine EL, Sablone M, Baumann D, Mir AK, Perry VH (2003) Focal lesions in the rat central nervous system induced by endothelin-1. J Neuropathol Exp Neurol 62:1276-1286.
Iadecola C, Xu X, Zhang F, el-Fakahany EE, Ross ME (1995) Marked induction of calcium-independent nitric oxide synthase activity after focal cerebral ischemia. J Cereb Blood Flow Metab 15:52-59.
Ikonomidou C, Turski L (2002) Why did NMDA receptor antagonists fail clinical trials for stroke and traumatic brain injury? Lancet Neurol 1:383-386.
Imura T, Kornblum HI, Sofroniew MV (2003) The predominant neural stem cell isolated from postnatal and adult forebrain but not early embryonic forebrain expresses GFAP. J Neurosci 23:2824-2832.
Inuzuka T, Hozumi I, Tamura A, Hiraiwa M, Tsuji S (1996) Patterns of growth inhibitory factor (GIF) and glial fibrillary acidic protein relative level changes

differ following left middle cerebral artery occlusion in rats. Brain Res 709:151-153.
Jander S, Sitzer M, Schumann R, Schroeter M, Siebler M, Steinmetz H, Stoll G (1998) Inflammation in high-grade carotid stenosis: a possible role for macrophages and T cells in plaque destabilization. Stroke 29:1625-1630.
Jankovski A, Sotelo C (1996) Subventricular zone-olfactory bulb migratory pathway in the adult mouse: cellular composition and specificity as determined by heterochronic and heterotopic transplantation. J Comp Neurol 371:376-396.
Jiang W, Gu W, Brannstrom T, Rosqvist R, Wester P (2001) Cortical neurogenesis in adult rats after transient middle cerebral artery occlusion. Stroke 32:1201-1207.
Jin K, Minami M, Lan JQ, Mao XO, Batteur S, Simon RP, Greenberg DA (2001) Neurogenesis in dentate subgranular zone and rostral subventricular zone after focal cerebral ischemia in the rat. Proc Natl Acad Sci U S A 98:4710-4715.
Jin K, Sun Y, Xie L, Peel A, Mao XO, Batteur S, Greenberg DA (2003) Directed migration of neuronal precursors into the ischemic cerebral cortex and striatum. Mol Cell Neurosci 24:171.
Johansson CB, Momma S, Clarke DL, Risling M, Lendahl U, Frisen J (1999) Identification of a neural stem cell in the adult mammalian central nervous system. Cell 96:25.
Kaplan MS (1981) Neurogenesis in the 3-month-old rat visual cortex. J Comp Neurol 195:323-338.
Kastrup A, Engelhorn T, Beaulieu C, de Crespigny A, Moseley ME (1999) Dynamics of cerebral injury, perfusion, and blood-brain barrier changes after temporary and permanent middle cerebral artery occlusion in the rat. J Neurol Sci 166:91-99.
Kato H, Walz W (2000) The initiation of the microglial response. Brain Pathol 10:137-143.
Kato H, Kogure K, Liu XH, Araki T, Itoyama Y (1996) Progressive expression of immunomolecules on activated microglia and invading leukocytes following focal cerebral ischemia in the rat. Brain Res 734:203-212.
Kempermann G, Jessberger S, Steiner B, Kronenberg G (2004) Milestones of neuronal development in the adult hippocampus. Trends Neurosci 27:447-452.
Kimelberg HK (1995) Current concepts of brain edema. Review of laboratory investigations. J Neurosurg 83:1051-1059.
Kirino T, Sano K (1984) Selective vulnerability in the gerbil hippocampus following transient ischemia. Acta Neuropathol (Berl) 62:201-208.
Kitamura A, Nakagawa Y, Sato M, Iso H, Sato S, Imano H, Kiyama M, Okada T, Okada H, Iida M, Shimamoto T (2006) Proportions of stroke subtypes among men and women > or =40 years of age in an urban Japanese city in 1992, 1997, and 2002. Stroke 37:1374-1378.
Koistinaho M, Malm TM, Kettunen MI, Goldsteins G, Starckx S, Kauppinen RA, Opdenakker G, Koistinaho J (2005) Minocycline protects against permanent cerebral ischemia in wild type but not in matrix metalloprotease-9-deficient mice. J Cereb Blood Flow Metab 25:460-467.
Koketsu D, Mikami A, Miyamoto Y, Hisatsune T (2003) Nonrenewal of neurons in the cerebral neocortex of adult macaque monkeys. J Neurosci 23:937-942.
Kokovay E, Li L, Cunningham LA (2006) Angiogenic recruitment of pericytes from bone marrow after stroke. J Cereb Blood Flow Metab 26:545-555.

Kolb B, Morshead C, Gonzalez C, Kim M, Gregg C, Shingo T, Weiss S (2006) Growth factor-stimulated generation of new cortical tissue and functional recovery after stroke damage to the motor cortex of rats. J Cereb Blood Flow Metab.

Komitova M, Zhao LR, Gido G, Johansson BB, Eriksson P (2005) Postischemic exercise attenuates whereas enriched environment has certain enhancing effects on lesion-induced subventricular zone activation in the adult rat. Eur J Neurosci 21:2397-2405.

Kondo T, Raff M (2000) Oligodendrocyte precursor cells reprogrammed to become multipotential CNS stem cells. Science 289:1754-1757.

Kornack DR, Rakic P (1999) Continuation of neurogenesis in the hippocampus of the adult macaque monkey. Proc Natl Acad Sci U S A 96:5768-5773.

Kornack DR, Rakic P (2001) Cell proliferation without neurogenesis in adult primate neocortex. Science 294:2127-2130.

Kreutzberg GW (1996) Microglia: a sensor for pathological events in the CNS. Trends Neurosci 19:312-318.

Kuno R, Wang J, Kawanokuchi J, Takeuchi H, Mizuno T, Suzumura A (2005) Autocrine activation of microglia by tumor necrosis factor-alpha. J Neuroimmunol 162:89-96.

Lammie GA (2000) Pathology of small vessel stroke. Br Med Bull 56:296-306.

Lammie GA, Brannan F, Wardlaw JM (1998) Incomplete lacunar infarction (Type Ib lacunes). Acta Neuropathol (Berl) 96:163-171.

Lee SM, Yune TY, Kim SJ, Park D W, Lee YK, Kim YC, Oh YJ, Markelonis GJ, Oh TH (2003) Minocycline reduces cell death and improves functional recovery after traumatic spinal cord injury in the rat. J Neurotrauma 20:1017-1027.

Lehrmann E, Christensen T, Zimmer J, Diemer NH, Finsen B (1997) Microglial and macrophage reactions mark progressive changes and define the penumbra in the rat neocortex and striatum after transient middle cerebral artery occlusion. J Comp Neurol 386:461-476.

Li X, Dancausse H, Grijalva I, Oliveira M, Levi AD (2003) Labeling Schwann cells with CFSE-an in vitro and in vivo study. J Neurosci Methods 125:83-91.

Li Y, Chopp M, Jiang N, Yao F, Zaloga C (1995a) Temporal profile of in situ DNA fragmentation after transient middle cerebral artery occlusion in the rat. J Cereb Blood Flow Metab 15:389-397.

Li Y, Sharov VG, Jiang N, Zaloga C, Sabbah HN, Chopp M (1995b) Ultrastructural and light microscopic evidence of apoptosis after middle cerebral artery occlusion in the rat. Am J Pathol 146:1045-1051.

Lichtenwalner RJ, Parent JM (2006) Adult neurogenesis and the ischemic forebrain. J Cereb Blood Flow Metab 26:1-20.

Lie DC, Dziewczapolski G, Willhoite AR, Kaspar BK, Shults CW, Gage FH (2002) The adult substantia nigra contains progenitor cells with neurogenic potential. J Neurosci 22:6639-6649.

Liebeskind DS, Kasner SE (2001) Neuroprotection for ischaemic stroke: an unattainable goal? CNS Drugs 15:165-174.

Liesi P, Kauppila T (2002) Induction of type IV collagen and other basement-membrane-associated proteins after spinal cord injury of the adult rat may participate in formation of the glial scar. Exp Neurol 173:31-45.

Lindvall O, Kokaia Z (2006) Stem cells for the treatment of neurological disorders. Nature 441:1094-1096.
Lindvall O, Kokaia Z, Martinez-Serrano A (2004) Stem cell therapy for human neurodegenerative disorders-how to make it work. Nat Med 10 Suppl:42.
Lipton P (1999) Ischemic cell death in brain neurons. Physiol Rev 79:1431-1568.
Liu J, Solway K, Messing RO, Sharp FR (1998) Increased neurogenesis in the dentate gyrus after transient global ischemia in gerbils. J Neurosci 18:7768-7778.
Liu Z, Fan Y, Won SJ, Neumann M, Hu D, Zhou L, Weinstein PR, Liu J (2007) Chronic treatment with minocycline preserves adult new neurons and reduces functional impairment after focal cerebral ischemia. Stroke 38:146-152.
Lledo PM, Alonso M, Grubb MS (2006) Adult neurogenesis and functional plasticity in neuronal circuits. Nat Rev Neurosci 7:179-193.
Lois C, Alvarez-Buylla A (1993) Proliferating subventricular zone cells in the adult mammalian forebrain can differentiate into neurons and glia. Proc Natl Acad Sci U S A 90:2074-2077.
Lois C, Alvarez-Buylla A (1994) Long-distance neuronal migration in the adult mammalian brain. Science 264:1145-1148.
Love S (2003) Apoptosis and brain ischaemia. Prog Neuropsychopharmacol Biol Psychiatry 27:267-282.
Lu G, Wai SM, Poon WS, Yew DT (2005) Ki67 and doublecortin positive cells in the human prefrontal cortices of normal aging and vascular dementia. Microsc Res Tech 68:255-257.
Luke LM, Allred RP, Jones TA (2004) Unilateral ischemic sensorimotor cortical damage induces contralesional synaptogenesis and enhances skilled reaching with the ipsilateral forelimb in adult male rats. Synapse 54:187-199.
Luskin MB (1993) Restricted proliferation and migration of postnatally generated neurons derived from the forebrain subventricular zone. Neuron 11:173-189.
Macrae IM, Robinson MJ, Graham DI, Reid JL, McCulloch J (1993) Endothelin-1-induced reductions in cerebral blood flow: dose dependency, time course, and neuropathological consequences. J Cereb Blood Flow Metab 13:276-284.
Magavi SS, Leavitt BR, Macklis JD (2000) Induction of neurogenesis in the neocortex of adult mice. Nature 405:951-955.
McAuley MA (1995) Rodent models of focal ischemia. Cerebrovasc Brain Metab Rev 7:153-180.
Mergenthaler P, Dirnagl U, Meisel A (2004) Pathophysiology of stroke: lessons from animal models. Metab Brain Dis 19:151-167.
Ming GL, Song H (2005) Adult neurogenesis in the mammalian central nervous system. Annu Rev Neurosci 28:223-250.
Morshead CM, Craig CG, van der Kooy D (1998) In vivo clonal analyses reveal the properties of endogenous neural stem cell proliferation in the adult mammalian forebrain. Development 125:2251-2261.
Muir KW, Grosset DG (1999) Neuroprotection for acute stroke: making clinical trials work. Stroke 30:180-182.
Nacher J, Crespo C, McEwen BS (2001) Doublecortin expression in the adult rat telencephalon. Eur J Neurosci 14:629.

Nakatomi H, Kuriu T, Okabe S, Yamamoto S, Hatano O, Kawahara N, Tamura A, Kirino T, Nakafuku M (2002) Regeneration of hippocampal pyramidal neurons after ischemic brain injury by recruitment of endogenous neural progenitors. Cell 110:429-441.

Namura S, Zhu J, Fink K, Endres M, Srinivasan A, Tomaselli KJ, Yuan J, Moskowitz MA (1998) Activation and cleavage of caspase-3 in apoptosis induced by experimental cerebral ischemia. J Neurosci 18:3659-3668.

Ni B, Wu X, Su Y, Stephenson D, Smalstig EB, Clemens J, Paul SM (1998) Transient global forebrain ischemia induces a prolonged expression of the caspase-3 mRNA in rat hippocampal CA1 pyramidal neurons. J Cereb Blood Flow Metab 18:248-256.

Nunes MC, Roy NS, Keyoung HM, Goodman RR, McKhann G, 2nd, Jiang L, Kang J, Nedergaard M, Goldman SA (2003) Identification and isolation of multipotential neural progenitor cells from the subcortical white matter of the adult human brain. Nat Med 9:439-447.

Nygren J, Wieloch T, Pesic J, Brundin P, Deierborg T (2006a) Enriched Environment Attenuates Cell Genesis in Subventricular Zone After Focal Ischemia in Mice and Decreases Migration of Newborn Cells to the Striatum. Stroke.

Nygren J, Wieloch T, Pesic J, Brundin P, Deierborg T (2006b) Enriched environment attenuates cell genesis in subventricular zone after focal ischemia in mice and decreases migration of newborn cells to the striatum. Stroke 37:2824-2829.

Ogita K, Hirata K, Bole DG, Yoshida S, Tamura Y, Leckenby AM, Ueda T (2001) Inhibition of vesicular glutamate storage and exocytotic release by Rose Bengal. J Neurochem 77:34-42.

Ohab JJ, Fleming S, Blesch A, Carmichael ST (2006) A neurovascular niche for neurogenesis after stroke. J Neurosci 26:13007-13016.

Ouyang YB, Tan Y, Comb M, Liu CL, Martone ME, Siesjo BK, Hu BR (1999) Survival- and death-promoting events after transient cerebral ischemia: phosphorylation of Akt, release of cytochrome C and activation of caspase-like proteases. J Cereb Blood Flow Metab 19:1126-1135.

Palmer TD, Ray J, Gage FH (1995) FGF-2-responsive neuronal progenitors reside in proliferative and quiescent regions of the adult rodent brain. Mol Cell Neurosci 6:474-486.

Palmer TD, Markakis EA, Willhoite AR, Safar F, Gage FH (1999) Fibroblast growth factor-2 activates a latent neurogenic program in neural stem cells from diverse regions of the adult CNS. J Neurosci 19:8487-8497.

Pan W, Zadina JE, Harlan RE, Weber JT, Banks WA, Kastin AJ (1997) Tumor necrosis factor-alpha: a neuromodulator in the CNS. Neurosci Biobehav Rev 21:603-613.

Panickar KS, Norenberg MD (2005) Astrocytes in cerebral ischemic injury: morphological and general considerations. Glia 50:287-298.

Paramore CG, Turner DA, Madison RD (1992) Fluorescent labeling of dissociated fetal cells for tissue culture. J Neurosci Methods 44:7-17.

Parent JM, Vexler ZS, Gong C, Derugin N, Ferriero DM (2002) Rat forebrain neurogenesis and striatal neuron replacement after focal stroke. Ann Neurol 52:802-813.

Pekny M, Nilsson M (2005) Astrocyte activation and reactive gliosis. Glia 50:427-434.

Pencea V, Bingaman KD, Freedman LJ, Luskin MB (2001a) Neurogenesis in the subventricular zone and rostral migratory stream of the neonatal and adult primate forebrain. Exp Neurol 172:1-16.
Pencea V, Bingaman KD, Wiegand SJ, Luskin MB (2001b) Infusion of brain-derived neurotrophic factor into the lateral ventricle of the adult rat leads to new neurons in the parenchyma of the striatum, septum, thalamus, and hypothalamus. J Neurosci 21:6706-6717.
Petreanu L, Alvarez-Buylla A (2002) Maturation and death of adult-born olfactory bulb granule neurons: role of olfaction. J Neurosci 22:6106-6113.
Picard-Riera N, Nait-Oumesmar B, Baron-Van Evercooren A (2004) Endogenous adult neural stem cells: limits and potential to repair the injured central nervous system. J Neurosci Res 76:223-231.
Planas AM, Justicia C, Sole S, Friguls B, Cervera A, Adell A, Chamorro A (2002) Certain forms of matrix metalloproteinase-9 accumulate in the extracellular space after microdialysis probe implantation and middle cerebral artery occlusion/reperfusion. J Cereb Blood Flow Metab 22:918-925.
Power C, Henry S, Del Bigio MR, Larsen PH, Corbett D, Imai Y, Yong VW, Peeling J (2003) Intracerebral hemorrhage induces macrophage activation and matrix metalloproteinases. Ann Neurol 53:731-742.
Price J, Turner D, Cepko C (1987) Lineage analysis in the vertebrate nervous system by retrovirus-mediated gene transfer. Proc Natl Acad Sci U S A 84:156-160.
Rafii S, Lyden D (2003) Therapeutic stem and progenitor cell transplantation for organ vascularization and regeneration. Nat Med 9:702-712.
Rakic P (2002) Adult neurogenesis in mammals: an identity crisis. J Neurosci 22:614-618.
Ramaswamy S, Goings GE, Soderstrom KE, Szele FG, Kozlowski DA (2005) Cellular proliferation and migration following a controlled cortical impact in the mouse. Brain Res 1053:38-53.
Reid JL, Dawson D, Macrae IM (1995) Endothelin, cerebral ischaemia and infarction. Clin Exp Hypertens 17:399-407.
Reynolds BA, Weiss S (1992) Generation of neurons and astrocytes from isolated cells of the adult mammalian central nervous system. Science 255:1707-1710.
Richard Green A, Odergren T, Ashwood T (2003) Animal models of stroke: do they have value for discovering neuroprotective agents? Trends Pharmacol Sci 24:402-408.
Ridet JL, Malhotra SK, Privat A, Gage FH (1997) Reactive astrocytes: cellular and molecular cues to biological function. Trends Neurosci 20:570-577.
Robinson MJ, Macrae IM, Todd M, Reid JL, McCulloch J (1990) Reduction of local cerebral blood flow to pathological levels by endothelin-1 applied to the middle cerebral artery in the rat. Neurosci Lett 118:269-272.
Rogelius N, Ericson C, Lundberg C (2005) In vivo labeling of neuroblasts in the subventricular zone of rats. J Neurosci Methods 142:285-293.
Roitberg B (2004) Transplantation for stroke. Neurol Res 26:256-264.
Romero JR, Babikian VL, Katz DI, Finklestein SP (2006) Neuroprotection and stroke rehabilitation: modulation and enhancement of recovery. Behav Neurol 17:17-24.

Saghatelyan A, Carleton A, Lagier S, de Chevigny A, Lledo PM (2003) Local neurons play key roles in the mammalian olfactory bulb. J Physiol Paris 97:517-528.
Sanai N, Tramontin AD, Quinones-Hinojosa A, Barbaro NM, Gupta N, Kunwar S, Lawton MT, McDermott MW, Parsa AT, Manuel-Garcia Verdugo J, Berger MS, Alvarez-Buylla A (2004) Unique astrocyte ribbon in adult human brain contains neural stem cells but lacks chain migration. Nature 427:740-744.
Sanchez-Alvarez R, Tabernero A, Medina JM (2004) Endothelin-1 stimulates the translocation and upregulation of both glucose transporter and hexokinase in astrocytes: relationship with gap junctional communication. J Neurochem 89:703-714.
Sanchez Mejia RO, Ona VO, Li M, Friedlander RM (2001) Minocycline reduces traumatic brain injury-mediated caspase-1 activation, tissue damage, and neurological dysfunction. Neurosurgery 48:1393-1399; discussion 1399-1401.
Sasaki C, Kitagawa H, Zhang WR, Warita H, Sakai K, Abe K (2000) Temporal profile of cytochrome c and caspase-3 immunoreactivities and TUNEL staining after permanent middle cerebral artery occlusion in rats. Neurol Res 22:223-228.
Savchenko VL, McKanna JA, Nikonenko IR, Skibo GG (2000) Microglia and astrocytes in the adult rat brain: comparative immunocytochemical analysis demonstrates the efficacy of lipocortin 1 immunoreactivity. Neuroscience 96:195-203.
Schaller B, Graf R (2004) Cerebral ischemia and reperfusion: the pathophysiologic concept as a basis for clinical therapy. J Cereb Blood Flow Metab 24:351-371.
Schmidt W, Reymann KG (2002) Proliferating cells differentiate into neurons in the hippocampal CA1 region of gerbils after global cerebral ischemia. Neurosci Lett 334:153-156.
Schroeter M, Jander S, Witte OW, Stoll G (1994) Local immune responses in the rat cerebral cortex after middle cerebral artery occlusion. J Neuroimmunol 55:195-203.
Schroeter M, Jander S, Huitinga I, Witte OW, Stoll G (1997) Phagocytic response in photochemically induced infarction of rat cerebral cortex. The role of resident microglia. Stroke 28:382-386.
Sheen VL, Macklis JD (1994) Apoptotic mechanisms in targeted neuronal cell death by chromophore-activated photolysis. Exp Neurol 130:67-81.
Sheen VL, Arnold MW, Wang Y, Macklis JD (1999) Neural precursor differentiation following transplantation into neocortex is dependent on intrinsic developmental state and receptor competence. Exp Neurol 158:47-62.
Shihabuddin LS, Ray J, Gage FH (1997) FGF-2 is sufficient to isolate progenitors found in the adult mammalian spinal cord. Exp Neurol 148:577-586.
Siesjo BK (1992a) Pathophysiology and treatment of focal cerebral ischemia. Part II: Mechanisms of damage and treatment. J Neurosurg 77:337-354.
Siesjo BK (1992b) Pathophysiology and treatment of focal cerebral ischemia. Part I: Pathophysiology. J Neurosurg 77:169-184.
Small DL, Morley P, Buchan AM (1999) Biology of ischemic cerebral cell death. Prog Cardiovasc Dis 42:185-207.
Smith DL, Woodman B, Mahal A, Sathasivam K, Ghazi-Noori S, Lowden PA, Bates GP, Hockly E (2003) Minocycline and doxycycline are not beneficial in a model of Huntington's disease. Ann Neurol 54:186-196.

Smith WS (2004) Pathophysiology of focal cerebral ischemia: a therapeutic perspective. J Vasc Interv Radiol 15:S3-12.
Snider BJ, Gottron FJ, Choi DW (1999) Apoptosis and necrosis in cerebrovascular disease. Ann N Y Acad Sci 893:243-253.
Snyder EY, Yoon C, Flax JD, Macklis JD (1997) Multipotent neural precursors can differentiate toward replacement of neurons undergoing targeted apoptotic degeneration in adult mouse neocortex. Proc Natl Acad Sci U S A 94:11663-11668.
Sofroniew MV (2005) Reactive astrocytes in neural repair and protection. Neuroscientist 11:400-407.
Sofroniew MV, Bush TG, Blumauer N, Kruger L, Mucke L, Johnson MH (1999) Genetically-targeted and conditionally-regulated ablation of astroglial cells in the central, enteric and peripheral nervous systems in adult transgenic mice. Brain Res 835:91-95.
Sohur S, Emsley JG, Mitchell BD, Macklis JD (2006) Adult neurogenesis and cellular brain repair with neural progenitors, precursors and stem cells. Philos Trans R Soc Lond B Biol Sci 361:1477-1497.
Song H, Stevens CF, Gage FH (2002) Astroglia induce neurogenesis from adult neural stem cells. Nature 417:39-44.
Stirling DP, Koochesfahani KM, Steeves JD, Tetzlaff W (2005) Minocycline as a neuroprotective agent. Neuroscientist 11:308-322.
Stoll G, Jander S, Schroeter M (1998) Inflammation and glial responses in ischemic brain lesions. Prog Neurobiol 56:149-171.
Streit WJ (1990) An improved staining method for rat microglial cells using the lectin from Griffonia simplicifolia (GSA I-B4). J Histochem Cytochem 38:1683-1686.
Streit WJ (2002) Microglia as neuroprotective, immunocompetent cells of the CNS. Glia 40:133-139.
Streit WJ, Walter SA, Pennell NA (1999) Reactive microgliosis. Prog Neurobiol 57:563-581.
Sugawara T, Fujimura M, Noshita N, Kim GW, Saito A, Hayashi T, Narasimhan P, Maier CM, Chan PH (2004) Neuronal death/survival signaling pathways in cerebral ischemia. NeuroRx 1:17-25.
Szele FG, Chesselet MF (1996) Cortical lesions induce an increase in cell number and PSA-NCAM expression in the subventricular zone of adult rats. J Comp Neurol 368:439-454.
Szymanska A, Biernaskie J, Laidley D, Granter-Button S, Corbett D (2006) Minocycline and intracerebral hemorrhage: influence of injury severity and delay to treatment. Exp Neurol 197:189-196.
Takagi Y, Nozaki K, Takahashi J, Yodoi J, Ishikawa M, Hashimoto N (1999) Proliferation of neuronal precursor cells in the dentate gyrus is accelerated after transient forebrain ischemia in mice. Brain Res 831:283-287.
Taupin P (2006a) Neurogenesis in the adult central nervous system. C R Biol 329:465-475.
Taupin P (2006b) BrdU immunohistochemistry for studying adult neurogenesis: Paradigms, pitfalls, limitations, and validation. Brain Res Brain Res Rev.
Teng YD, Choi H, Onario RC, Zhu S, Desilets FC, Lan S, Woodard EJ, Snyder EY, Eichler ME, Friedlander RM (2004) Minocycline inhibits contusion-triggered

mitochondrial cytochrome c release and mitigates functional deficits after spinal cord injury. Proc Natl Acad Sci U S A 101:3071-3076.
Terasaki M, Jaffe LA (1991) Organization of the sea urchin egg endoplasmic reticulum and its reorganization at fertilization. J Cell Biol 114:929-940.
Thomas WE (1999) Brain macrophages: on the role of pericytes and perivascular cells. Brain Res Brain Res Rev 31:42-57.
Thored P, Arvidsson A, Cacci E, Ahlenius H, Kallur T, Darsalia V, Ekdahl CT, Kokaia Z, Lindvall O (2006) Persistent production of neurons from adult brain stem cells during recovery after stroke. Stem Cells 24:739-747.
Tikka T, Fiebich BL, Goldsteins G, Keinanen R, Koistinaho J (2001) Minocycline, a tetracycline derivative, is neuroprotective against excitotoxicity by inhibiting activation and proliferation of microglia. J Neurosci 21:2580-2588.
Tilley BC, Alarcon GS, Heyse SP, Trentham DE, Neuner R, Kaplan DA, Clegg DO, Leisen JC, Buckley L, Cooper SM, Duncan H, Pillemer SR, Tuttleman M, Fowler SE (1995) Minocycline in rheumatoid arthritis. A 48-week, double-blind, placebo-controlled trial. MIRA Trial Group. Ann Intern Med 122:81-89.
Tokita Y, Keino H, Matsui F, Aono S, Ishiguro H, Higashiyama S, Oohira A (2001) Regulation of neuregulin expression in the injured rat brain and cultured astrocytes. J Neurosci 21:1257-1264.
Tomita M, Fukuuchi Y (1996) Leukocytes, macrophages and secondary brain damage following cerebral ischemia. Acta Neurochir Suppl 66:32-39.
Toresson H, Parmar M, Campbell K (2000) Expression of Meis and Pbx genes and their protein products in the developing telencephalon: implications for regional differentiation. Mech Dev 94:183-187.
Tramontin AD, Garcia-Verdugo JM, Lim DA, Alvarez-Buylla A (2003) Postnatal development of radial glia and the ventricular zone (VZ): a continuum of the neural stem cell compartment. Cereb Cortex 13:580-587.
Traystman RJ (2003) Animal models of focal and global cerebral ischemia. ILAR J 44:85-95.
Tropepe V, Coles BL, Chiasson BJ, Horsford DJ, Elia AJ, McInnes RR, van der Kooy D (2000) Retinal stem cells in the adult mammalian eye. Science 287:2032-2036.
Tsai PT, Ohab JJ, Kertesz N, Groszer M, Matter C, Gao J, Liu X, Wu H, Carmichael ST (2006) A critical role of erythropoietin receptor in neurogenesis and post-stroke recovery. J Neurosci 26:1269-1274.
Tsuji M, Wilson MA, Lange MS, Johnston MV (2004) Minocycline worsens hypoxic-ischemic brain injury in a neonatal mouse model. Exp Neurol 189:58-65.
Turley KR, Toledo-Pereyra LH, Kothari RU (2005) Molecular mechanisms in the pathogenesis and treatment of acute ischemic stroke. J Invest Surg 18:207-218.
Velier JJ, Ellison JA, Kikly KK, Spera PA, Barone FC, Feuerstein GZ (1999) Caspase-8 and caspase-3 are expressed by different populations of cortical neurons undergoing delayed cell death after focal stroke in the rat. J Neurosci 19:5932-5941.
Vercelli A, Repici M, Garbossa D, Grimaldi A (2000) Recent techniques for tracing pathways in the central nervous system of developing and adult mammals. Brain Res Bull 51:11-28.

Walz W, Juurlink B (2002) Homestatic Properties of Astrocytes. In: The Neuronal enviroment: brain homestasis in health and disease (Walz W, Tortowa N, eds), pp 159-186: Humana Press.
Wang CX, Shuaib A (2002) Involvement of inflammatory cytokines in central nervous system injury. Prog Neurobiol 67:161-172.
Wang K, Walz W (2003) Unusual topographical pattern of proximal astrogliosis around a cortical devascularizing lesion. J Neurosci Res 73:497-506.
Wang K, Bekar LK, Furber K, Walz W (2004) Vimentin-expressing proximal reactive astrocytes correlate with migration rather than proliferation following focal brain injury. Brain Res 1024:193.
Wang X, Louden C, Yue TL, Ellison JA, Barone FC, Solleveld HA, Feuerstein GZ (1998a) Delayed expression of osteopontin after focal stroke in the rat. J Neurosci 18:2075-2083.
Wang Y, Sheen VL, Macklis JD (1998b) Cortical interneurons upregulate neurotrophins in vivo in response to targeted apoptotic degeneration of neighboring pyramidal neurons. Exp Neurol 154:389-402.
Wardlaw J (2004) ACCESS: the acute cerebral CT evaluation stroke study. Emerg Med J 21:666.
Warlow C, Sudlow C, Dennis M, Wardlaw J, Sandercock P (2003) Stroke. Lancet 362:1211-1224.
Watson BD, Dietrich WD, Busto R, Wachtel MS, Ginsberg MD (1985) Induction of reproducible brain infarction by photochemically initiated thrombosis. Ann Neurol 17:497-504.
Weickert CS, Webster MJ, Colvin SM, Herman MM, Hyde TM, Weinberger DR, Kleinman JE (2000) Localization of epidermal growth factor receptors and putative neuroblasts in human subependymal zone. J Comp Neurol 423:359-372.
Weiss S, Dunne C, Hewson J, Wohl C, Wheatley M, Peterson AC, Reynolds BA (1996) Multipotent CNS stem cells are present in the adult mammalian spinal cord and ventricular neuroaxis. J Neurosci 16:7599-7609.
Wells JE, Hurlbert RJ, Fehlings MG, Yong VW (2003) Neuroprotection by minocycline facilitates significant recovery from spinal cord injury in mice. Brain 126:1628-1637.
Westerlund U, Moe MC, Varghese M, Berg-Johnsen J, Ohlsson M, Langmoen IA, Svensson M (2003) Stem cells from the adult human brain develop into functional neurons in culture. Exp Cell Res 289:378-383.
Weston SA, Parish CR (1990) New fluorescent dyes for lymphocyte migration studies. Analysis by flow cytometry and fluorescence microscopy. J Immunol Methods 133:87-97.
Whishaw IQ (2000) Loss of the innate cortical engram for action patterns used in skilled reaching and the development of behavioral compensation following motor cortex lesions in the rat. Neuropharmacology 39:788-805.
Wichterle H, Garcia-Verdugo JM, Alvarez-Buylla A (1997) Direct evidence for homotypic, glia-independent neuronal migration. Neuron 18:779-791.
Windle V, Szymanska A, Granter-Button S, White C, Buist R, Peeling J, Corbett D (2006) An analysis of four different methods of producing focal cerebral ischemia with endothelin-1 in the rat. Exp Neurol.

Winner B, Cooper-Kuhn CM, Aigner R, Winkler J, Kuhn HG (2002) Long-term survival and cell death of newly generated neurons in the adult rat olfactory bulb. Eur J Neurosci 16:1681-1689.

Xu L, Fagan SC, Waller JL, Edwards D, Borlongan CV, Zheng J, Hill WD, Feuerstein G, Hess DC (2004) Low dose intravenous minocycline is neuroprotective after middle cerebral artery occlusion-reperfusion in rats. BMC Neurol 4:7.

Yagita Y, Kitagawa K, Ohtsuki T, Takasawa K, Miyata T, Okano H, Hori M, Matsumoto M (2001) Neurogenesis by progenitor cells in the ischemic adult rat hippocampus. Stroke 32:1890-1896.

Yamada M, Onodera M, Mizuno Y, Mochizuki H (2004) Neurogenesis in olfactory bulb identified by retroviral labeling in normal and 1-methyl-4-phenyl-1,2,3,6-tetrahydropyridine-treated adult mice. Neuroscience 124:173-181.

Yamamoto S, Nagao M, Sugimori M, Kosako H, Nakatomi H, Yamamoto N, Takebayashi H, Nabeshima Y, Kitamura T, Weinmaster G, Nakamura K, Nakafuku M (2001) Transcription factor expression and Notch-dependent regulation of neural progenitors in the adult rat spinal cord. J Neurosci 21:9814-9823.

Yamashita K, Vogel P, Fritze K, Back T, Hossmann KA, Wiessner C (1996) Monitoring the temporal and spatial activation pattern of astrocytes in focal cerebral ischemia using in situ hybridization to GFAP mRNA: comparison with sgp-2 and hsp70 mRNA and the effect of glutamate receptor antagonists. Brain Res 735:285-297.

Yamashita T, Ninomiya M, Hernandez Acosta P, Garcia-Verdugo JM, Sunabori T, Sakaguchi M, Adachi K, Kojima T, Hirota Y, Kawase T, Araki N, Abe K, Okano H, Sawamoto K (2006) Subventricular zone-derived neuroblasts migrate and differentiate into mature neurons in the post-stroke adult striatum. J Neurosci 26:6627-6636.

Yang L, Sugama S, Chirichigno JW, Gregorio J, Lorenzl S, Shin DH, Browne SE, Shimizu Y, Joh TH, Beal MF, Albers DS (2003) Minocycline enhances MPTP toxicity to dopaminergic neurons. J Neurosci Res 74:278-285.

Yong VW, Wells J, Giuliani F, Casha S, Power C, Metz LM (2004) The promise of minocycline in neurology. Lancet Neurol 3:744-751.

Yrjanheikki J, Keinanen R, Pellikka M, Hokfelt T, Koistinaho J (1998) Tetracyclines inhibit microglial activation and are neuroprotective in global brain ischemia. Proc Natl Acad Sci U S A 95:15769-15774.

Yrjanheikki J, Tikka T, Keinanen R, Goldsteins G, Chan PH, Koistinaho J (1999) A tetracycline derivative, minocycline, reduces inflammation and protects against focal cerebral ischemia with a wide therapeutic window. Proc Natl Acad Sci U S A 96:13496-13500.

Zang DW, Cheema SS (2003) Leukemia inhibitory factor promotes recovery of locomotor function following spinal cord injury in the mouse. J Neurotrauma 20:1215-1222.

Zhang R, Zhang Z, Wang L, Wang Y, Gousev A, Zhang L, Ho KL, Morshead C, Chopp M (2004) Activated neural stem cells contribute to stroke-induced neurogenesis and neuroblast migration toward the infarct boundary in adult rats. J Cereb Blood Flow Metab 24:441-448.

Zhang RL, Zhang ZG, Zhang L, Chopp M (2001) Proliferation and differentiation of progenitor cells in the cortex and the subventricular zone in the adult rat after focal cerebral ischemia. Neuroscience 105:33-41.
Zhang Z, Chopp M, Powers C (1997) Temporal profile of microglial response following transient (2 h) middle cerebral artery occlusion. Brain Res 744:189-198.
Zhao M, Momma S, Delfani K, Carlen M, Cassidy RM, Johansson CB, Brismar H, Shupliakov O, Frisen J, Janson AM (2003) Evidence for neurogenesis in the adult mammalian substantia nigra. Proc Natl Acad Sci U S A 100:7925-7930.
Zheng Z, Yenari MA (2004) Post-ischemic inflammation: molecular mechanisms and therapeutic implications. Neurol Res 26:884-892.
Zhu S, Stavrovskaya IG, Drozda M, Kim BY, Ona V, Li M, Sarang S, Liu AS, Hartley DM, Wu DC, Gullans S, Ferrante RJ, Przedborski S, Kristal BS, Friedlander RM (2002) Minocycline inhibits cytochrome c release and delays progression of amyotrophic lateral sclerosis in mice. Nature 417:74-78.
Ziaja M, Janeczko K (1999) Spatiotemporal patterns of microglial proliferation in rat brain injured at the postmitotic stage of postnatal development. J Neurosci Res 58:379-386.